AN AUTOMATED CALIBRATION SETUP FOR LASER BEAM POSITIONING SYSTEMS IN VISUAL INSPECTION APPLICATIONS

A THESIS SUBMITTED TO
THE GRADUATE SCHOOL OF NATURAL AND APPLIED SCIENCES
OF
MIDDLE EAST TECHNICAL UNIVERSITY

BY

ERCAN KİRAZ

IN PARTIAL FULFILMENT OF THE REQUIREMENTS
FOR
THE DEGREE OF MASTER OF SCIENCE
IN
MECHANICAL ENGINEERING

JANUARY 2013

Approval of the thesis:

AN AUTOMATED CALIBRATION SETUP FOR LASER BEAM POSITIONING SYSTEMS IN VISUAL INSPECTION APPLICATIONS

submitted by **ERCAN KİRAZ** in partial fulfillment of the requirements for the degree of **Master of Science in Mechanical Engineering Department, Middle East Technical University** by,

Prof. Dr. Canan Özgen _____
Dean, Graduate School of **Natural and Applied Sciences**

Prof. Dr. Süha Oral _____
Head of Department, **Mechanical Engineering**

Assist. Prof. Dr. Melik Dölen _____
Supervisor, **Mechanical Engineering Dept., METU**

Examining Committee Members:

Prof. Dr. Eres Söylemez _____
Mechanical Engineering Dept., METU

Assist. Prof. Dr. Melik Dölen _____
Mechanical Engineering Dept., METU

Assist. Prof. Dr. A. Buğra Koku _____
Mechanical Engineering Dept., METU

Assist. Prof. Dr. Yiğit Yazıcıoğlu _____
Mechanical Engineering Dept., METU

Assist. Prof. Dr. Kutluk Bilge Arıkan _____
Mechatronics Engineering Dept., Atılım University

Date: 23.01.2013

I hereby declare that all information in this document has been obtained and presented in accordance with academic rules and ethical conduct. I also declare that, as require by these rules and conduct, I have fully cited and referenced all material and results that are not original to this work.

Name, Last Name : Ercan, Kiraz

Signature :

ABSTRACT

AN AUTOMATED CALIBRATION SETUP FOR LASER BEAM POSITIONING SYSTEMS IN VISUAL INSPECTION APPLICATIONS

Kiraz, Ercan
M.Sc., Department of Mechanical Engineering
Supervisor: Assist. Prof. Dr. Melik Dölen

January 2013, 150 pages

In this study, a calibration setup for laser beam positioning systems used in visual inspection applications in industry is designed and manufactured. The laser positioning systems generate movable parallel laser lines on the projection surface. There are several translational and angular error sources affecting the positioning accuracy of the laser lines on the projection surface. Especially, since the laser line positioning error caused by angular error sources increases with the distance between the laser system and the projection surface, angular parameters of the laser sources should be measured and adjusted precisely. The calibration setup developed in this study detects the laser line positions at two different projection distances by means of laser sensing cameras which are positioned precisely along the laser lines and laser positioning axis which is perpendicular to these lines. Cameras detect the positions of the laser lines which are directed to the camera sensors with micrometer repeatability by means of some special imaging algorithms. The precise positioning of the cameras requires a special camera positioning system. For this reason, the disturbances like temperature changes and vibration should be minimized. In order to provide a suitable environment for the calibration system, special tests are conducted and a special calibration room is constituted. Construction inside the room is also made by considering the required ambient parameters. Finally, several verification tests of the calibration system are conducted.

Keywords: Laser Calibration, Laser Positioning, Laser Line Detection, Calibration System, Laser Sensing

ÖZ

GÖRSEL KONTROL UYGULAMALARINDA KULLANILAN LAZER POZİSYONLAMA SİSTEMLERİ İÇİN OTOMATİKLEŞTİRİLMİŞ BİR KALİBRASYON SİSTEMİ

Kiraz, Ercan
Yüksek Lisans. Makina Mühendisliği Bölümü
Tez Yöneticisi: Yrd. Doç. Dr. Melik Dölen

Ocak 2013, 150 sayfa

Bu çalışmada, sanayideki görsel kontrol uygulamalarında kullanılan lazer konumlama sistemleri için bir kalibrasyon sisteminin tasarımı ve üretimi gerçekleştirilmiştir. Lazer konumlama sistemleri doğrultulan yüzeyde hareketli paralel lazer çizgileri oluşturmaktadır. Projeksiyon yüzeyindeki lazer çizgilerinin konumlama doğruluğunu etkileyen çeşitli öteleme ve açı hata kaynakları mevcuttur. Özellikle açısal hata kaynaklarının sebep olduğu lazer çizgisi konumlama hataları lazer sistemi ve projeksiyon yüzeyi arasındaki mesafe ile arttığı için lazer kaynaklarının açı parametreleri hassas bir şekilde ölçülüp ayarlanmalıdır. Bu çalışmada geliştirilen kalibrasyon sistemi, lazer çizgileri ve bu çizgilere dik olan lazer konumlama ekseni boyunca hassas bir şekilde konumlanan lazer algılayıcı kameralar aracılığı ile lazer çizgilerinin iki farklı yükseklikte konumlarını algılamaktadır. Kameralar, özel görüntü işleme algoritmaları kullanarak algılayıcılara doğrultulmuş lazer çizgilerinin konumunu mikrometre tekrarlanabilirlikle belirlemektedir. Kameraların hassas konumlaması özel bir kamera konumlama sistemi gerektirmektedir. Bu nedenle sıcaklık değişimi ve titreşim gibi dış etkilerin en aza indirilmesi gerekmektedir. Kalibrasyon sistemine uygun bir ortam sağlamak için özel testler gerçekleştirilmiş ve özel bir kalibrasyon odası oluşturulmuştur. Bu odanın içyapısı da gerekli ortam koşulları düşünülerek hazırlanmıştır. Son olarak da kalibrasyon sisteminin çeşitli sistem doğrulama testleri gerçekleştirilmiştir.

Anahtar Kelimeler: Lazer Kalibrasyon, Lazer Konumlama, Lazer Çizgisi Belirleme, Kalibrasyon Sistemi, Lazer Algılama

To my family

ACKNOWLEDGEMENT

I would like to express my special thanks to my supervisor Assist. Prof. Dr. Melik Dölen for his guidance, support, and encouragement throughout this study and in my university life.

I would also like to thank Assist. Prof. Dr. Buğra Koku and Assist. Prof. Dr. Yiğit Yazıcıoğlu for their help during the progress of this thesis study.

I am grateful to my family for their endless love, patience, and encouragement.

I am also very grateful to Mr. Onur Yarkınoğlu for his support and special effort at each step of the study.

I would like to thank Mr. Erhan Yarkınoğlu and Mr. Hasan Tepebaşı for their invaluable effort in the construction of the mechanical system.

This study is supported by Modesis Machine Technologies Company and The Scientific and Technological Research Council of Turkey (TÜBİTAK) with project number 7100648.

TABLE OF CONTENTS

LIST OF FIGURES

FIGURES

LIST OF TABLES

TABLES

CHAPTER 1

INTRODUCTION

1.1 Motivation

Visual inspection techniques depending on laser line positioning are widely used in textile and automotive industry, tire production, packaging systems, medical and aerospace applications. Patient alignment with laser lines for radiation therapy, diagnostic radiology, and nuclear medicine are some examples of the medical applications. In industry, laser projectors generate precise outlines, templates, patterns or other shapes on surfaces by projecting laser lines during the manufacturing or assembling processes. These applications depend on generation of laser lines with a desired form and positioning of these lines according to the pre-determined accuracy.

1.2 Scope of the Thesis

In this thesis, it is aimed to develop a calibration setup for a laser positioning system used in visual inspection applications in industry. This system generates planar laser beams which form laser lines on the target surface. The laser system which is desired to be calibrated is elaborated in Chapter 3 in detail.

Calibration of the laser beam positioning system (LBPS) depends on determining the positions, angles, and forms of the laser lines. For this purpose, several laser sensing devices and methods are investigated. Finally, CCD cameras are selected as the sensing device. In the calibration system, two CCD cameras at two different projection distances and a 2D positioning system are utilized. Position and form information of the laser lines are obtained by using these cameras and positioning system. The CCD cameras are precisely positioned along the linear motion system and the laser lines are detected on two different projection distances. Repeating this position sensing action for several points along the laser lines and also along the movement range of the laser sources, exit angles of the laser beams, projection angles of the laser lines, and positions of the laser sources are determined.

The 2D positioning system is developed to provide the camera positioning with high precision along the laser lines and also along the translation axis of the laser positioning system. During the design and manufacturing of this system a lot of accuracy considerations and system requirements are taken into account. These are elaborated in Chapter 4.

The accuracy considerations for the calibration system are precise positioning of the cameras along the translation axes, orientation of the cameras on the system, vibration, and the accuracy of the camera outputs. The first three problems are mechanical issues. Mechanical design of the calibration system is focused on these three parameters. Mechanical elements, manufacturing techniques, position feedback devices, system assembly, and selection the place of the calibration system are determined according to these considerations. The forth problem arises from the CCD sensor capabilities. However, it is possible to improve the repeatability of the camera measurements by developing some imaging algorithms. For this purpose, some repeatability tests are conducted with the cameras. During these tests, some imaging algorithms are also developed

and tested. Depending on the test results, a best method of position determination according to camera output is selected.

The contribution of this thesis is a new approach for calibration of laser position and form by positioning laser sensing devices (i.e. CCD cameras) along the projected laser lines. This method is quite different than ordinary image processing methods in which the whole laser lines are directed to a screen and captured by cameras via focusing lenses. The drawback of such a system is the distortions caused by additional optical elements and difficulty of measuring the beam exit angle. In the developed method, projected lines are mapped on two different projection planes having different projection distance by means of a precise positioning system enabling to measure the beam exit angles without any additional optical elements.

1.3 Organization

In the organization of the thesis, the chapters are constituted as follows. Chapter 2 includes the current state of the art about the relevant subjects. Chapter 3 elaborates the Laser Beam Positioning System which is to be calibrated. Chapter 4 includes development steps of the calibration setup. Chapter 5 is dedicated to modeling of the calibration system. Chapter 6 is related to system integration. All software and communication structure are included in this chapter. Chapter 7 presents the tests and measurements related to calibration system. In Chapter 8, which is the final chapter, conclusions and future work are elaborated.

CHAPTER 2

REVIEW OF THE STATE OF THE ART

2.1 Introduction

In this part of the thesis, the current state of the art about the relevant subjects is investigated. This literature review consists of three main parts. In the first part, types of laser sources commonly used in industry and medical are explained. Several examples depending on positioning, measurement, and inspection applications using these sources are also presented. In the second part, three main laser sensing devices are introduced and explained. Studies using these laser sensing devices are added to the part of each device. Finally, calculation methods developed for laser position determination from a discrete image data are given.

2.2 Types of Laser Sources

Hundreds of different types of lasers are available today. However, operation properties of these sources should be optimized for specific applications. As a result, a few of these lasers are commercially available (Drake, 2006).

There are basically four types of laser which are commonly utilized in industrial and scientific applications. These are gas lasers, solid state lasers, liquid lasers, and semiconductor lasers (Dahotre, 2008).

2.2.1 Gas Lasers

In gas lasers, the active laser medium is gaseous materials like Helium-Neon and Argon. There are several studies conducted by using gas lasers.

One of the studies conducted by using gas lasers depending on laser position detection is the surveying system developed by the SPring-8 (Super Photon ring-8 GeV) project team (Chida, 1995). The SPring-8 (Super Photon ring-8 GeV) Storage Ring is a 8 GeV synchrotron radiation source with 1436 m circumference and consists of 44 double bend achromatic cells (Chasman Green cell) and 4 straight section cells (Tsumaki, 2002). Each cell except for the 4 cells is composed of three straight sections and two bending magnets. Each straight section consists of five or seven quadrupole and sextupole magnets on one 4 or 5 m girder (Chida, 1995). A surveying system using a laser and a CCD camera with image processing is developed for several alignment purposes. The first one is to align magnets on 5 m long girder to an accuracy of 10 μm (Matsui, 1995). The second application is the alignment of magnets on 50 mm straight section with misalignment tolerance of ± 0.2 mm and ± 0.1 mm along horizontal and vertical axes, respectively (Matsui, 2002). The same surveying system is also employed in rearrangement of the magnets on 30 m long straight sections (Tsumaki, 2002). In this surveying system, a 633 nm

wavelength He-Ne gas laser with 2mW exit power is used. Diameter of the laser spot ($1/e^2$) and the expending angle of the laser beam are 0.8 mm and 1.3 mrad respectively (Chida, 1995).

2.2.2 Solid State Lasers

In solid-state lasers, active medium consists of a small percentage of impurity ions doped in a solid host material. Nd:YAG laser is the one which is most commonly utilized in the industrial applications like laser machining. This laser type consists of crystalline YAG with a chemical formula $Y_3Al_5O_{12}$ as a host material with contribution of 2 % Nd^{3+} ions doped in YAG (Dahotre, 2008).

In the STAR experiment at RHIC (Relativistic Heavy Ion Collider), a laser calibration system is built to calibrate and monitor the tracking performance of TPC (Time Projection Chamber) which is the primary tracking detector for the STAR experiment (Lebedev, 2002). In this laser system, Nd:YAG laser with multiple beams (200 - 400) is operated to imitate straight charged particle tracks in the tracking volume. The laser beams are utilized to measure the drift velocity and drift distortions that can arise from errors in the E and B fields. The laser light is frequency quadrupled to 266 nm and the resulting UV beam is expanded and collimated in a telescope. During the RHIC run, the laser system shows the stability of the TPC electronics and to measure drift velocities with approximately 0.02% accuracy.

In the study related to solid state lasers conducted in Aachen University for high-speed melt pool detection in laser welding applications, three different image processing methods are developed for the detection of the melt pool circle (i.e. its position and radius) in Nd:YAG laser welding applications by using a CMOS image sensor (Stache, 2006). In the first one of these methods, each captured frame is matched to a set of idealized binary prototype melt pool images with varied but defined parameters. The best match then leads directly to the sought parameters. In the second method, periphery points named as N, S, E, and W are calculated for the captured images and a circle that is closest in parameter space to the previously determined one is picked according to the smallest Euclidean distance to the previous picked one. The third proposed method is very similar to the second with the difference of determining the smallest distance. In this case, the smallest distance is calculated with the least squares approach.

Another study conducted in Aachen University related to solid state laser positioning is the calibration of a laser welding system equipped with a galvanometer scanner (Stache, 2007). In this study, a laser welding system using Nd:YAG laser source is calibrated. The welding system depends on 2D positioning of the laser by using a galvanometer scanner. In the calibration system of the study, an imaging system with a high speed (high frame rate) CMOS camera is employed for process monitoring and position recognition of the parts to be welded. This study addresses the problem arises from the chromatic aberrations resulting from different wave lengths of welding laser passing from f-theta optics of the scanner. Since these elements are generally designed for a certain wavelength, different wavelength laser beams are subjected to positioning problems on the lateral axes of the lenses. In this study it is claimed that a cheap and flexible compensation method is introduced. In this method, there are two techniques for automatic calibration by use of the system-incorporated camera. The first one is based on creating laser spots and detecting them. In this technique, system automatically generates laser spots, evaluates their positions and possible offsets and finally fits an affine compensation model. The second technique is related to calibration of the camera in order to estimate its field of view position precisely. For this purpose a specially coded test pattern is used.

A study on precise positioning of diode pumped solid state lasers is introduced in *Institute of Digital Image Processing* in Austria (Kulcke, 2002). This study depends on the calibration of high

precision laser projection systems using green solid state laser sources and galvanometric laser scanners. Related projection systems are utilized in industrial environments to project CAD drawings onto large working areas generally larger than 1 m x 1 m. Such applications require external calibration to ensure a constant precision and quality. A special calibration system is developed for this purpose. The calibration system consists of 4 to 10 (depending on the dimensions of the projection area) standard machine vision black and white cameras. The laser projectors are mounted together with the cameras and the electronic system on a rigid frame which is in turn attached to a ceiling crane system or mounted stationary in the ceiling. The calibration procedure depends on defining different coordinate frames (world coordinate frame, table coordinate frame, projector coordinate frame, and camera coordinate frame) for the elements of the whole system and generating mathematical transformations from one to each other. The main purpose of the calibration method presented in this study is to obtain the transformation between table and projector coordinate systems. As a result, the projected data on the work area precisely matches the CAD drawing and it is not affected by the factors like positioning errors and drift.

In the *National Institute of Metrology* in Thailand, traceability in wavelength measurement of 633 nm iodine He-Ne lasers is investigated (Ranusawud, 2009). NIMT, maintains the standard of length in accordance with the definition of the meter through a 633 nm iodine stabilized He-Ne laser. Its accuracy is transferred to stabilized and non-stabilized lasers regarding to beat frequency method and direct measurement using a wavelength meter. The iodine stabilized He-Ne laser is self-calibrated by using the master and slave beat frequency system.

2.2.3 Liquid Lasers

Liquid lasers or liquid dye lasers consist of liquid solutions (organic dyes dissolved in suitable liquid solvents) as active laser materials. One of the most important characteristics of the dye lasers is that they can be used over a wide range of wavelengths (0.2–1.0 μm). This property makes them quite suitable for tunable lasers and pulsed lasers (Dahotre, 2008).

2.2.4 Semiconductor Lasers

Semiconductor lasers use semiconductor materials as active medium. The light emission from semiconductor diode lasers is generally associated with the radiative recombination of electrons and holes. This occurs at the junction of an n-type material with excess electrons and a p-type material with excess holes. The excitation is provided by an external electric field applied across the p-n junction that causes the two types of charges to come together (Drake, 2006).

By using a semiconductor planar laser diode, a CCD camera, and a special image processing method, a simple, low cost, 3D scanning system is presented in Carleton University (Bradley, 2009). This method depends on laser sectioning technique. This technique involves measuring the position of an object's surface profile by recording where the profile intersects a laser light plane. An important property of the proposed system is the ability of the camera system to rotate about an object with the required number of degrees of freedom making it flexible for numerous applications; particularly for biomedical applications where the apparatus would ideally rotate about a patient and not vice versa (Bradley, 2008). In a second study conducted in Carleton University, two different calibration techniques are presented for the same laser system for biomedical purposes. The techniques depend on analytical and least squares methods. In this study, both methods are evaluated according to their ability to cope with noise in the input calibration data.

Another semiconductor laser related medical study is conducted with a calibration method consisting of a laser projection device and the corresponding image processing method for automated detection of laser calibration marks (Wurzbacher, 2008). In the study, the laser projection device is attached to an endoscope and projects two parallel laser lines with a known distance to each other as calibration information onto the vocal folds. Image processing methods automatically identify the pixels belonging to the projected laser lines in the image data. The combination of the laser projection device and the image processing enables the calibration of laryngeal endoscopic images within the vocal fold plane and thus provides quantitative metrical data of vocal fold dynamics.

By using a semiconductor laser line generator and two cameras, a novel stereo vision calibration procedure is presented by (Vilaca, 2008). This procedure is based on a laser line projection plane in order to ensure the precision of the measurement of complex 3D object surfaces using non-contact laser scanning systems. In the proposed calibration procedure, the laser is located at the same physical distance from both cameras, and the cameras are oriented at 30° to the horizontal line. In the calculations, only radial distortion is considered because it is the most relevant distortion in industrial machine vision applications, and only the laser line projection plane is calibrated since measurements are only made along the plane defined by the laser line.

2.3 Laser Sensing Devices

Calibration of the laser beam positioning system which is the main subject of this thesis work depends on the determination of the laser positions. There are various laser sensing devices and methods which can be used for this purpose. The most significant laser sensing devices which can be used to determine the laser position together with several laser parameters are Charge Coupled Devices (CCD), Complementary Metal Oxide Semiconductors (CMOS), and Position Sensitive Detectors (PSD).

2.3.1 CCD and CMOS Sensors

Both CCD and CMOS sensors are widely used solid state image sensors in today's imaging technology. These sensors consist of an array of light sensing units named as pixel. Each pixel includes a photo-detector and devices for readout. An area image sensor has a two dimensional pixel array with dimensions of $m \times n$ where these range from 320×240 to 7000×9000. Pixel size ranges from $15\mu m \times 15\mu m$ down to $3\mu m \times 3\mu m$. Minimum pixel size is limited by dynamic range and the cost of related optics (Xinqiao, 2002). In most applications small pixel size is desirable. Thus, there are studies to develop smaller pixel sizes. The first submicron pixel size is reported by Keith Fife et al. (Fife, 2007). At this study, a CCD array with a 0.5 μm pixel size is fabricated and the performance parameters are stated to be within the consumer image sensors.

In CCD and CMOS sensors incident radiant power (photon/second) falling onto the photo-detector is converted into photocurrent which is proportional to the radiant power (Xinqiao, 2002). In the photo sensitive area of each pixel incident light is converted into electrons that is collected in a semiconductor just like a bucket accumulated with water (Hanumolu, 2001).

The basic difference between CCD and CMOS image sensors is the readout architecture. CCD image sensors generally use interline charge transfer. The sensor consists of array of photo-detectors and vertical and horizontal CCDs for readout. At the instant of exposure, charge is integrated in each photo-detector. After that, it is simultaneously transferred to vertical CCDs at

the end of exposure for all the pixels. The charge is then sequentially readout through the vertical and horizontal CCDs by charge transfer. In CMOS image sensors, the pixels in the array are addressed through the horizontal word line and the charge or voltage signal is readout from each pixel through the vertical bit line. The readout is done by transferring one row at a time to the column storage capacitors (Xinqiao, 2002).

There are plenty of studies related to laser position determination by using CCD and CMOS image sensors. Some of them are presented in this part.

An inspection system for in-tray laser IC (integrated circuit) marking system is developed by (Lin, 2010) with a new calibration model. The inspection system developed uses a high-speed high-resolution line scan CCD and a servo drive positioning system. In order to determine the laser marking locations precisely, image processing of the data coming from the high speed CCD scan is performed according to a novel algorithm. The calibration of the inspection system is conducted by using a template with known geometric properties and the mentioned algorithm. The total processing time for laser correction marking, scanning, and identification is mentioned as about 2 ~ 2.5 sec, and the positioning accuracy as ±9 mm.

The surveying system of SPring-8 storage ring mentioned in Section *2.2.1 Gas Lasers* consists of a laser, a CCD camera, and an image processing computer (Chida, 1995). During the study, lenses in front of the camera are removed and the attenuated laser spot is directly injected on the sensor plane. Some positioning tests are also carried out on the CCD camera. Pixel size of the tested camera is 11 μm and the distance between the laser source and the camera plane is 600 mm. In these tests, CCD camera is placed on the stage with a micrometer of which the minimum division is 2 μm and moved horizontally. The shift of this stage is checked by a laser interferometer. The tests results show that the accuracy of the camera position measurements is ± 4 μm for ± 1 mm translation and ± 1.5 μm for ± 0.1 mm translation. Rotating the camera by 90°, the same accuracy is observed also in the vertical direction.

In *Netherlands Institute for Metals Research*, a monitoring system to visualize the CW Nd:YAG laser keyhole welding process is presented (Aalderink, 2005). The mentioned monitoring system uses a diode laser to illuminate the welding process combined with an interference optical filter and a CMOS camera. In this method, the camera is not over radiated by the emissions of the sample material. The used camera system is a CCAM CCf_{1000} system, which contains a silicon based Fuga 1000 CMOS chip. A CMOS chip is quite favourable for such applications depending on visualization of images containing large intensity differences under the favour of the CMOS sensor's large dynamic range.

2.3.2 PSD Sensors

(PSD) is an optical sensor which is utilized for determination of the centroid location of the intensity distribution on the sensor in one or two dimensions. PSD is an analogue device and provides high sensitivity, short response time, and independency from spot light size, shape, and intensity (Hou, 2011). It is a useful element for real time measurements of position, displacement, and vibration. Compared with CCD and CMOS sensors, PSDs are more favourable with their high sensitivity, high response, and simple circuit structure. However, it is easily affected by environment stray light, and its output signal cannot be further processed like image processing of the digital signal of CCD device (Song, 2006).

A study based on the centroid determination of obstructed focused laser beam is conducted by (St. John, 2009). The laser beam investigated has a Gaussian intensity distribution and the obstruction

is a vertically oriented opaque cylinder treated as a flat hard aperture. In the study, theoretical centroid position is compared with the experimental results. Theoretical data of diffraction of the obstructed focused Gaussian laser beam is obtained by using the Huygens–Fresnel diffraction integral. The experimental setup consists of a 514 nm wavelength laser source, obstruction cylinder, and a PSD. Obstruction cylinders are precise gauge pins with diameters from 4 to 100 mm. The theory was found to agree well with experimental measurements.

Two different displacement sensor configurations based on PSD is presented and described by (Song, 2006). The sensor configurations depend on triangulation method for displacement measurements. Determination of the dimension, sensing resolution, and comparison of the two different configurations are presented in the study. The factors affecting the performance of the laser displacement sensor were discussed and two methods, which can eliminate the affection of dark current and environment light, are proposed. The displacement sensor configurations proposed in the study are given in Figure 2.1.

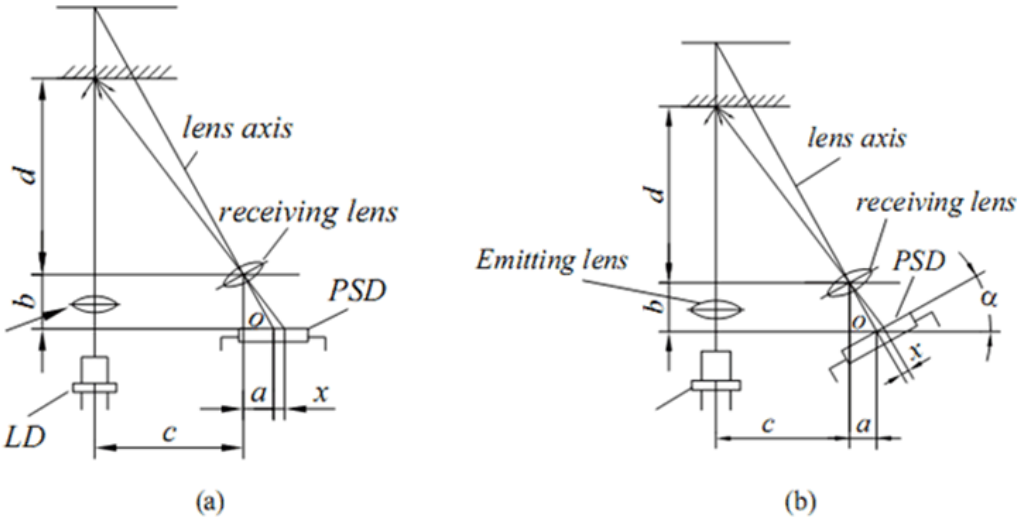

Figure 2.1: Configurations of PSD based laser displacement sensor (Song, 2006).

In the first configuration given as Figure 2.1 (a), PSD is parallel to the emitting lens. In the second configuration given as Figure 2.1 (b), PSD is parallel to the receiving lens. The aim in both configurations is to determine the parameter “d”.

2.4 Position Detection Algorithms

Centroid estimation algorithms are used in digital imaging to locate target images with subpixel accuracy (Welch, 1993). There are two tasks to be performed in the process of computing the subpixel locations of target images: recognition and location. The detection of the target images is required to unambiguously identify targets within a scene. The location of the target image is

generally a second process which precisely and accurately determines the target image center within the digital image frame (Shortis, 1994).

Centroid calculation algorithms are commonly used for laser position detection applications. The basic ones are average of perimeter method, binary centroid method, center of gravity method, weighted center of gravity method, Gaussian fit method. In addition to these centroid calculation methods, some pre-processing methods like threshold removal and blob testing are performed together with one of the mentioned centroid calculation algorithms.

2.4.1 Average of Perimeter Method

This method takes the average of the perimeter of the target image determined by using a pre-determined threshold (Shortis, 1994). The equation is given by

$$\bar{x} = \frac{1}{n} \cdot \sum_{i=1}^{n} x_i \tag{2.1}$$

where x_i is the x coordinate of ith pixel; n is the number of coordinates; and $\bar{x}$ is the subpixel centroid location of the target image.

2.4.2 Binary Centroid Method

In this method, intensity values of the pixels which are above the pre-determined threshold value are taken as one and the others are assumed to be zero. (Shortis, 1994). The equation is given by

$$\bar{x} = \frac{\sum_{i=1}^{n} i \cdot I_i}{\sum_{i=1}^{n} I_i} \tag{2.2}$$

where I_i is one or zero depending on the threshold and intensity value at pixel location with index number *i*.

2.4.3 Center of Gravity Method

In this method, intensity value of each pixel is multiplied by the pixel position before divided by the total intensity (Vyas, 2009). The equation is given by

$$\overline{x} = \frac{\sum_{i=1}^{n} x_i \cdot I_i}{\sum_{i=1}^{n} I_i} \tag{2.3}$$

where I_i is the intensity value of the i[th] pixel and x_i is the position of i[th] pixel. A modified version of this method named as squared center of gravity is obtained by taking the squares of the intensity values in the equation.

2.4.4 Weighted Center of Gravity Method

This method depends on the multiplication of the numerator of Equation (2.3) by a weighting function (Vyas, 2009). The related equation appears as

$$\overline{x} = \frac{\sum_{i=1}^{n} x_i \cdot I_i \cdot W_i}{\sum_{i=1}^{n} I_i} \tag{2.4}$$

where W_i is the weight for the i[th] pixel. In laser applications, laser spots generally have a Gaussian intensity distribution. Then, the weighting function can be written as follows:

$$W(x) = \exp\left(-\frac{(x-\overline{x})^2}{2\sigma^2} \right) \tag{2.5}$$

This method has an advantage over center of gravity when the Gaussian spot shape is maintained and if the spot does not shift by a large amount from the image center. It is disadvantageous and sometimes even useless in the presence of strong noise background or even in conditions of barely few photons. Since the weighting function in Equation (2.5) depends on the position of the centroid and the spot size which is not under control, and an iterative process should be followed. As an initial guess, the image center is taken as the centroid estimate and one quarter of the image length is taken as the spot width. In the iterations, spread in the spot and the position of the centroid are progressively corrected after every iteration (Vyas, 2009).

2.4.5 Gaussian Fit Method

An idea for determining the centroid of an intensity distribution which is close to a Gaussian form is to fit a Gaussian curve on the distribution and take the peak position as the centroid (Jukic, 2005). Form of a Gaussian distribution is represented by

$$f\left(x,K,\sigma,\mu\right)=K\cdot\exp\left(-\frac{\left(x-\mu\right)^2}{2\sigma^2}\right) \tag{2.6}$$

Parameters K and μ represent the maximum peak height and its position, respectively. σ is related to width of the distribution.

2.5 Closure

In this chapter, the background knowledge about the laser sensing, laser positioning, and laser calibration related subjects are presented. For this purpose, these subjects are divided into three groups as *types of laser sources*, *laser sensing devices*, and *position detection algorithms*. Several types of laser sources and some related applications of these types are given in the first group. The second group includes the three basic laser sensing devices (CCD, CMOS, and PSD) and the studies conducted by utilizing these devices. In the third group, several centroid calculation methods for position detection depending on digital image data are presented.

CHAPTER 3

LASER BEAM POSITIONING SYSTEM (LBPS)

3.1 Introduction

The laser beam positioning system is a commercial laser projection device developed and manufactured by MODESIS Machine Technologies Company in METU Technopolis. This device is used in visual inspection applications in industry. It generates planar laser beams which form laser lines on the target surface. A photo of one of the commercial models is given in the following figure.

Figure 3.1: A photo of the laser beam positioning system (Model No: 2SH1S – 1800)

The basic application of this system is the visual inspection for operators during tire manufacturing. In tire production, operators should take plenty of measurements on the layers of the tire. This process is quite time consuming and tedious work without such a system. The laser beam projection system generates reference laser lines at different operation locations on the tire at each step of the manufacturing.

In this chapter, general structure and working principles of this laser system are described. Structural components and their functions are also included. System parameters and the required tolerances for translational and angular errors of the laser lines on the projection surface and the laser beams exiting from the laser positioning system are explained.

3.2 General Structure and Working Principles of LBPS

The laser beam positioning system which is used in visual inspection applications in industry generates planar laser beams which are parallel to each other. These laser beams are perpendicular to projection surface. Moreover, the laser lines obtained on the projection surface are moved and positioned along a translation axis which is perpendicular to these lines. In Figure 3.2 a schematic view of these laser lines is seen.

The laser beams exiting from laser positioning system are projected on working surface. The center laser source is stationary and the outer laser sources are positioned symmetrically on the projection surface along a translational axis which is perpendicular to the parallel laser lines on the surface. The aim of this system is to show the pre-determined symmetrical working locations on the surface to the operator with a high precision. Thus, the operator gets rid of the necessity of taking a lot of symmetrical measurements along a distance sometimes reaching to about 2 meters. Using this system enhances the product quality and production speed substantially.

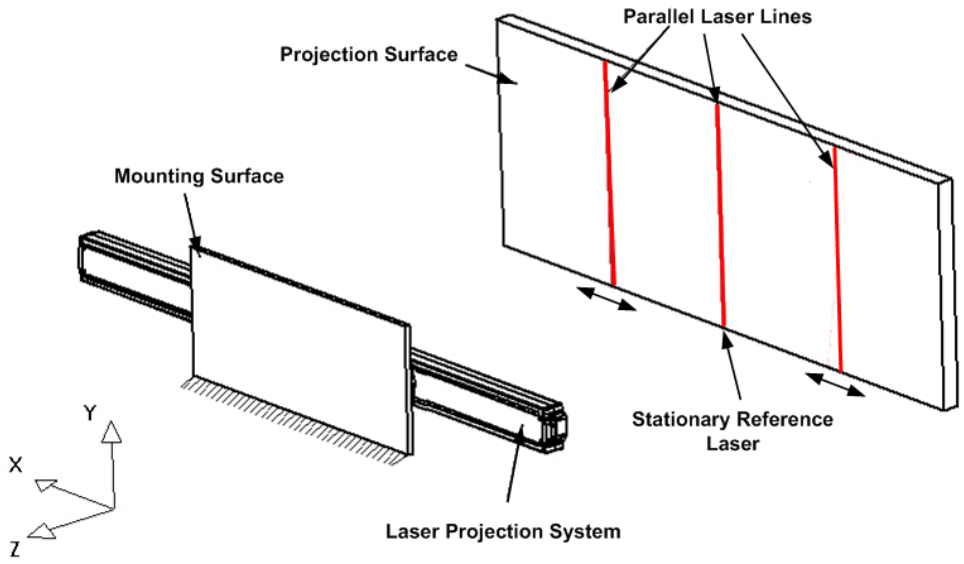

Figure 3.2: A schematic view of laser lines produced by laser positioning system

The axis designation is also given on Figure 3.2. Throughout this thesis work, this coordinate designation is used. According to this presentation, x-axis is the translation axis of the laser sources, y-axis is the axis along the laser lines, and z-axis is the axis along the laser beams.

Laser beam positioning system consists of several main parts. These are outer casing, positioning system, laser sources, adjustment mechanisms of laser sources, and electronic control system.

3.2.1 Outer Casing

One of the most important parts of the laser positioning system is outer casing. It is designed and manufactured according to industrial requirements such as facing, structural strength, corrosion resistance, and electrical properties. Each casing consists of two parts as upper and lower ones. Upper and lower parts of the casing are mounted by means of countersunk screws. And also, a circular cross section sealing plastic material is used between them. Under the favor of constant cross section of the casing throughout the length, the casing is produced by means of aluminum extrusion method with aluminum alloy 6061 T5. Thus, a low cost, light weight, and rigid casing structure is obtained. In Figure 3.3 the cross section of the outer casing is given.

As can be seen from Figure 3.2, dimensions of the outer casing cross section are 140 × 80 mm. The length of the casing changes according to the maximum positioning distance of the laser system. As standard dimensions, there are five different models with respect to maximum "positioning distance" (i.e. the distance between the movable laser lines on the right and left sides of the center laser line). These are 800 mm, 1200 mm, 1600 mm, 1800 mm, and 2000 mm. The weight of the overall system is less than 30 kg for the longest model. In Figure 3.1, an assembled casing of laser beam positioning system is seen.

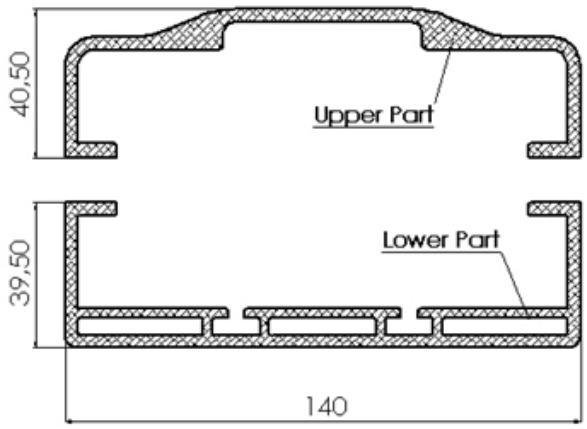

Figure 3.3: Cross section of lower and upper parts of the outer casing

There are also two adjustable mounting feet assembled to the outer casing. These parts are used to mount the system to the location where it will be used in the factory. A view of one of these two mounting feet is given in Figure 3.4.

As can be seen on Figure 3.4, the casing has slots on the back surface. The feet can slide along these slots and can be fixed where it is necessary. This makes it quite easy to mount the casing to the place where it will be used. In addition to the translational adjustment of the mounting feet

along the casing, it is also possible to adjust the laser system with an angular manner around the same axis. This also makes it possible to adjust the angular orientation of the casing between 0° and 45°.

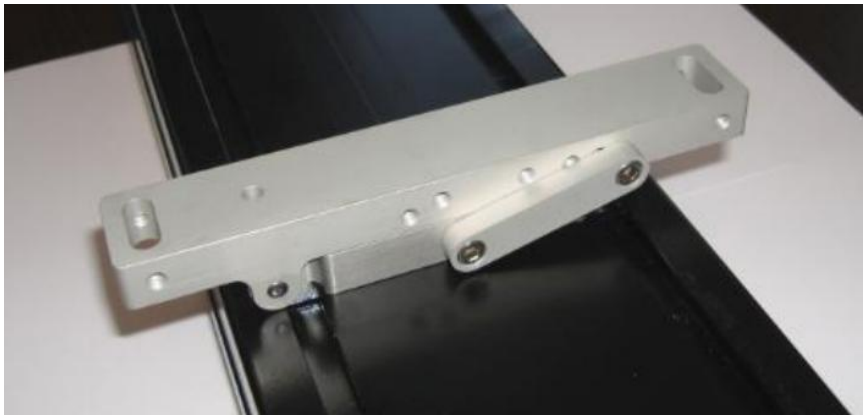

Figure 3.4: Laser beam positioning system mounting foot assembly

Another important point about the outer casing is environmental effects on the system. The outer casing must fulfill the requirements related to industrial environment for water contact and dust problem. Hence, for power and serial communication, high safety industrial connectors are used on the casing. Moreover, outer casing must have a high resistance to effects it can be subjected in industrial environment such as heat, moisture, and chemicals. For this reason, the casing is exposed to chemical coating which is followed by electrostatic painting.

Depending on cross sectional area and the length, the outer casing is prone to be subjected to distortions in time. Mounting of the system on its working place also causes distortions. For this reason, laser positioning system has a special internal structure on which the positioning of the laser sources is carried out.

3.2.2 Positioning System

Positioning system is an internal structure which provides the required positioning of the laser sources with the desired accuracy. Positioning accuracy and the resistance to the angular errors are determined by this structure. Positioning system consists of three main element groups which are linear positioning, power transmission, and position control elements.

3.4.1.1 Linear Positioning Elements

Linear positioning elements are the machine elements providing the translation of the laser sources along the same axis of motion with minimum translational and angular errors. These elements are

laser positioning chassis, linear guideway, and carriages. In Figure 3.5, linear positioning elements assembled to outer casing (without upper cover part) is given.

Figure 3.5: Laser positioning chassis, linear guideway, and carriages mounted to outer casing

Laser positioning chassis seen on Figure 3.5 is an L-shaped special aluminum structure. The vertical face is precisely ground and used for precise mounting of linear guideway. Geometrical problems on this surface cause angular error on the laser beams along their movement range. As a result, the positions of the laser lines on the projection surface may exceed the tolerance limits. The horizontal surface is used for special mounting of positioning system to the outer casing. This mounting prevents the precise internal structure from the distortions of outer casing.

Linear guideways are the elements providing the precise linear motion of the carriages on which the laser sources are mounted. A guideway and carriage assembly with critical reference plane indications is given in Figure 3.6.

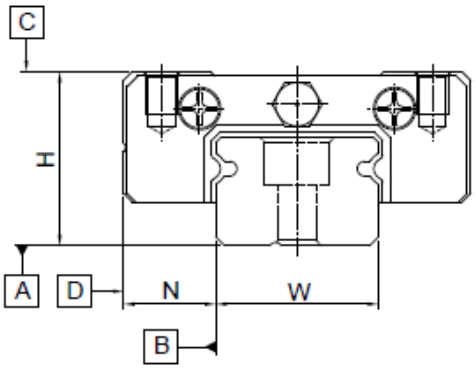

Figure 3.6: Linear guideway (rail) and carriage assembly with indicated reference planes (Hiwin, 2012)

One of the main sources of the angular errors is the linear guideway and carriage assembly shown in Figure 3.6. There are two types of errors caused by linear guideway and carriages. These are the

angular errors caused by the clearance of the linear guideway and carriage assembly and the angular errors caused by the running parallelism of this assembly. For this reason, preloaded precision class linear guideways are used in the laser positioning system. Preloaded rail and carriage assembly comes from the manufacturer as coupled and mounted. By this way minimum clearance between the rail and carriage is provided. Using precision class guideways minimizes the running parallelism errors along the rail. Running parallelism accuracy between surfaces A and C and between B and D (Figure 3.6) is 2 μm for a rail segment shorter than 50 mm (Hiwin, 2012).

3.4.1.2 Power Transmission Elements

Linear motion of the laser sources is derived by a stepper motor. Power transmission elements provide the translation of the moving elements by transferring the motor torque to these elements. A timing belt and pulley mechanism is used for this purpose. In Figure 3.7 a schematic view of this system is illustrated.

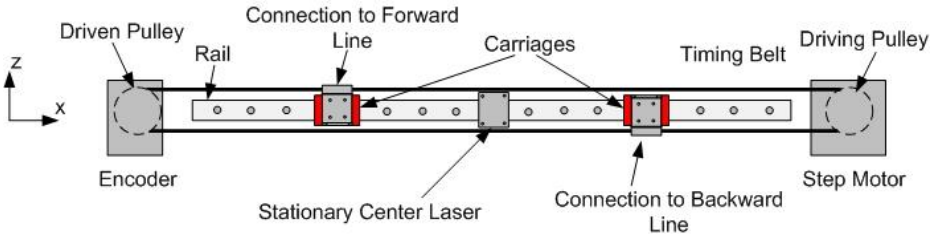

Figure 3.7: A schematic view of the power transmission system

In the laser beam positioning system the two movable laser sources on the right and left sides of the stationary center laser translates along the rail symmetrically. In order to obtain this symmetric motion with respect to center laser, one of the carriages is connected to the forward line of the timing belt and the other one is connected to the backward line with respect to the driving pulley (Figure 3.7). Thus, the counterclockwise rotation of the step motor provides an increasing action for the distance between the movable lasers and similarly clockwise rotation does the opposite.

3.4.1.3 Position Control Elements

Position control elements consist of a stepper motor and a rotary encoder which is able to read the instantaneous position of the laser sources.

In the laser beam positioning system, the load profile is constant throughout the application. Moreover, there is no need for a path generation. Instead of it, only the last position has to be controlled. Under these conditions, a stepper motor satisfies the system driving requirements.

3.2.3 Laser Sources

In the laser beam positioning system, continuous wave uniform line generator semiconductor diode lasers with 635 nm wavelength and 1 mW exit power are used. An outer view of the laser sources used in the system is given in Figure 3.8.

Figure 3.8: Uniform line generator diode laser sources (Diode Laser Concepts, 2012)

These sources generate uniformly distributed laser lines on the projection surface. A schematic view of line generation is shown in Figure 3.9.

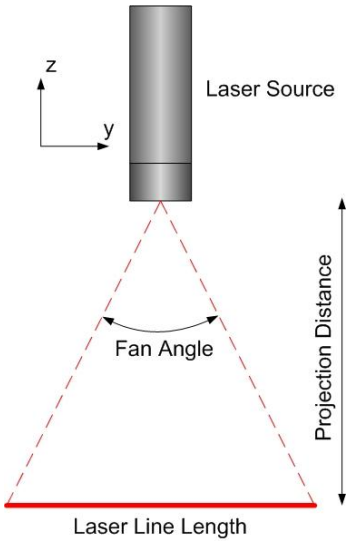

Figure 3.9: A schematic view of line generation

As can be seen from Figure 3.9, line length is determined by the exit fan angle and the projection distance. Several alternatives for the fan angle and line width are presented by Diode Laser Concepts Inc. company. A fan angle of 45º is used in the system. Line width is 0.6 mm at 1.5 m projection distance and has a divergence of 0.5 mrad. This means that line width is focused at 1.5 m distance and it is thicker than 0.6 mm for any projection distance which is less or greater than 1.5 m.

Pointing accuracy of the laser sources is less than 2 mrad. This value is the parallelism of the laser beam with the laser casing. Stability of the laser under temperature changes is given as less than 10 µrad/.

Due to the alignment problems of the lens assemblies of the line generators, generated laser lines are not perfectly straight. They have a curvature shape instead. This problem causes straightness problem on the projected laser lines. That problem also results in position error on the projection surface. In order to prevent this problem, line generators are ordered as special straightness specifications. Moreover, laser sources are inspected first and then, mounted to the laser positioning system by coupling their curvature side and magnitude. For example, three laser sources having the same straightness error are mounted together.

The generated lines have a Gaussian distribution along the section of line width. On the other hand, light strength is almost constant along the line length. This condition is illustrated in Figure 3.10.

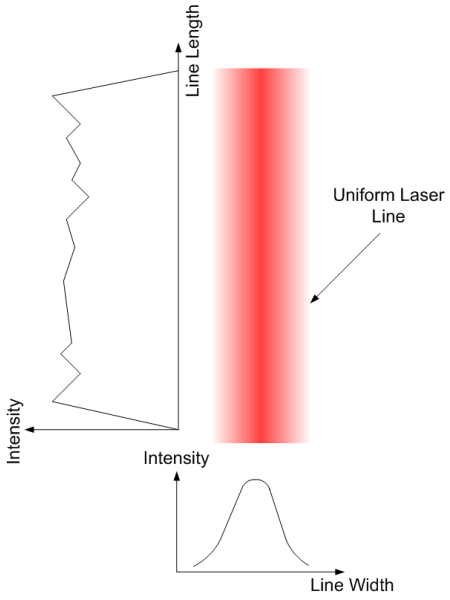

Figure 3.10: Laser intensity distribution

Line uniformity along the laser line length seen in Figure 3.10 is 20 % for 80 % portion of the line. Figure 3.11 shows the uniformity of the generated line along the line length in a schematic fashion. This property given in Figure 3.11 gives the name of *uniform line generator* to this laser sources.

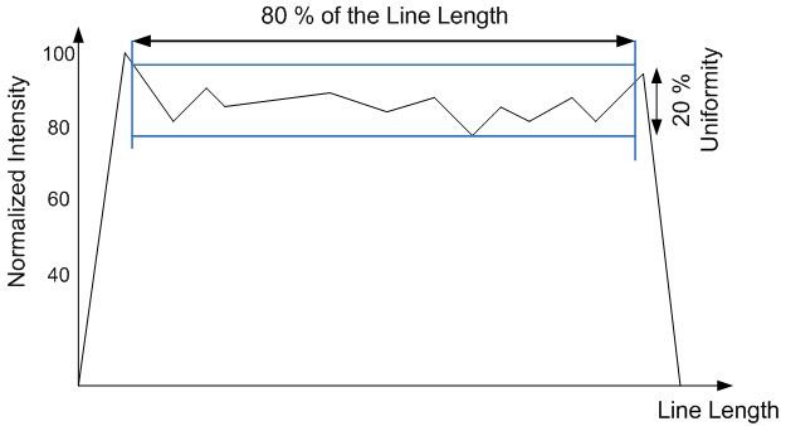

Figure 3.11: Laser line uniformity along the line length

3.2.4 Adjustment Mechanisms of Laser Sources

In addition to positioning error of the laser sources, angular error of the laser beam with respect to the normal of the mounting surface and the angular error of the laser line on the projection surface with respect to the translation axis are the other error sources affecting the laser line position accuracy on the projection surface.

The first angular error is the laser beam exit angle error. For an ideal system, laser beam is expected to be along the same direction with the normal of the mounting surface. A schematic view of the laser beam exit angle is shown in Figure 3.12.

As can be seen from Figure 3.12, exit angle error of the laser beam causes the laser line on the projection surface to be deflected towards right or left depending on the direction of the angle.

Since the pointing accuracy of the laser sources can reach up to 2 mrad, without an adjustment mechanism, laser beam cannot be directed precisely even if the outer casing of the laser source is perfectly mounted to the system. For this reason, exit angle of each laser beam is adjusted by means of setscrews assembled with the laser mountings.

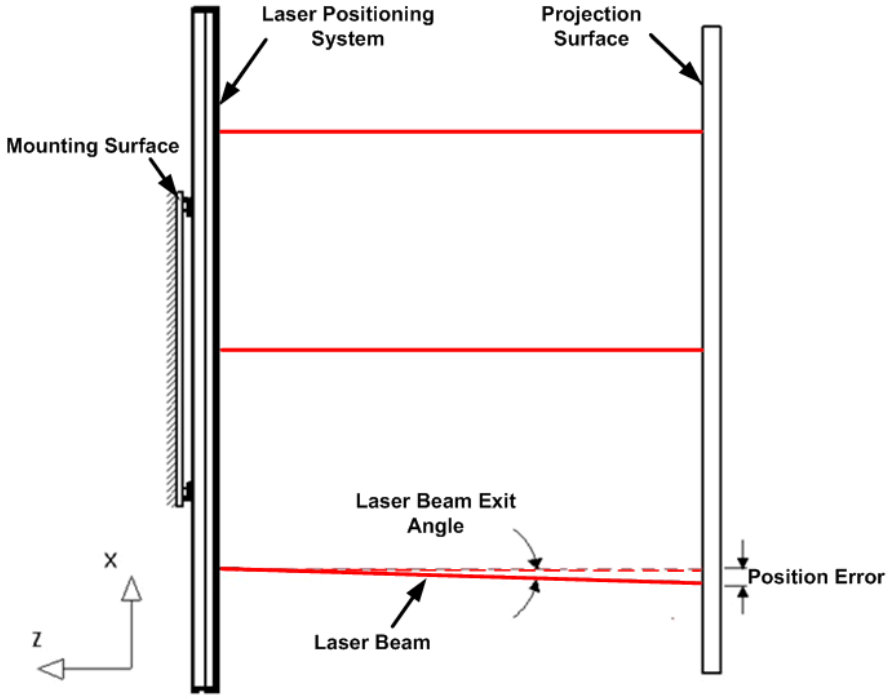

Figure 3.12: A schematic view of the laser beam exit angle

The second angular error is the laser line angle error on the projection surface. Precise positioning of the midpoint of the laser line is not enough for the position accuracy of the whole laser line. Rotation of the laser line around its midpoint causes an angular error between the laser line and the translation axis of the laser lines. Figure 3.13 shows the schematic representation of the laser line angle on the projection surface.

The laser line should be perpendicular to translation axis of the lines (x-axis on Figure 3.13). The effect of the laser line angle error on the position accuracy of the laser line increases with the line length.

On the laser mountings, there is a special mechanism providing precise adjustment of the laser lines. This mechanism provides the rotation of the laser source around z-axis on Figure 3.13 with a 1/500 rotation reduction. In other words, one rotation of the setscrew on the mechanism provides 1/500 of full rotation of the laser line. Thus, it enables to adjust the line angle precisely.

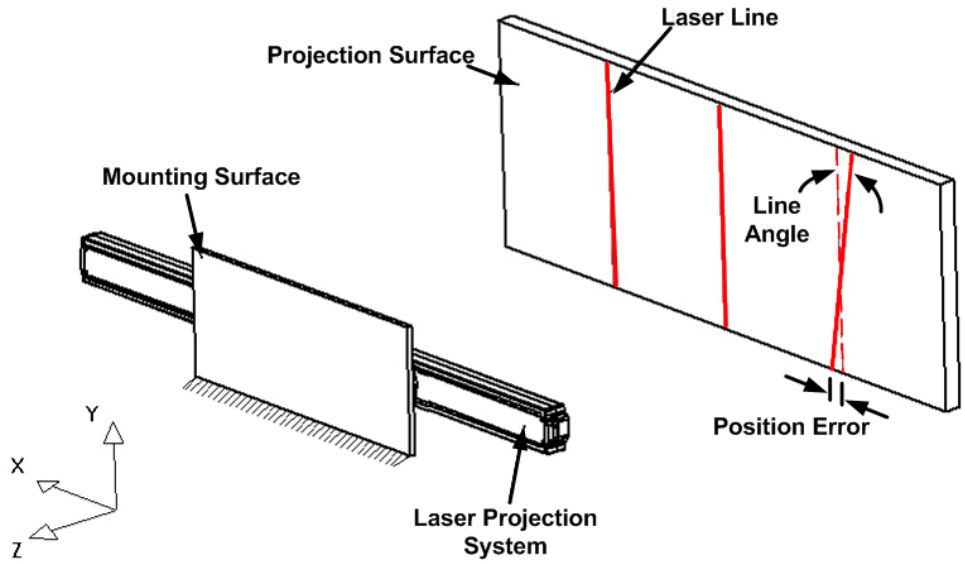

Figure 3.13: A schematic view of laser line angle on the projection surface

3.2.5 Electronic Control System

Electronic control system consists of a main control card, an encoder card, four connection cards, and embedded system software. Data exchange, processing of the received data, precise positioning of the motor, and control of the laser sources are carried out by the control system. The main control card of the system is given in Figure 3.14. On the main control card, Microchip dsPIC30F6015 is utilized as the micro controller.

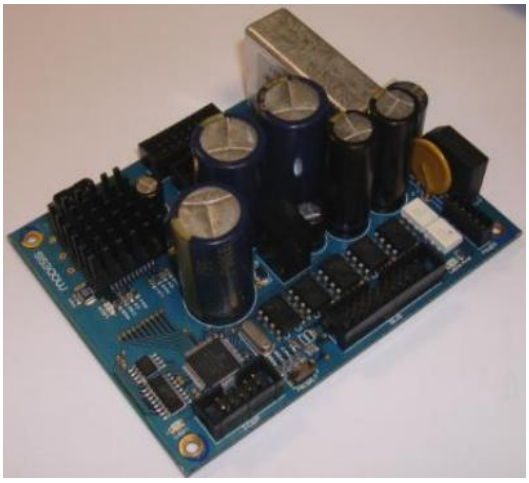

Figure 3.14: Main control card of the system

For the flexibility of the communication with the system on different automation solutions, there are parallel, RS232, and RS485 communication interfaces on the main control card. System also satisfies industrial safety regulations like high voltage protection, low voltage protection, and EMC filtering up to certain levels. Moreover, the main control card has the property of 8x micro stepping, high speed encoder interface, and laser controller.

3.3 System Requirements of LBPS

There are several error components determining the positioning of the laser line on the projection surface. These are positioning error of laser sources, exit angle error of the laser beams, and angle error of the projection lines. Positioning error of the laser sources and beam exit angle error determines the positioning accuracy at the middle of the laser line on the projection surface. Line angle error together with positioning error of laser source and beam exit angle determines the positioning accuracy at the tips of the laser line on the projection surface. All these parameters are with respect to the stationary center laser.

The positioning error of the laser sources is caused by several parameters like timing belt inaccuracies and pulley run-out. Laser source positioning error does not change with projection distance.

The laser beam exit angle error is caused by mounting error of the laser source, mounting error of the linear guideway, clearance between carriage and the guideway, and running parallelism of the guideway. Laser beam exit angle error increases with the projection distance.

Considering these error components, MODESIS Machine Technologies Company defines the tolerance bands under a reference condition which is given as 1.5 m projection distance and 1.0 m (±500 mm from the center) part of the laser line. Although the laser line length on the projection surface at projection distance of 1.5 m is 1.2 m, only 1.0 m of this line is under consideration for this reference condition. The mentioned reference case is given in the following figure.

Tolerance bands on the projection plane for this reference condition are defined for center of the laser line and tip points of the laser lines. Laser positioning error tolerance at the center of the laser line is required to be under 0.3 mm. Moreover, that is to be 0.5 mm at the tip points. The two components of the position error at the center caused positioning error of the laser source and beam exit angle error are required to be less than 0.1 mm and 0.2 mm, respectively. In addition to these components, the other laser position error component at the laser tip points is laser line angle error which is given in Figure 3.13. The defined tolerance for this component is 0.2 mm in the reference condition. Tolerance definitions for the error components are summarized in Table 3.1.

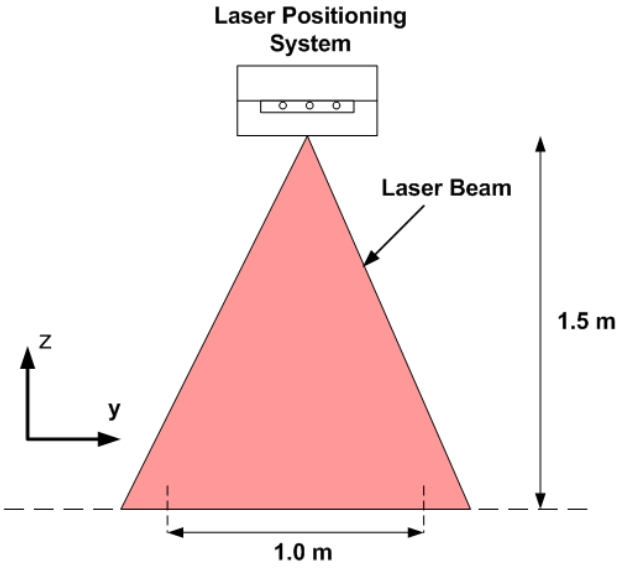

Figure 3.15: Reference condition for the accuracy parameters

Table 3.1: Error components and their contributions under the reference condition

Location	Positioning	Exit angle	Line angle	Total
Line Center	0.1 mm	27.5 arcsec (0.2 mm/1.5 m)	--	0.3 mm
Line Tip	0.1 mm	27.5 arcsec (0.2 mm/1.5 m)	82.5 arcsec (0.2 mm/0.5 m)	0.5 mm

Considering the accuracy requirements given in Table 3.1, 0.10 mm of 0.30 mm tolerance band at line center for 1.5 m of projection distance is laser source position error and the remaining 0.20 mm is the position error caused by laser beam exit angle error. Similarly, considering a projection distance of 4.0 m, 0.15 mm of 0.75 mm at 4 m of projection distance is again laser source positioning error since it does not change with projection distance. However, position error at the middle of the laser line on the projection surface increases to 0.53 mm with the same beam exit angle error which is 27,5 arcsec. Contributions of laser beam exit angle error and laser source position error to total laser position error is illustrated in Figure 3.16.

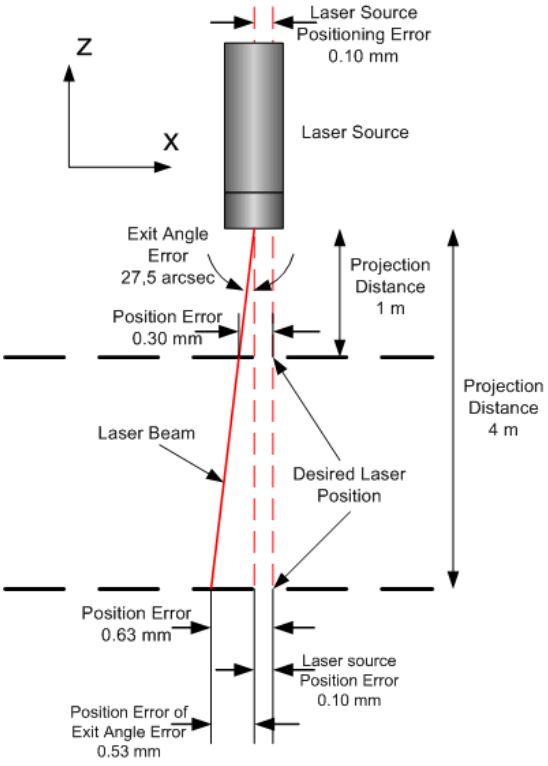

Figure 3.16: Illustration of laser position (kinematic) error components

Figure 3.16 shows that the laser source position error is independent from the projection distance. On the other hand, since there is an offset between the adjustment axis and the functional axis (projection surface), position error caused by exit angle error increases with the projection distance. Considering the parameters like running parallelism of the rail, mounting inaccuracies of the carriage-rail assembly, and thermal factors, it is seen that to remain the exit angle error less than 27,5 arcsec requires special measuring and adjustment methods together with a proper mechanical structure of the laser system. For example, only the angular displacement of the carriage due to the running parallelism of 2 µm between the surfaces B and D (Figure 3.6) may cause the exit angle error to deviate about 20 arcsec. To sum up, measurement and adjustment of the angular and translational errors of the laser beam has a vital importance for laser beam positioning system.

3.4 Closure

In this chapter, Laser beam positioning system is presented in detail. Functions and working principle of the system are explained. General mechanical and electronic structure of the system is given by explaining the subsystems and their components. The error sources and their contributions to the resultant position error are clarified. It is shown that the error sources may divided into two components basically. These are translational and angular errors. Translational errors are caused by inaccurate positioning of the laser sources. This component can be minimized with a special care on power transmission system and positioning software. On the other hand,

since the angular errors increase with the projection surface offset, very small angular measurements and adjustments should be handled.

CHAPTER 4

CALIBRATION SETUP

4.1 Introduction

In this part of the thesis, the development of the calibration setup is to be elaborated step by step. For this purpose, problem to be solved about the requirements of the laser beam positioning system given in Chapter 3 is defined and related design specifications are determined. After this step, a conceptual design procedure is followed. Design alternatives for several parameters are determined and evaluated at this stage. Moreover, four different concepts for the overall system are generated and evaluated according to several design parameters. Consequently, the detailed design of the calibration system is started. In detailed design stage, the system which is desired to be manufactured is specified and engineering calculations about several parts are conducted. Finally, methods, applications, and relevant technologies followed during the manufacturing and assembling procedure of the setup are explained.

4.2 Problem Definition and Design Specifications

Laser beam positioning system explained in Chapter 3 with its details provides precise laser lines on the projection surface. Ideally, the system generates three parallel laser beams. These beams form three ideally parallel laser lines on the surface to which they are projected. The laser lines on the right and left sides of the stationary center laser line moves symmetrically with respect to center laser line. As explained in Section *3.3 System Requirements of LBPS*, laser sources should be positioned with ± 0.1 mm accuracy. Moreover, laser beams should remain inside ± 27.5 arcsec angular envelope throughout the movement range of the laser sources according to beam exit angle parameter. The last accuracy requirement introduced in *3.3 System Requirements of LBPS* is angular tolerance of ± 82.5 arcsec for laser line on the projection plane. For this reason, position and angular errors along the translation ranges should be measured, optimized, and adjusted accordingly.

The setup to be designed for this purpose must measure the following properties:

- Straightness of all three laser lines,
- Center laser beam exit angle,
- Center laser line position and angle on the projection plane,
- Exit angles of movable laser beams throughout their translation axis,
- Positions and angles of the movable laser lines on the projection plane.

In order to make these measurements within the given tolerances, the designed system must satisfy the following specifications:

- Measurement range along x-axis: 1600 mm,
- Measurement range along y-axis: 600 mm,
- Translational speed along both axes: 300 mm/sec,
- Acceleration and deceleration time (for 0 - 300 mm/sec): 0.1 sec,
- Laser source position measurement tolerance: ±20 μm,
- Laser projection line angle measurement tolerance: ±8 arcsec,
- Laser beam exit angle measurement tolerance: ±3 arcsec.

There are two main alternatives for laser line detection methods. The first one is to project the laser beams on a surface, to take images of the laser lines on the surface by optical means, and to determine the laser positions via image processing techniques. The second method is to position the laser detecting sensor precisely, to direct the laser beams to the sensor plane, and to determine the laser line positions by moving the sensor on the projection surface. Since the determination of the laser detection method changes all other design alternatives, it should be determined before the conceptual design.

In the first alternative shown in Figure 4.1, the laser beams are directed to a surface and the image of the surface is taken by several cameras with some optics. Images obtained in this method include some distortion problems since a wide area is imaged with a small sensor area by means of some optics. These distortions cause position problems to be handled. Another problem with this alternative is the measurement of the laser beam exit angle. It is not possible to decouple the laser source positioning error and laser beam exit angle in a calibration set up with stationary projection surface in this configuration. It may be possible to identify the beam exit angle by translating the projection surface along z-axis.

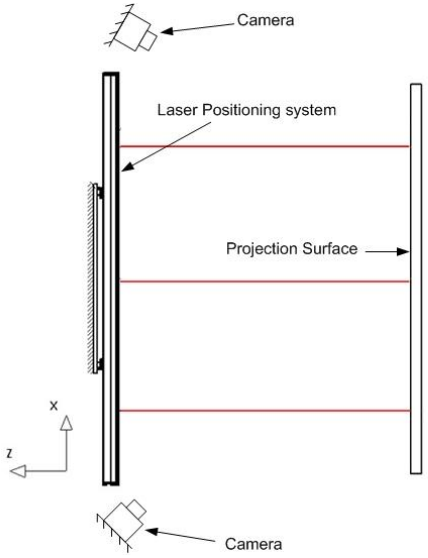

Figure 4.1: First alternative for laser line detection method

In the second alternative (Figure 4.2), the laser line is directed on the sensor. Position of the laser segment on the sensor can be detected precisely in this method. The problem of this alternative is the determination of the position of the sensor. As long as the position of the sensor is set and measure precisely, it is possible to perform relatively accurate measurements. Measurement of the laser beam exit angle can be performed by using camera positioning along different elevations in this alternative.

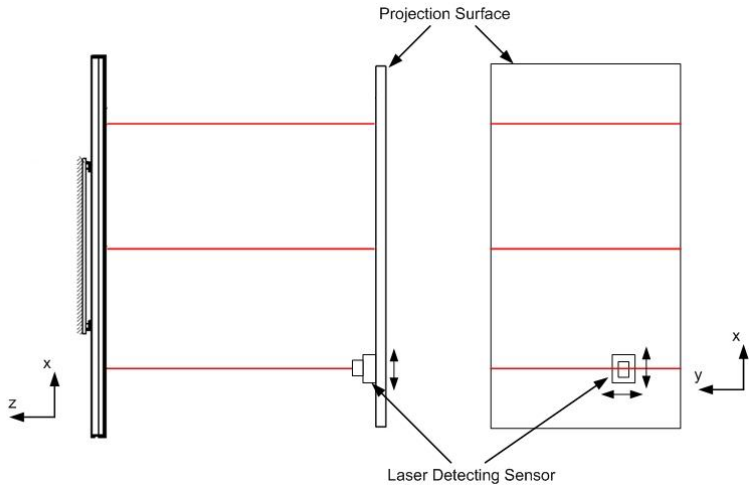

Figure 4.2: Second alternative for laser line detection method

Due to the optical distortions on the laser position which should be handled further and laser beam exit angle measurement problems of the first alternative, the second alternative is considered to be more applicable, cost effective and more suitable to obtain the required accuracy. Thus, the conceptual design is carried out according to how accurately the sensor can be positioned and how much laser position detection accuracy can be obtained by a sensor.

4.3 Conceptual Design

Before the detailed design, a conceptual design procedure should be conducted to determine the most suitable system components and methods. Conceptual design of the calibration system consists of generation and evaluation of the design alternatives depending on several aspects.

4.3.1 Concept Development

In this concept development part, design alternatives for different system components and different methods for the tasks to be performed are presented. Advantages and disadvantages of each alternative are also introduced.

4.3.1.1 Laser Detection Device

The system which is desired to be calibrated generates laser lines which are originated from semiconductor laser diodes. Properties of the laser are given in Section *3.2.3 Laser Sources* in detail.

There are four alternatives for laser detection device of the calibration system. These are CCD cameras, CMOS cameras, laser beam profilers, and PSD sensor. Background information about the CCD, CMOS, and PSD sensors are given in Chapter 2. Beam profilers are CCD or CMOS based laser sensing devices with special software support for determination of several laser properties.

CCD cameras are imaging devices using CCD sensors for light sensing detectors. These devices have high light sensitivity. They provide bright and clear view together with stable image quality. In addition to these, CCD cameras are affected from background noise less. Beside these advantages CCD cameras suffer from low saturation limits (Hanumolu, 2001).

CMOS cameras use CMOS sensors for imaging. The most significant advantage of CMOS cameras is the high saturation limits. However, these cameras are less sensitive and they are affected by the noise more than other alternatives (Hanumolu, 2001).

Beam profilers are special purpose devices for determining several laser quality parameters. They present special hardware and software for this purpose. Although these devices provide position data of the laser quite precisely, since they are capable of measuring different laser parameters, they are quite expensive. They cost a few thousands American dollars (Edmund, 2012).

PSD sensors are analogue devices generating the centroid of the light intensity distribution falling on its surface by means of simply the ratio of the voltages at the edges. PSD sensors have futures of high sensitivity, high response, and simple circuitry requirements. However, they are easily affected by the background light and their output signal cannot be further processed like image processing in CCD sensors (Song, 2006).

4.3.1.2 Laser Power Attenuation Method for the Laser Sensor

When using a digital laser detecting sensor, it is essential to perform attenuation to the incident power to prevent the sensor cells from damage and saturation. For this purpose three types of optical alternatives exist. These are beam splitters, absorptive neutral density filters, and reflective density filters.

Beam splitters are optical elements splitting incident light into two. A schematic view of the working principle of beam splitters is shown in Figure 4.3. It is possible to use such an element to decrease the transmitted laser power. Although they can be quite precise, this is a rather expensive solution. Although, there are plenty of beam splitter types, a moderate non-polarizing beam splitter may cost about € 200-300 (Newport, 2012).

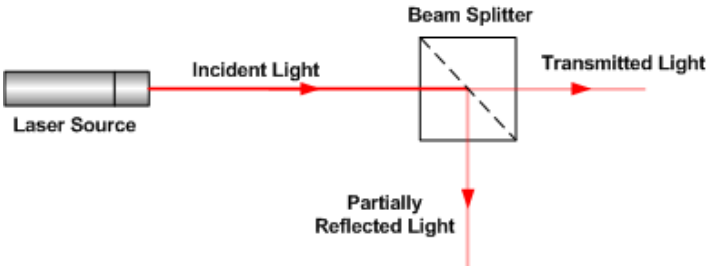

Figure 4.3: Schematic representation of a beam splitter

Neutral density (ND) filters are optical parts which are capable of providing quite high attenuation to the light passing through them. They are divided into two groups according to their light power attenuation technique. These are reflective and absorptive type ND filters.

Reflective type ND filters transmits some portion of the light while reflecting the remaining. Working principle of this type of ND filters is given in Figure 4.4 (a). There is a metallic layer on the surface of reflective ND filters for reflective action. Roughness of the film directly influences the uniformity of the laser. That may results in accuracy problems on the laser position determination.

Absorptive type ND filters attenuate the incident light power by absorbing a certain portion of the power (Figure 4.4 (b)). It is possible to manufacture quite precise absorptive type ND filters. Laser light may remain almost unmodified while its power is decreased with desired amount. However, absorptive filters suffer from temperature increase due to absorbed energy.

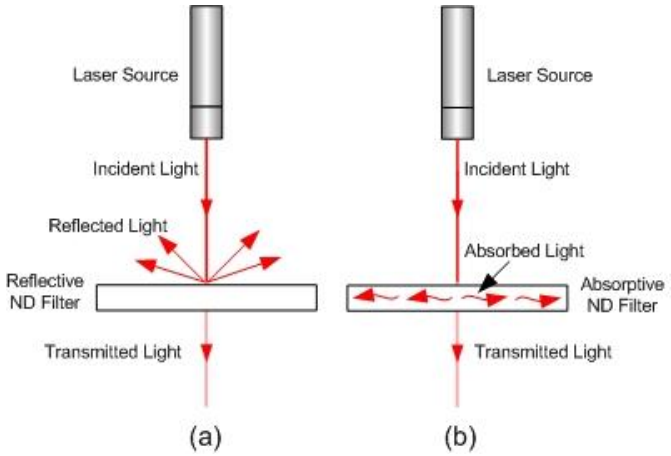

Figure 4.4: Schematic view of working principles of ND filters, (a) Reflective ND filter (b) Absorptive ND Filter

4.3.1.3 Laser Exit Angle Measurement Method

One of the most important requirements of the calibration setup is to measure the laser beam exit angle precisely. For this purpose, it is necessary to make measurements at different levels along z-axis.

There are three alternative methods for laser exit angle measurement. These are using an inclined plane with a positioning system and a single laser sensor, using two positioning systems and two sensors at two different elevations along z-axis, and using a single positioning system with two sensors at two different elevations along z-axis.

In the first alternative, a sensor is positioned on a plane which is rotated around x-axis to give an inclination along the laser lines. A schematic representation of this system is given in Figure 4.5. This alternative enables to measure the position of the laser line at different elevations along z-axis. However, since the measured segment of the line is not the same line segment at each time, decoupling the laser beam exit angle error and the projected laser line angle error is a problem for this design.

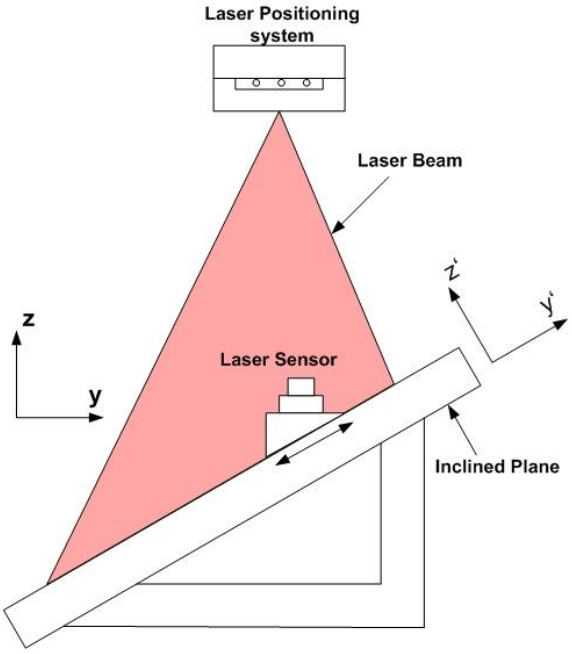

Figure 4.5: Schematic representation of "*inclined plane*" design

The second design alternative for laser exit angle measurement is to use two laser sensors which are positioning independently from each other at two elevations along z-axis. A schematic illustration is given in Figure 4.6.

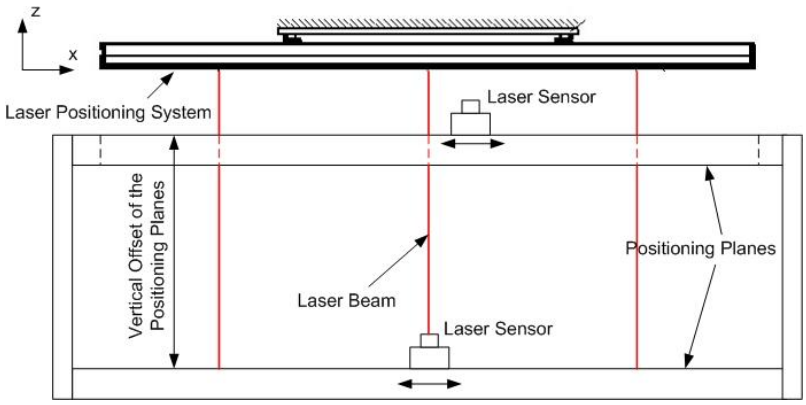

Figure 4.6: Schematic side-view of "*two positioning systems at two different elevations*" design

In the design shown in Figure 4.6, two different laser sensors are precisely positioned on two positioning planes at two different elevations along z-axis. Laser beams passes from the cavity on the upper plane without any interference. At a position, lower sensor takes snap and determine the laser position on lower plane. Consequently, the upper sensor gets to a position, takes a snapshot and determines the laser line position on the upper plane. Using the vertical offset distance of the planes and the position information of the sensors, the exit angle of the laser beam can be calculated. Since the same line segment is to be measured at each time, the exit angle can be easily decoupled other kinematic error components. An important advantage associated with this configuration is that the vertical offset between the positioning planes can be kept rather long. This simplifies measuring the exit angle by decreasing accuracy requirement of the position data. Problem with this design is the precise alignment of the upper and lower positioning systems.

The third alternative is a single positioning plane with two laser sensors at different elevations along z-axis (Figure 4.7).

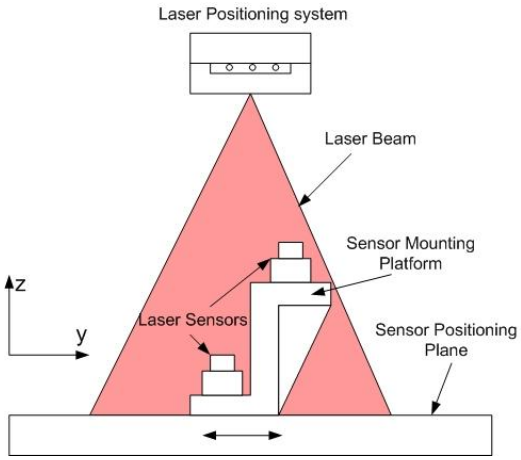

Figure 4.7: Schematic view of "*two sensors at two elevations with a single positioning system*" design

In the design shown in Figure 4.7, two sensors at two different elevations (with an offset between them along y-axis) are used. The lower sensor is positioned first, takes a snapshot, and determines the position of a laser segment on the lower sensor plane. Then, the upper camera which is positioned over the same laser segment repeats the acquisition procedure mentioned above. Using the offset distance along z-axis and the position data of the sensors, the exit angle of the laser beam can be calculated. The main challenge of this design is the sensor positioning and laser beam position sensing accuracies. A shorter z-axis offset is desirable but to shorten the offset value depends on the accuracy obtained. More precise measurements leads to a shorter z-axis offset.

4.3.1.4 Laser Projection line angle Measurement Method

One of the laser line position error components is the projection line angle error on the projection surface. There are two alternatives to measure this error. The first one is to use a 1D positioning system on which a sensor platform having multiple sensors on it is positioned. The second one is to use a single sensor with a 2D positioning system. These two design alternatives are seen on Figure 4.8.

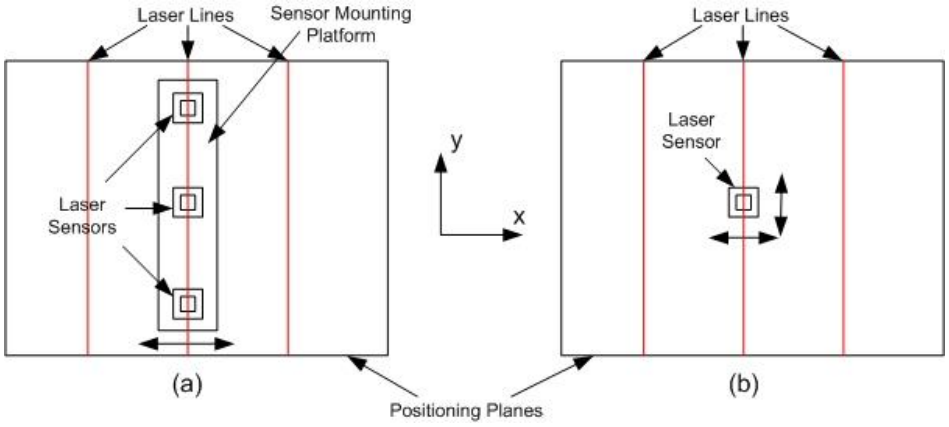

Figure 4.8: Laser line exit angle measurement methods

The first method (in Figure 4.8 (a)) which is to use multiple sensors along laser lines with a positioning system along x-axis is easier to implement. But the challenge in this method is to align each sensor with respect to each other precisely. It requires an extra sensor position calibration process. Moreover, this method gives partial information along the whole laser length. As explained in *3.2.3 Laser Sources*, laser lines have some form errors so they do not resemble perfect straight lines. Additionally, it is desirable to obtain data about the form of the laser lines. This method presents position information of limited points along y-axis.

In the second method (in Figure 4.8 (b)), a single sensor can be positioned along x-axis to measure the position of the laser lines while it is also positioned along the y-axis to measure the position of the laser lines at different locations along y-axis. In this method, it is possible to obtain the laser line form error together along with the projection line angle error. However, this method has some drawbacks. This design requires two different precise positioning systems. Furthermore, although

the extra calibration in the first alternative is not required for this case, the translation mechanism along y-axis must be manufactured with high accuracy.

4.3.1.5 Main Structure

Main structure of the calibration setup is the body on which all the positioning system elements are mounted. There are three alternatives for main structure: i) aluminum body with connection parts of sigma profiles, ii) gray cast iron body, iii) granite structure.

The first alternative aluminum body is a light weight and cheap solution. It is also easy to manufacture. However, it is affected by vibration excessively.

The second alternative gray cast iron presents a good vibration damping property and good machinability. It is also quite stable material with thermal annealing. The drawbacks of this alternative are the requirement of special casting model and mold designs and its weight problem.

The third alternative, which is based on granite, offers great material stability and good vibration absorption characteristics (Precision Granite Castings, 2012). However, it is also a bulky solution and is not easy to manufacture. Moreover, granite as a base material is more expensive than the other alternatives.

4.3.1.6 Actuator

For the actuation unit of the calibration system, three alternatives are considered. These are stepper motors, DC servo motors, and linear motors.

Stepper motors are cheaper than similar servo motors. They generate finite number of discrete steps for a single rotation. A typical four phase stepper motor can produce 200 full steps, 400 half steps, and 25,000 micro steps per revolution. This is useful for smoothness of the motion. However, stepper motors are generally open loop devices and their positioning accuracy rather poor especially when using micro stepping. Moreover, stepper motors have very poor torque characteristics at higher speeds. It is possible to improve this condition with micro stepping; however, unless the stepper is used in a closed loop mode, it does not usually perform as well as a servo (Techno Inc., 2011).

Servo motors are relatively expensive solutions compared with the stepper motors. However, they have some superiority when the requirements of the calibration system are considered. These closed loop devices can achieve the available resolution and maintain the positional accuracy. Servo motors can produce torque values two to four times that of same size stepper motors (Techno Inc, 2011)

A linear brushless servo motor consists of a stationary magnet track and a moving coil assembly (ABB, 2012). The most common type is U-channel synchronous linear motor. This type of linear motors consists of two parallel magnet tracks facing to each other with the forcer between the plates. The forcer is supported in the magnet track via a bearing system. Since there is no backlash or windup a linear motor system may have a repeatability of the encoder count (Aerotech, 2012). However, the stroke of the linear motors is limited by several hundreds of millimeters. Moreover, linear motors are relatively more expensive then the stepper and servo motors.

4.3.1.7 Linear Positioning Elements

In the calibration setup, laser detecting sensors are desired to be precisely positioned along two translational axes. To provide a precise translational motion, two alternatives are considered: i) linear polymer friction bearings, ii) linear recirculating ball bearings.

The first alternative polymer friction bearings are cheaper solutions. However, the axial clearance between the rail and the carriage (bearing) may affect the positioning accuracy of such a precise system negatively. Another disadvantage of this alternative is the high friction force which should be overcome.

The second alternative (recirculating ball bearings) has a low friction coefficient and low clearance. The price of this choice is higher than that of the polymer friction bearings.

4.3.1.8 Power Transmission

In the calibration set-up, the motor torque should be transmitted to the moving elements by means of a power transmission method. There are three design alternatives for power transmission method: i) ball screws, ii) lead screws, iii) belt-pulley mechanisms.

Ball screws are high precision power transmission elements. They offer high-positioning-accuracy motion with low friction. On the other hand, they require special end support configurations (mounting) and they are relatively expensive.

Lead screws are relatively cheaper solutions at the expense of lowered accuracy and higher friction. They are also required special end supports with bearings.

Belt-pulley mechanisms are the cheapest solutions of all offering simple mounting. However, especially for long positioning systems, belt-pulley mechanisms causes accuracy and control problems.

4.3.1.9 Linear Position Sensing Device

One of the basic ideas of the calibration setup is the precise positioning of the laser sensing devices. Two alternatives appear for this subject. One of them is to use a rotary encoder mounted to the motor shaft. The other one is to use a linear encoder along the translation axes.

Using a rotary encoder is a cheap method and it is easy to integrate to the system. However, the exact data about the position of the sensor cannot be known by the controller. Inaccuracies caused by power transmission and linear positioning element are not possible to handle.

Although the linear encoders (or linear scales) are quite expensive devices relative to rotary encoders, they perform quite high accuracy measurements. Using linear encoder requires some extra machining and mounting work.

4.3.1.10 LBPS Mounting Method

One of the important issues to be addressed about the calibration system is how the laser positioning system is to be mounted on the set-up. There are two basic design solutions behind this problem.

The first solution is to obtain a monolithic structure together with the calibration setup and the laser positioning system. In other words, mounting the laser positioning system onto a platform which is attached to the positioning system by means of some structural elements like columns provides the system to behave like a single rigid body.

The second solution is to attach the laser positioning system without any direct connection to the calibration setup. Hence, the vibrations generated in the sensor positioning system do not affect the laser sources.

The first solution requires the attachment of the laser positioning system onto a platform connected to the sensor positioning system. On the other hand, the second one mounts it without any connections to the sensor positioning system. If the vibration introduced by outside sources to the calibration system is high, the first alternative becomes more viable. However, if an environment with low vibration sources is provided, the second alternative appears to be advantageous.

4.3.2 Evaluation of Concepts

In this part, the evaluation of each element of the design alternatives is presented. The alternatives are compared according to related design parameters by means of their inferior and superior properties. A weighting percentage is assigned to each criterion. Then, each alternative is graded out of five for these criteria.

4.3.2.1 Laser Detection Device

There are four alternatives for laser detection device. They are CCD cameras, CMOS cameras, beam profilers, and PSD sensors. These alternatives are evaluated according to parameters light sensitivity, background noise, saturation, cost, and processing of the output. Evaluation is given in Table 4.1.

Table 4.1: Evaluation of laser detection devices

	Sensitivity	Noise	Saturation	Cost	Processing	**Grade**
CCD Camera	5	4	3	4	5	**4.3**
CMOS Camera	3	3	4	4	5	**3.8**
Beam Profiler	5	4	4	3	3	**3.8**
PSD Sensor	4	3	5	5	1	**3.3**
Weight (%)	**20**	**25**	**15**	**15**	**25**	

4.3.2.2 Laser Power Attenuation Method for the Laser Sensor

Three alternatives are introduced for laser power attenuation method as beam splitter, reflective ND filter, and absorptive ND filter. The evaluation parameters are determined as laser uniformity, heat generation, and cost. Evaluation is given in Table 4.2. It is considered that the laser uniformity has the greatest importance for the calibration setup. Hence, its weight is assigned accordingly.

Table 4.2: Evaluation of laser power attenuation methods

	Laser Uniformity	Heat Generation	Cost	**Grade**
Beam Splitter	5	4	2	**3.9**
Reflective ND	3	4	4	**3.6**
Absorptive ND	5	3	4	**4.1**
Weight (%)	**40**	**35**	**25**	

4.3.2.3 Laser Exit Angle Measurement Method

There are three alternatives for laser exit angle measurement. They are “inclined surface” method, “two positioning system at two different elevations” method, and “two sensors at two elevations with a single positioning system” method. The methods are evaluated according to five criteria. These are decoupling capability of laser exit angle and laser projection line angle errors, accuracy requirement to measure the angle, sensor and axis alignment problem, ease to implement, and cost. Evaluation results are presented in Table 4.3.

Table 4.3: Evaluation of laser exit angle measurement methods

	Inclined Plane	Two Positioning Systems at Two Elevations	Single Positioning System with Two Sensors	**Weight (%)**
Decoupling Angles	2	4	4	**20**
Accuracy Requirement	3	4	3	**25**
Alignment Problem	4	2	4	**30**
Ease to Implement	4	3	4	**15**
Cost	4	2	4	**10**
Grade	**3.4**	**3.1**	**3.8**	

4.3.2.4 Laser Projection line angle Measurement Method

Two alternatives are given for laser projection line angle error measurement method. They are a linear sensor array aligned along the laser line direction (y-axis) with a 1D positioning system and a single sensor with 2D positioning system. The evaluation parameters of the alternatives are alignment problem along y-axis, laser line profiling capability, ease to implement, and the cost. The results are presented in Table 4.4.

Table 4.4: Evaluation of laser projection line angle error measurement methods

	Alignment Problem	Line Profiling	Ease to Implement	Cost	**Grade**
Multiple Sensors Single Axis	3	2	4	3	**2.8**
Single Sensor Double Axes	4	4	3	3	**3.6**
Weight (%)	**20**	**40**	**20**	**20**	

4.3.2.5 Main Structure

Three basic alternatives are presented as the main body structure. They are aluminum body, gray cast iron body, and granite body. Evaluation parameters appear as ease of manufacturing, performance under vibration disturbances, material stability, weight of the required volume, and the cost. Evaluation is presented in the following table.

Table 4.5: Evaluation of main structure alternatives

	Manufacturing	Vibration	Stability	Weight	Cost	**Grade**
Aluminum	5	2	3	5	5	**3.8**
Cast Iron	4	4	4	4	4	**4.0**
Granite	3	4	5	4	3	**3.9**
Weight (%)	**20**	**25**	**25**	**15**	**15**	

4.3.2.6 Actuator

Three alternatives of the actuator unit are given as stepper motor, DC servo motor, and linear. Evaluation parameters are determined as positioning resolution, positioning accuracy, load capacity, stroke, and cost. This evaluation is given in Table 4.6.

Table 4.6: Evaluation of actuator alternatives

	Resolution	Accuracy	Load	Stroke	Cost	**Grade**
Stepper	4	3	3	5	5	**3.5**
DC Servo	5	4	4	5	4	**4.0**
Linear	5	5	3	2	2	**3.4**
Weight (%)	**20**	**25**	**20**	**20**	**15**	

4.3.2.7 Linear Positioning Elements

Evaluation of linear positioning elements is carried out upon two alternatives: linear polymer friction bearings and linear recirculating ball bearings. Evaluation criteria are clearance between the rail and carriage, friction generated between the carriage and rail, and cost. The related evaluation result is given in Table 4.7.

Table 4.7: Evaluation of linear positioning elements

	Clearance	Friction	Cost	**Grade**
Friction Bearing	2	3	5	**2.9**
Ball Bearing	4	5	3	**4.1**
Weight (%)	**50**	**30**	**20**	

4.3.2.8 Power Transmission

Three alternatives for power transmission mechanism are presented. These are ball screws, lead screws, and belt-pulley mechanisms. Evaluation is conducted according to positional accuracy, convenience of mounting, controllability, and cost. Table 4.8 gives the evaluation results.

Table 4.8: Evaluation of power transmission alternatives

	Accuracy	Mounting	Control	Cost	**Grade**
Ball Screw	5	3	4	3	**4.0**
Lead Screw	4	3	4	4	**3.8**
Belt-Pulley	3	4	3	5	**3.6**
Weight (%)	**35**	**25**	**25**	**15**	

4.3.2.9 Linear Position Sensing Device

To measure the position of the laser detecting sensors two alternatives of position sensing devices are presented as rotary encoders and linear encoders. They are evaluated with respect to accuracy, ease to integrate to the system, and cost. The results are given in Table 4.9.

Table 4.9: Evaluation of linear position sensing devices

	Accuracy	Integration	Cost	**Grade**
Rotary Encoder	3	5	5	**4.0**
Linear Encoder	5	4	3	**4.3**
Weight (%)	**50**	**30**	**20**	

4.3.2.10 LBPS Mounting Method

Two methods are given for LBPS mounting to the calibration system. The first one is to mount the LBPS to a platform connected to the sensor positioning system. The second alternative is to mount LBPS to a platform separated from the sensor positioning system. This parameter which is one of the most critical problems of the calibration system is dependent to vibration disturbance coming from the environment. For this purpose, a series of tests are conducted and presented in Section *7.3 Calibration Room Vibration Tests*. The results show that the vibration coming from the ambient is not significant. Hence, the vibration generated by the sensor positioning system is more critical. Consequently, it is seen that the second alternative is superior on the basis of vibration disturbance.

4.3.3 Concept Alternatives for the Overall System and Their Evaluations

In this section, four different concept alternatives for overall calibration system are generated. These concepts are evaluated according to *Pugh's Concept Selection Method* (Dieter, 2009). This method depends on comparing conceptual alternatives w.r.t. a reference concept. The generated concepts are presented in Table 4.10.

Concept (4) given in Table 4.10 is selected as the reference concept and the remaining concepts are compared on the basis of the following criteria:

- Convenience of implementation,
- Manufacturing Cost,
- Ease to supply,
- Exposure to vibration,
- Base material stability,

- Measurement accuracy,
- Resolution of the output data,
- Processing of the output data.

Table 4.10: Concepts of the calibration setup

	Concepts			
Function	**(1)**	**(2)**	**(3)**	**(4)**
Main Structure	Aluminum	Granite	Cast Iron	Aluminum
Laser Exit Angle Measurement Method	Two Positioning Systems at Two Elevations	Single Positioning System with Two Sensors	Single Positioning System with Two Sensors	Single Positioning System with Two Sensors
Laser Projection line angle Measurement Method	Single Sensor Double Axes	Multiple Sensors Single Axis	Single Sensor Double Axes	Single Sensor Double Axes
Laser Detection Device	CCD Camera	CMOS Camera	CCD Camera	PSD Sensor
Laser Power Attenuation Method	Absorptive ND	Reflective ND	Absorptive ND	
Actuator	Stepper Motor	Servo Motor	Servo Motor	Servo Motor
Linear Positioning Elements	Friction Bearing	Recirculating Ball Bearing	Recirculating Ball Bearing	Recirculating Ball Bearing
Power Transmission	Belt-Pulley	Ball screw	Ball screw	Ball screw
Linear Position Sensing Device	Rotary Encoder	Linear Scale	Linear Scale	Linear Scale
LBPS Mounting Method	Connected Mounting	Connected Mounting	Separate Mounting	Separate Mounting

According to the mentioned criteria, the generated concepts are evaluated in the following table.

Table 4.11: Comparison of the concepts

	Concepts			
Criterion	(1)	(2)	(3)	(4)
Convenience of implementation	–	S	+	
Manufacturing Cost	+	–	–	
Ease to supply	S	–	S	REFERENCE
Exposure to vibration	–	+	+	
Base material stability	S	+	+	
Measurement accuracy	–	S	S	
Resolution of the output data	–	–	–	
Processing of the output data	+	+	+	
∑ +	2	3	4	
∑ -	4	3	2	
∑ **S**	2	2	2	

where "+" represents the parameters of the relevant concept which are better than the related parameter of the reference concept, "–" represents the worse ones, and "*S*" represents the ones which are about the same.

According to the evaluation results given in Table 4.11, concept (3) is selected as the best concept for the design of the calibration setup. After this point, detailed design of the system is to be conducted.

4.4 Detailed Design

In this part, the detailed design for the selected concepts is elaborated. Properties of the designed system are explained firstly. At this step, general structure and working principle of the calibration system is presented. Engineering calculations of some elements of the system are given. Finally, manufacturing plan of some elements is presented.

4.4.1 Properties of Designed System

Calibration system consists of two basic parts as camera positioning system and laser positioning system mounting.

Camera positioning system is a 2D stage driven by two servo motors and drivers. All system is on a gray cast iron bed. Cast iron saddle translates along the bed by means of linear guideways and recirculating ball bearing carriages. Translation of the saddle generates the x-axis motion of the camera. On the saddle, linear motion of the table which carries the camera stage is performed along an axis perpendicular to the motion of the saddle. Translation of the table generates the y-axis motion of the camera. A schematic view of this translational system is illustrated in Figure 4.9. A camera mounting stage is assembled on the top of the table seen on Figure 4.9. There are two camera connections on this stage, one is for lower camera and the other one is for upper camera. This stage enables the laser exit angle measurement explained in Section *4.3.1.3 Laser Exit Angle Measurement Method*.

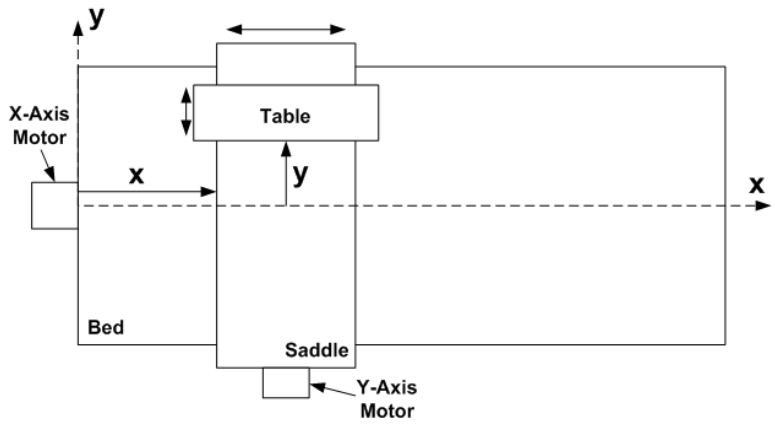

Figure 4.9: Schematic view of working principle of the camera positioning system

Cameras are mounted to the camera stage with two different elevations. Properties of the cameras used in the system are presented in *7.2.1 Properties of the Camera*.

Power transmission is achieved by ball screws and backlash free couplings. Ball screws are mounted to the bed and the saddle by means of FK-FF type end supports. FK-FF type end supports are attached to the end of the ball screws and to the plane perpendicular to the translational axis. Ball bearings on FK side are fixed but ball bearing on FF side is free along the ball screw for dimensional fluctuations. These supports enable the elimination of some distortions caused by assembly and manufacturing of the tables, rails, and ball screw nuts by means of the mounting freedom on y-z plane. However, to be able to guarantee that this method works, the surfaces to which the end supports are mounted should be precisely machined.

Ball screw nuts are not directly mounted to saddle and table, but they are mounted by means of thermal insulation plates made of fiberglass epoxy (called thermal break) in order to prevent the interference of heat generated on the nuts to the system elements. Temperature of ball screw nuts

may reach up to 50 – 60 ºC during operation (Hiwin, 2012b). Conduction of the heat generated affects the system accuracy adversely. These fiberglass epoxy plates and screw head housings provide quite good insulation against transmission of heat. A schematic representation of related mountings is given in Figure 4.10.

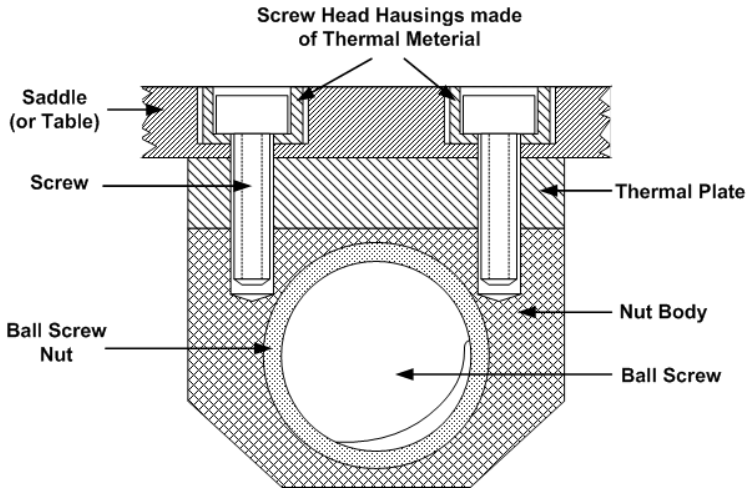

Figure 4.10: Schematic sketch of nut body mounting with thermal elements

Thermal plate and screw head housings made of fiberglass epoxy prevent the direct contact of system table and nut body. Under favour of screw head housings, heat carried by screws is blocked.

Due to the reliability considerations, LS-type Heidenhain linear encoders are selected as position measuring elements. Translational positions of the camera stage along x and y axes are determined by these two linear encoders with ±3 μm accuracy and 250 nm measuring resolution. One of the encoders is attached to saddle, and the other one is attached to table. In order to be able to determine the yaw error of the saddle during the translation, connections for two more linear encoders are available on the saddle (for encoder head) and on the bed (for encoder body). These two extra encoders are mounted to the left and right sides of the main encoder. Comparison between the encoder counts enables the determination of the yaw error of the saddle. Outputs of the two extra encoders are to be read by extra electronic cards.

Measuring ranges of the encoders on the bed and on the saddle are 1640 mm and 640 mm respectively. Outputs of the main encoders are fed to the motor drivers. Hence, this data is used to determine the position of the camera stage precisely.

One of the problematic issues in the camera positioning system is the cabling. It is very important to determine the fixed connections and movement of the cables which are mounted to the translational elements. Bending radius values of the cables for fixed and frequent flexing conditions should be determined carefully. A schematic representation of these two conditions is illustrated in Figure 4.11.

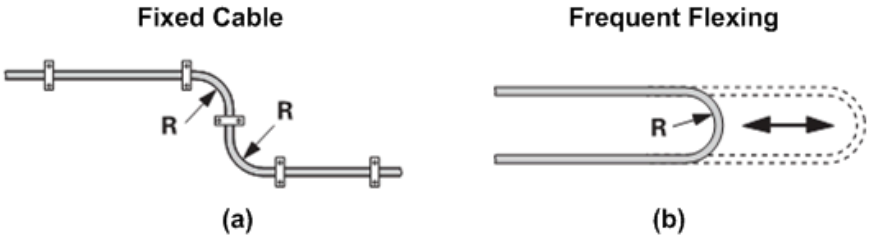

Figure 4.11: Schematic representation of cable mountings, (a) Fixed Cable (b) Frequent Flexing

The radius values seen on Figure 4.11 have some lower limits for each cable types. For fixed cable mountings, cable tapes and crochets are used in the system by considering the minimum allowable bending radii. In movable cable case, bending radius lower limits are higher than that of fixed condition. Moreover, all path of the cable motion should be controlled. For this purpose, special movable cable guides are used. After determining the dimensions of the cable guide (height, width, and length), the most important parameter which should be determined is the bending radius of the cable guide. Since frequent flexing of the cables results in deformation of the cable material for small bending radii, the bending radius of the cable channel is determined according to the data given in catalogues of the cables used for translational elements which are cameras, encoder heads, y-axis motor and motor encoder, y-axis limit switches, and y-axis homing switch. As a result, a value of 150 mm is selected as bending radius of both cable guides mounted to translational axes.

Camera positioning system with all its elements is placed to the ground by means of special machine feet which are mounted to the bed from the bottom. A drawing of the machine feet used in the system is given in Figure 4.12.

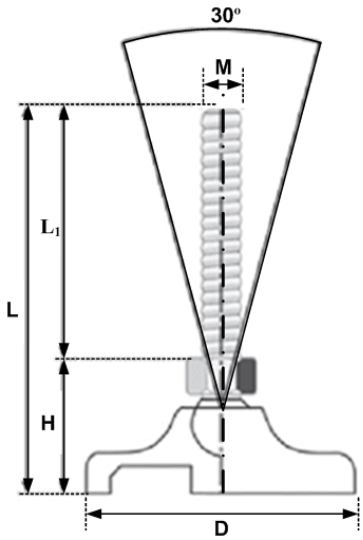

Figure 4.12: Drawing of the feet mounted to the bed (Esersan, 2012)

The foot shown in Figure 4.12 is mounted to the bed by means of an adapter part which has the same thread size M. The foot is mounted to the part stepping to the ground with a spherical joint to prevent the distortions of the bed originated from the mounting of the foot.

The upper side of the calibration system (on which the laser beam positioning system is attached) is constructed with I-beams. Although the construction carries only the laser system which has a weight less than 20 kg, it is designed quite sturdy for vibration and safety considerations. IPN-200 type profiles are used for this purpose. Four I-beams are mounted to counter walls in pairs and they also mounted to each other by means of three I-beams. The constructional view of the structure is given in Figure 4.13.

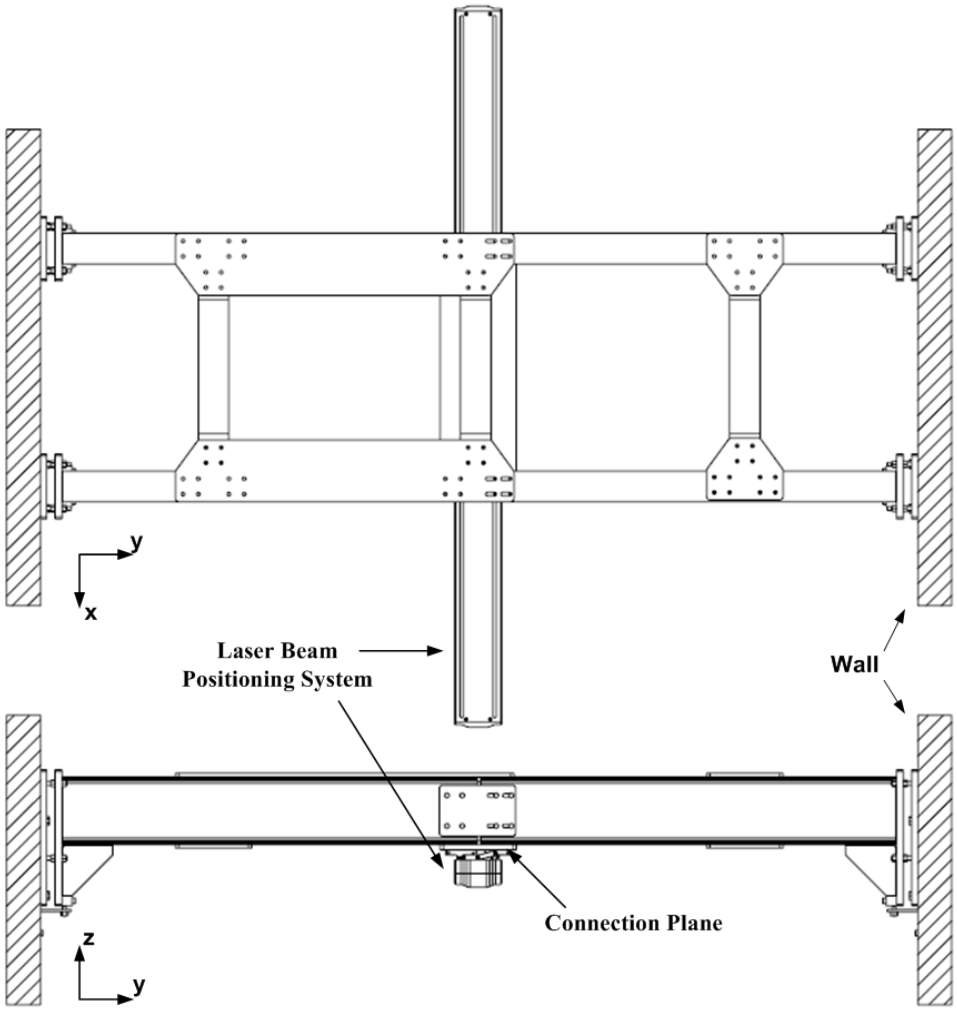

Figure 4.13: Constructional views of upper side of the calibration system

The middle one of the three I-beams connecting the two long beams to each other seen in Figure 4.13 is used for connection of the laser beam positioning system to the calibration setup via a 10-mm-thickness plate. Connection faces of the plates and the I-beams are precision ground. Parallelism of the camera positioning system and the plane to which the laser positioning system mounted is adjusted by using a high precision (0.02mm / 1m) spirit level (elaborated in *4.6 Assembling Procedure*).

The basic idea behind this design of which the basic parts and the properties are explained here is to meet with the positional and angular requirements of laser positioning system. For this purpose: position, exit angle, projection line angle, straightness values of stationary center laser are measured and adjusted first. After that, the same parameters of the movable laser sources are measured and adjusted according to this reference laser source.

4.4.2 Engineering Calculations

During the selection of some elements of the calibration system, some calculations are conducted. These elements are the bed of the camera positioning system, ball screws used for power transmission, motors actuating the translational motions along the x and y axes, and ND filters used for power attenuation of the laser reflected onto the camera sensor.

4.4.2.1 Bed Static Deflection

In the design of the bed, saddle, table, and several other mechanical elements Solid Works 2012 and Solid Works Simulation are used as design and analysis tools. Static deflection analysis of the bed, which is one the most critical elements of the system due to its dimensions and weight, is carried out on Solid Works Simulation via finite elements method.

In this analysis, curvature based meshes are utilized. In this method more elements are created in higher-curvature areas automatically without need for mesh control. Maximum element size is set to 91 mm. This size is used for boundaries with lowest curvature. Minimum element size is taken as 18 mm. This size is for the boundaries with highest curvature. Minimum number of elements in a circle is set to 8. Element size growth ratio specifies the global element size growth ratio starting from regions of high curvatures in all directions. This parameter is set to 1.6.

Result of the conducted analysis is presented in Figure 4.14. The bed is supported by fixed supports from six locations at the bottom. These locations represent the machine foot locations in the system. Deflection increases with the distance to any foot. The maximum static deflection is about 4 μm.

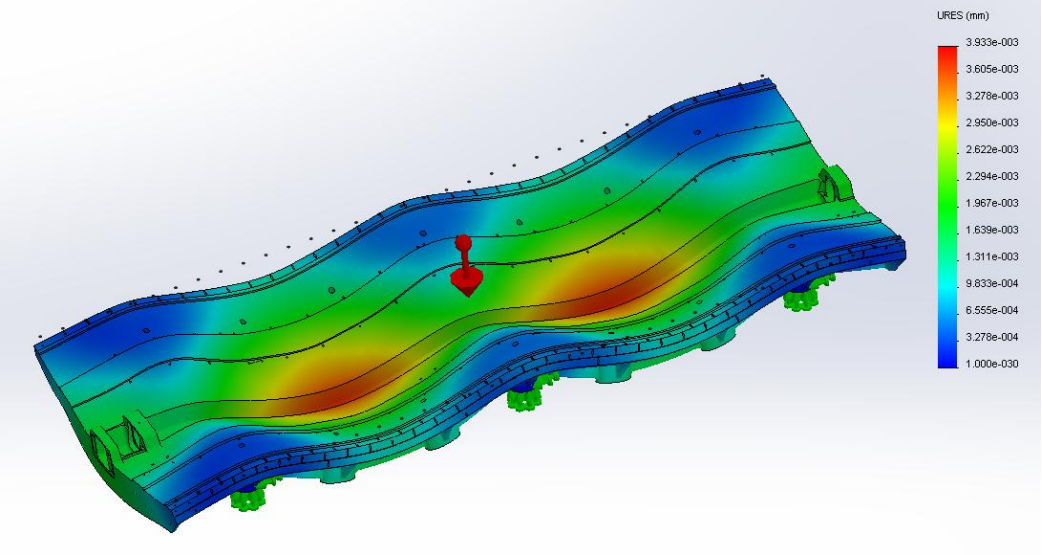

Figure 4.14: Static deflection analysis result of the bed

The important deflection which affects the performance of the camera positioning system directly is the deflection along the linear guideway plane. The graph of the deflection curve along the linear guideway connection plane is plotted in Figure 4.15. In this graph, maximum deflection appears as about 1µm. Since the width of the saddle is about 300 mm, this amount of deflection causes maximum angular error (pith error elaborated in Section *7.4 Camera Positioning System Verification Tests*) error less than 1 arcsec. This result shows that the machining and precision grinding of the bed together with the assembling are the dominant factors for the mentioned angular error.

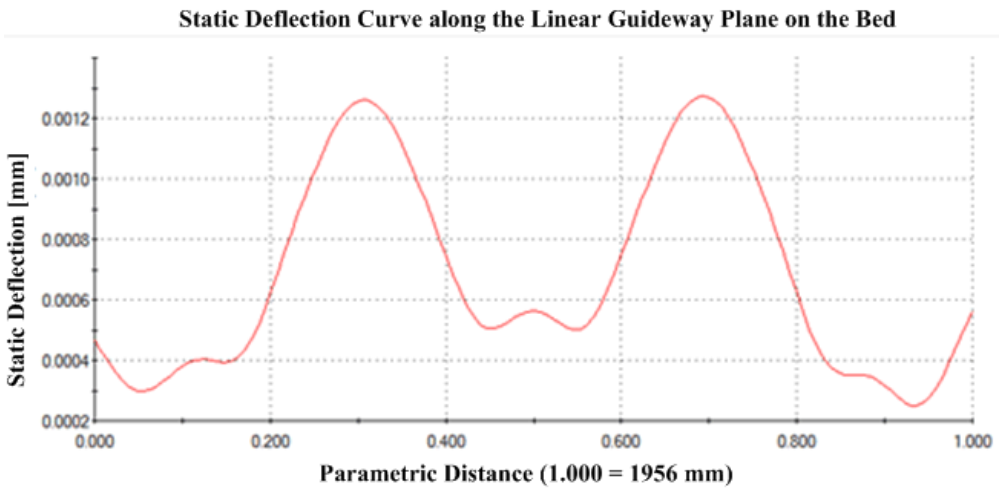

Figure 4.15: The graph of the static deflection curve along the linear guideway plane on the bed

4.4.2.2 Ball Screw Dimensions

On the power transmission of the camera positioning system, FSC type Hiwin ball screws are used. This type presents lower noise and smaller nut diameter than the other types. Selection of the diameter and the lead of the ball screw require some calculations.

Small ball screw diameter is desirable but critical speed of the screw restricts the minimum screw diameter. Lead, on the other hand, directly determines the rotational speed of the screw. In the design specifications, positioning speed of the camera positioning system is decided to be 300 mm/sec. A smaller lead increases the required rotational speed and causes the ball screw to reach critical speed. The critical speed is said to exist when the rotational frequency of a shaft equals the first natural frequency of the shaft. This will cause the ball screw to bend under the stress of vibration coupled with the centrifugal forces due to the rotation and cause the shaft to vibrate violently. Therefore, the rotational speed of the ball screw should be set to below the value indicated by critical speed (Hiwin, 2012b). Especially x-axis, which is the longer axis, suffers from this problem. Increasing the lead solves the problem but this time system inertia increases and the rotor inertia of the motor required to be increased.

Considering the restrictions some calculations are conducted and screw diameter of 25 mm and lead of 25 mm is selected for x-axis. Diameter of 20 mm and lead of 20 mm is selected for y-axis. The relevant calculations are given in the appendix.

4.4.2.3 Motor Parameters

Actuation units of the translational axes are servo motors. Depending on the required rotational speed, system inertia, and required torque values suitable motor parameters should be determined.

Motor parameters should be determined are rated rotational speed, rotor moment of inertia, and effective value of the torque.

ECMA-C10807GS and ECMA-C10604GS model Delta servo motors are selected for x and y axes respectively. Values of the related parameters of each motor are given in Table 4.12.

Table 4.12: Parameters of the selected motors

Axis	**Model**	**Rated Power [W]**	**Rated Rotational Speed [rpm]**	**Rated Torque [N.m]**	Rotor Inertia [10^{-4} kg.m^2]
x-axis	ECMA-C10807GS	750	3000	1.27	0.227
y-axis	ECMA-C10604GS	400	3000	2.39	1.13

4.4.2.4 Grade of ND Filters

ND filter is an element providing attenuation to the incident light power. In the calibration system, absorptive ND filter is selected to decrease the laser power transmitted to the camera sensor. These elements are explained in Section *4.3.2.2 Laser Power Attenuation Method for the Laser Sensor*.

ND filters have grades like ND1, ND2, and so on. The number in the name represents the power of 10 which is the attenuation rate. For example, a filter with grade ND2 passes 1/100 of the incident power.

Determination of the ND grade depends on the saturation limits of the camera sensor under the working conditions. The cameras use Sony ICX445 CCD sensors. Saturation performance of these sensors is related to the wave length of the incident light, quantum efficiency of the sensor for this wave length, and shutter time used.

In laser positioning system the laser sources with 635 nm wavelength are used. One photon at 635 nm wavelength is equal to 1.95 eV. This value also equals to 3.12×10^{-19} J.

Quantum efficiency of the sensor ICX445 at 635 nm can be determined from the graph given in Figure 4.16.

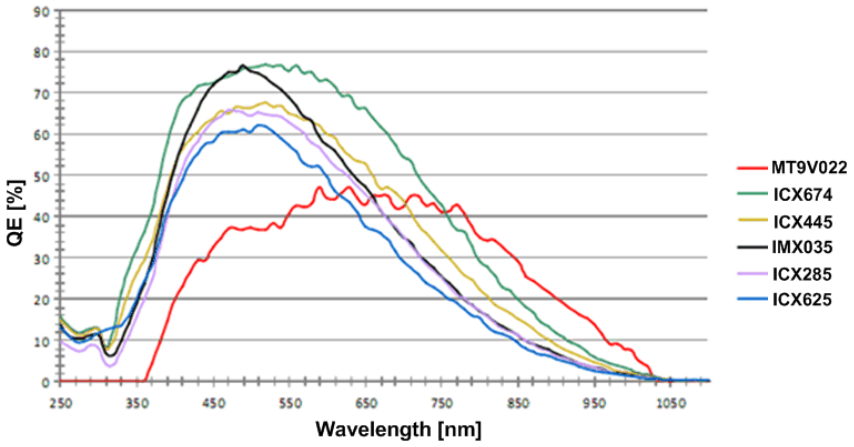

Figure 4.16 Quantum efficiency values of the sensors (Point Grey, 2012)

Using the graph given in Figure 4.16, quantum efficiency of sensor used in calibration system (ICX445) at 635 nm is determined as 55%. Every 2 photons result in one electron charge energy. Since 55% of photons are registered, 3.64 photons (at 635 nm wavelength) hitting the cell result in 1 electron charge being built over the device. The full well depth capacity on the sensor (the amount of electrons one cell can hold on the sensor) is at about 6800 electrons. Thus, for one pixel to saturate at 635 nm light, it needs to be hit by around 24700 photons.

Assuming a shutter time S, full saturation occurs with hit of 24700 photons in time S. Considering a single photon carries 3.12×10^{-19} J at this wavelength, this resulting energy is equivalent to 7.73×10^{-15} J per pixel in time S. Each CCD cell on the sensor has dimensions of 3.75 µm × 3.75

μm. This makes 0.55 J/m^2. For a shutter time of 0.5 sec, area density of the saturation power is 1.1 mW/m^2.

The laser sources (i.e. uniform line generators used in the laser positioning system) have an exit power of 1 mW. According to the specifications of these sources, line thickness at 1.5 m projection distance is about 0.6 mm. Since the fan angle is 45º, line length at this projection distance is about 1.24 m. Thus, the area on which the laser power distributed is 7.44×10^{-4} m^2. This means that the exit power area density of the laser sources is about 744 mW/m^2.

For projection distance of 1.5 m between the camera and the laser source, power density of 744 mW/m^2 should be decreased to 1.1 mW/m^2. For this purpose, an attenuation of 1/1000 is required. Therefore, neutral density filter grade of ND3 is selected for the system.

4.5 Manufacturing of the System Parts

Calibration system has several parts should be manufactured. These parts are tables of the camera positioning system (bed, saddle, and table), foot adapters, rail supports, mechanical stoppers, sheet plates of switches and cable channels, ends of ball screws, ball screw nut bodies, thermal plates, camera mounting stage, motor mounting adapters, and upper construction of the calibration system. In this part, manufacturing methods and technologies, which are utilized during the production of these parts, are explained.

4.5.1 Tables of the Camera Positioning System

There are three main components of the camera positioning system: i) bed, ii) saddle, iii) table. Manufacturing of these gray cast iron tables consists of six steps. These steps are manufacturing of wooden models, casting of the tables, CNC machining, stress relieving heat treatment, grinding, and painting.

4.5.1.1 Manufacturing of Wooden Models

To be able to form the casting molds, wooden models of the tables are designed and manufactured. Due to the nature of casting and system parameters, designed models should satisfy some requirements. They are as follows:

- Avoiding from sharp corners,
- Using suitable draft angles for the ease of mold and material separation,
- Giving suitable allowances to the surfaces to be machined,
- Determination of separation plane,
- Compensating shrinkage of the material in the design,

- Providing uniform thickness throughout the part.

In the design of the models, suitable radius values are given to all external and internal corners of the tables. During the manufacturing of the models these geometries are obtained by using some simple apparatus and steel putty.

One of the most important parameters to be taken into account with the casting model design and manufacturing is the draft angles which are the ones introduced to the model surfaces perpendicular to the separation plane between upper and lower half of the mold. During the model design, the draft angles of the side surfaces are given as 4º.

During the design of the wooden models machining allowances are given depending on the machining length and the direction of the surface (upper, lower, and side) to be machined.

Due to the geometrical considerations, mold separation plane is determined as the upper surface for the bed and the tip of the ribs for the saddle.

All dimensions of the wooden models are scaled such that the models are bigger than the actual ones as much as 1 % due to the shrinkage of the cast material.

Special efforts are put forward to obtain uniform material thickness throughout the models during the design phase. Sharp increases in the cross-sections and bulky parts (where molten material is difficult to feed during casting) are avoided.

Models are manufactured by using plywood obtained from beech tree. These plates are cut to the suitable dimensions with required angles by means of sawing machine with adjustable saw angle. In Figure 4.17, manufactured wooden model of the bed is given.

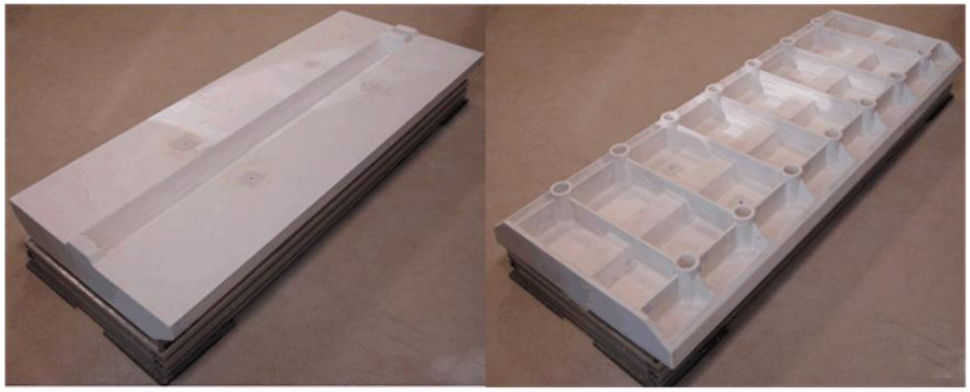

Figure 4.17: Wooden model of the bed (a) Upper side (b) Lower side

In the model seen in Figure 4.17, specific geometries are provided. These are machining surfaces for linear encoders, linear guideways, and guide supports, cavity for ball screw and ball screw nut, flanges for motor and FK-FF end supports, ribs, and cylinders for foot connections. Wooden model of the saddle is given in Figure 4.18.

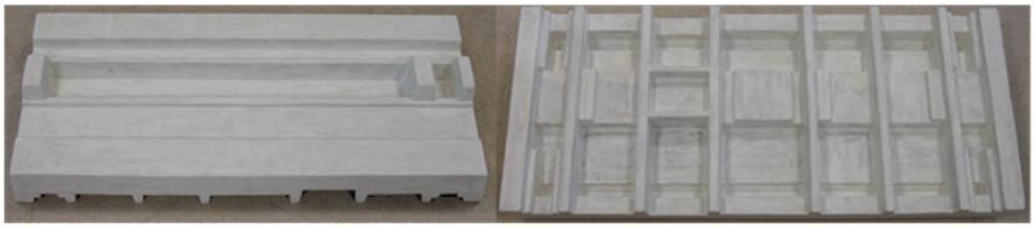

Figure 4.18: Wooden model of the saddle (a) Upper side (b) Lower side

Provided geometries with the model of the saddle given in Figure 4.18 are machining surfaces for linear encoder, linear guideways, and guide supports, cavity for ball screw and ball screw nut, flanges for motor and FK-FF end supports, ribs, and surfaces for encoder heads, ball screw nut body, and linear guideway carriages.

Model of the table does not have any complex geometry. Hence, it is formed as a block material instead. Required geometries for encoder head and linear guideway carriages are obtained by machining this block after casting.

4.5.1.2 Casting of the Parts

Using the wooden models manufactured, casting of the parts is conducted. The composition of the casting material is as follows: 2.86% C, 2.05% Si, 0.75% Mn, 0.017% P, 0.015% S, 0.40% Cr, 0.062% Ni, 0.79% Mo, 0.07% Cu, 0.02% Al, and 0.05% Ti. With this compound, the hardness of 240 - 270 HB is achievable.

During the formation of mold geometries, the upper surface of the bed and the tip of the ribs of the saddle are selected as the mold separation planes. In order to be able to obtain smoother geometries on the surfaces (where the encoder body and guideways are to be mounted), these surfaces are oriented towards downwards (with respect to gravity).

4.5.1.3 CNC Machining

After casting rough machining of the parts is performed via CNC machining center. Since the cutting forces in machining cause additional residual stresses in the material, rough machining of the parts are scheduled before the heat treatment in the manufacturing plan.

During CNC machining of the parts, surfaces requiring dimensional precision like encoder body interface and linear guideway mounting surface are machined to allow 0.5 mm for grinding.

4.5.1.4 Stress Relieving Heat Treatment

In order to reduce residual stresses due to casting and machining, parts (on which the rough machining is performed) are subjected to stress relieving heat treatment process in a PLC controlled industrial scale electrical furnace.

Parts are heated up to 600 - 650 ºC and held at this temperature for a few hours and then slowly cooled in still air.

4.5.1.5 Grinding

After stress relieving process, planes for encoder bodies, linear guideways, guideway carriages, encoder heads, and ball screw nut bodies are precision ground.

4.5.1.6 Painting

After precision grinding of the parts, surfaces (not requiring dimensional accuracy) are painted to prevent corrosion. Portions of ground surfaces that are exposed to air are covered by metal protecting chemicals.

4.5.2 Foot Adapters

Foot adapters are used to mount the machine feet shown in Figure 4.12 to the cylindrical parts at the bottom of the bed. These parts are manufactured from aluminum.

Parts are machined in CNC turning center and then M16 treads are cut at the center of each part. Finally all parts are covered by zinc-phosphate coating.

4.5.3 Rail Supports

Rail supports are parts fixing the linear guideways to the ground supporting face. These parts are manufactured from low carbon steel. These relatively simple parts are machined via a CNC machining center and then coated with zinc-phosphate.

4.5.4 Mechanical Stoppers

Translations in camera positioning system are to be limited by the controller (i.e. software). In addition, each axis has limit switches. However, to avoid full crash due to unforeseeable reasons (hardware malfunction, “bugs” in the control software, etc.), ends of the axes constitute

mechanical stoppers. These parts are machined out of aluminum. Note that the rubber material (of 10 mm in thickness is attached) onto the so as to stop smoothly an over travelled carriage.

4.5.5 Sheet Plates of Switches and Cable Channels

Homing and limit switches (along with cable channels) are mounted onto the camera positioning system by means of sheet metals with 1 mm thickness. The sheets are cut from low carbon steel (ST-37) plates by using laser cutting. After obtaining the required planar sheet geometries, parts are bent to their final shapes. These parts are also coated with zinc-phosphate.

4.5.6 Ends of Ball Screws

One of the most important machining works of the system is the end machining of each ball screw. In order not to face with any contraction and obtain a smooth translation on the axes, ends of the ball screws must be machined quite precisely. Dimensional and geometric tolerances of these operations are only few microns. Especially, for the ball screw of the long axis (x-axis), it is rather difficult to obtain such tolerances. Grinding works of the ball screw ends are conducted by using special apparatus providing linear alignment of the shaft during grinding. The most difficult issue about these machining is to find the machines and machinists capable of performing such delicate applications without failure.

4.5.7 Ball Screw Nut Bodies

Ball screw nuts are mounted onto the saddle and table by means of nut bodies. Aluminum is used for these parts due to its high thermal conductivity. Thus, the heat is removed effectively from the nut.

The perpendicularity of the face, on which the ball screw nut flange is mounted and the surface to be meshed with the saddle or the table should be precisely obtained. For this purpose, aluminum nut bodies are machined via CNC machining center and the mentioned surfaces are precision ground.

4.5.8 Thermal Plates

Thermal plates (shown in Figure 4.10), are used to protect the precise sensors from heat generated by the ball screw nuts. These thermal insulation plates (i.e thermal breaks) are made of fiberglass epoxy with good machinability characteristics. In manufacturing of these parts, screw holes are drilled in CNC machining center and upper and lower surfaces are precision ground to the required dimensions.

4.5.9 Camera Mounting Stage

As mentioned earlier, camera mounting stage is obtained from ST 37 sheet plates with 8 mm thickness. In order to form the stage geometry, plates are cut by using laser cutter. Furthermore, the plates are arc-welded to each other. In order to get rid of the residual stresses caused by thermal effects during the welding operation, the stage is subjected to stress relief heat treatment. Finally, top and bottom surfaces of the stage are precision ground to obtain parallelism between the two cameras to be mounted.

4.5.10 Motor Mounting Adapters

Motor adapters are parts used to mount the motors to the bed and the saddle. Motor mounting adapters have two functions: The first one is to provide the integration of the motor to the system. The second one is to provide a proper mounting according to ball screw alignment. These parts enables fixing the motor to the system according to the alignment of the ball screw as explained in Section *4.4.1 Properties of Designed System*.

These parts are manufactured out of low carbon steel plates (ST-37) of 10 mm thickness. Firstly, the overall geometry is machined in a CNC machining center with 1 mm machining allowance on the hole for the centering flange of the motor. Hence, the two faces of the plate are ground to provide the perpendicularity between the motor axis and the mounting surface. Finally, diameter of the hole is machined in CNC machining center to a H7 tolerance and the screw holes are drilled.

4.5.11 Upper Construction of the Calibration System

Upper construction provides integration of the laser positioning system to the calibration system with proper mounting planes. As explained in Section *4.4.1 Properties of Designed System*, this construction is manufactured out of I-beams and steel plates (ST-37) of 10 mm thickness. Holes of the beams and the plates are drilled in CNC machining center. These plates are welded to the I-beams. Consequently, these structures are subjected to stress relief (heat) treatment. Finally, to obtain the parallelism between the laser system mounting plane and the camera positioning plane, mating surfaces of the relevant parts and upper/lower faces of the I-beams are precision ground.

4.6 Assembling Procedure

Calibration system consists of two main subassemblies which are laser positioning system attachment structure (i.e. upper structure) and camera positioning system. Assembling procedure of the calibration system is based on the individual integration of each of these two subassemblies and their alignments relative to each other.

4.6.1 Assembling of the Upper Structure

The upper structure of the calibration system (Figure 4.13) which is used to attach the laser beam positioning system to the calibration setup consists of four IPN-200 I-beams, connection plates, adjustment plates, and perpendicular angle brackets. These elements are presented in Figure 4.19.

Each one of the four I-beams is permanently connected (arc welded) to an adjustment plate which provides adjustment for the position and the orientation of the I-beam. The adjustment plate is connected to another plate which is fixed to the wall via four bolts. Four other bolts connect the adjustment plate to the fixed one. The clearance of the holes on the adjustment plate provides translational and rotational freedoms in small range (1 to 2 mm in translations and 1 to 5 degrees for rotations). This property provides great convenience during the assembly of the structure and enables leveling the laser beam positioning system connection plate.

After the required position and orientation of the I-beam are obtained, the adjustment plate is fixed by tightening the counter nuts. Whenever, the laser beam positioning system connection plate leveling is required, one can loosen the nuts and adjust it vie the bolts on the adjustment plate and the angle bracket.

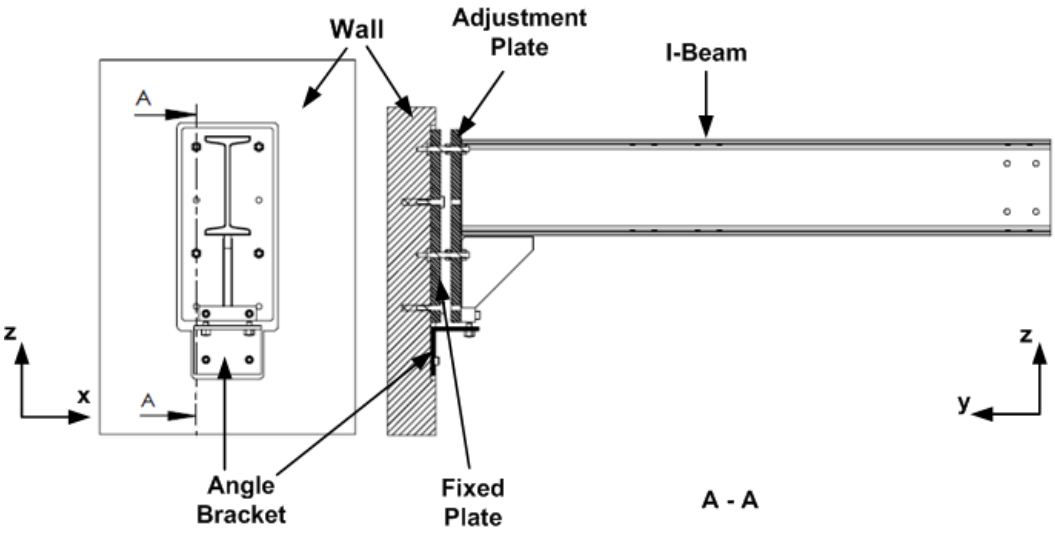

Figure 4.19: Wall connection of one of the four I-beams with adjustment parts

4.6.2 Assembling of the Camera Positioning system

Camera positioning system is a 2D positioning stage which is elaborated in Section *4.4.1 Properties of Designed System* in detail. Assembling of this system consists of plenty of elements. However, the elements of which the connections require special care are linear guideways and their carriages, ball screws and their end supports, and linear scales.

Planes which are to be used for references of linear guideways and carriages are precision ground on both the bed and saddle. Linear guideway and carriage mounting strategy which is followed for both positioning systems along x and y axes is illustrated in the following figure.

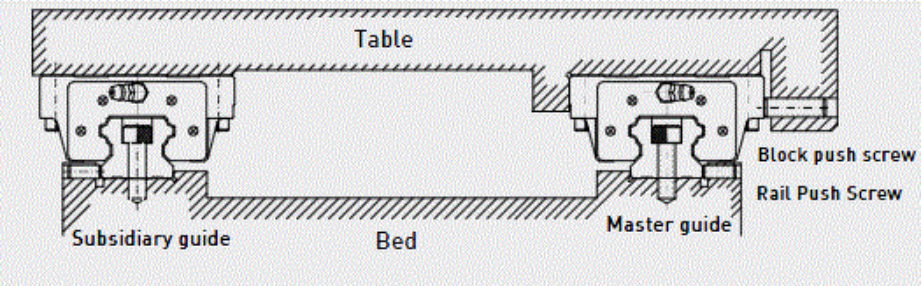

Figure 4.20: Linear guideway and carriage mounting strategy (Hiwin, 2012a)

Different from the configuration given in Figure 4.20, in order to support the rails of both master and subsidiary guides, push plates are utilized instead of rail push screws. This configuration is presented in the following figure.

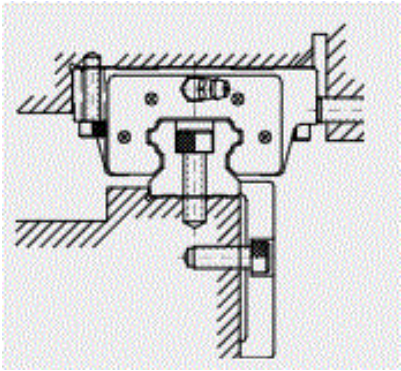

Figure 4.21: Mounting of the rail and the carriage via push plate and push screw, respectively (Hiwin, 2012a)

The most important points of the guideway and carriage attachment are the cleanliness of the reference planes (no dust, oil, or moisture), and tightening the bolts with same torque. Tightening torque for HGR 25 and HGR 15 guideways suggested by Hiwin are 13.7 N.m and 3.9 N.m respectively. For this purpose a torque limiting wrench is utilized.

The power transmission elements (i.e. ball screws) are supported by FF and FK type end supports (Explained in Section *4.4.1 Properties of Designed System*). While assembling the ball screw along the x-axis (on the bed), ball screw ends are mounted to the supports by means of ball

bearings, supports are temporarily connected to mounting surfaces on the bed, and ball screw nut is mounted and fixed to the saddle. Then, the saddle is pulled to the motor side (FK side) and FK support is permanently fixed to the bed by tightening the mounting screws. Motor adapter is also tightened at this stage. Consequently, the saddle is moved to the other side (FF side). At this stage, FF support can freely move on y-z plane. Thus, it aligns itself according to ball screw. Finally, this support is also fixed to the mounting surface. A schematic view of the FK-FF type end supports integrated to the bed is shown in Figure 4.22.

Ball screw of y-axis is also mounted to the saddle with the same method explained and shown in Figure 4.22. But this time, nut is mounted to table carrying the camera stage.

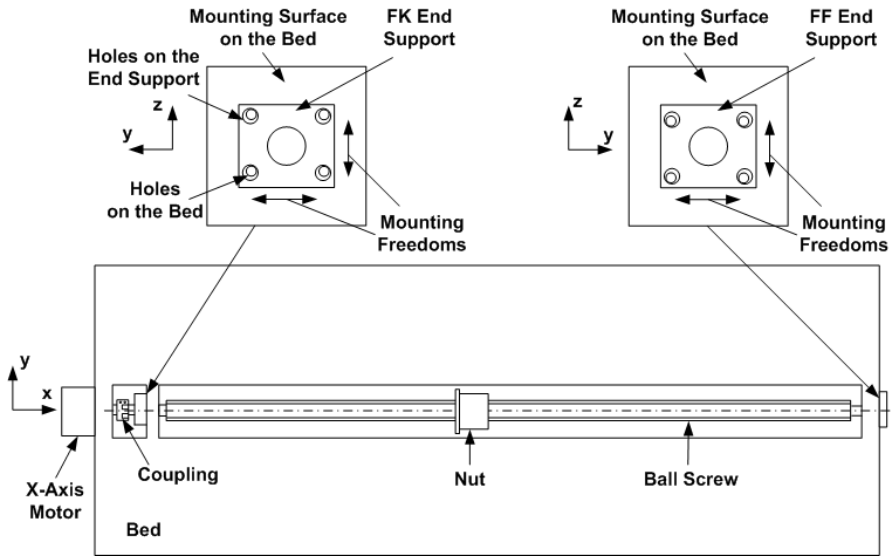

Figure 4.22: Schematic view of the end supports used for ball screw mounting

Linear position feedback is obtained via Heidenhain LS-type linear scales (i.e. linear encoders). Although these devices are quite precise measurements tools, their assembly is an important parameter to be able to get accurate position feedback. Mounting configuration used in the system and the dimensions are given in the following figure.

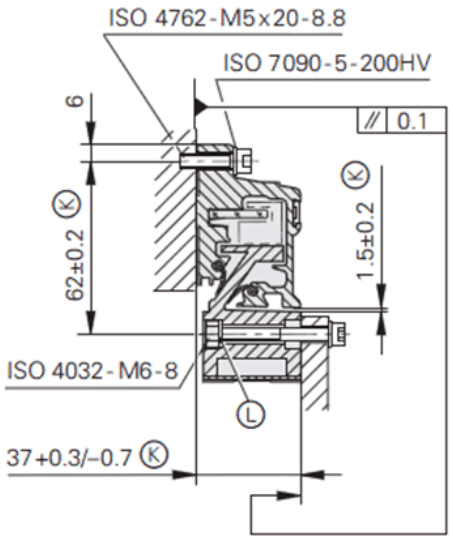

Figure 4.23: Linear scale mounting dimensions (Heidenhain, 2002)

To be able to provide the parallelism of the mounting surfaces, reference planes on the bed, saddle, and table are precision ground. These planes are illustrated in Figure 4.24.

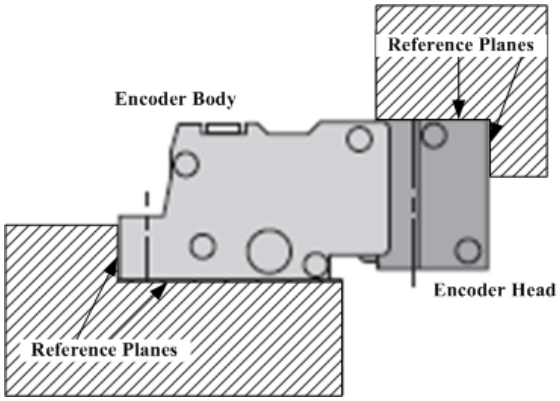

Figure 4.24: Illustration of the reference planes constituted for linear encoder attachment

In the assembling procedure of the linear encoders, encoder head is pushed to the vertical reference plane on the encoder head side (Figure 4.24) and fastened via bolts and nuts with the required torque. After that, encoder body is pushed to the vertical plane on the encoder body side and the screws are tightened in the required order and with the required torque. The tightening torque values for the head and the body, and tightening order of the screws on the body are given in the following figure.

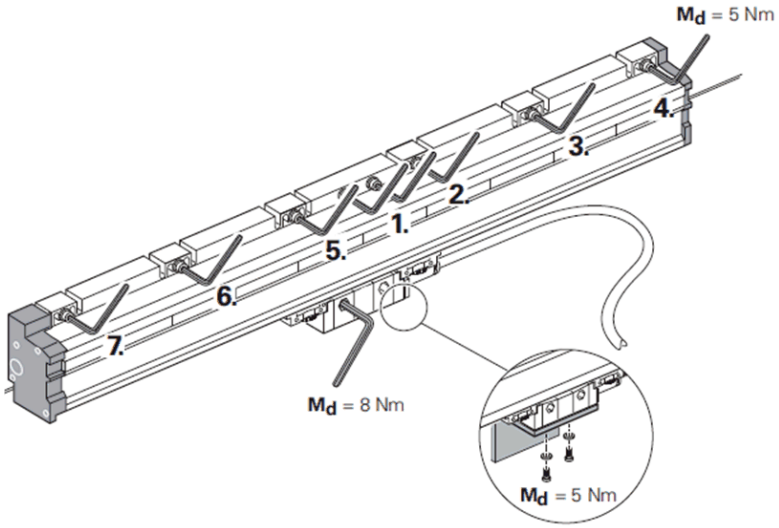

Figure 4.25: Tightening torque values and the order (Heidenhain, 2002)

As can be seen in Figure 4.25, bolts of the encoder head are tightened with torque value of 8 N.m while the screws of the body are tightened with 5 N.m starting from the middle one.

4.6.3 Levelling and Alignment

Two parameters of the calibration system having major importance are: i) parallelism of the laser positioning system mounting and camera positioning system x-y plane, ii) alignment of the laser positioning system translation axis and camera positioning system x-axis. In order to satisfy the design specifications of the system, static rotational errors of the laser positioning around x-axis and y-axis of the global coordinate frame (see Section 5.3 Coordinate Frames) should be less than 0.003 rad (Section *5.10 Determination of the Static and Dynamic Errors*). To be able to obtain the required parallelism and alignment values some strategies are followed. These are: i) leveling the laser beam positioning system connection plane w.r.t. gravity via precision spirit level, ii) aligning the camera positioning system bed via a reoriented laser line and alignment mechanisms, iii) leveling the camera positioning system w.r.t. gravity via precision spirit level and machine feet.

4.6.3.1 Leveling the Laser Beam Positioning System Connection Plane

Laser beam positioning system is attached to the connection plane on the upper structure (Figure 4.13) of the calibration system. The upper structure is designed and manufactured in an adjustable manner (elaborated in Section *4.6.1 Assembling of the Upper Structure*). At the final stage, to be able to provide the parallelism of this plane w.r.t. camera positioning system, both connection plane and camera positioning system are adjusted w.r.t. gravity. For this purpose, a high precision (0.02 mm / 1000 mm) spirit level is utilized. A photo of this spirit level is presented in the following figure.

Figure 4.26: A photo of the spirit level used in the level adjustments of the system

Translational change of the bubble (seen in Figure 4.1) from the central location of the long vial with an amount of one line corresponds to an angular change of 4 arcsec (0.02 mm / 1000 mm).

During the angular adjustments of the connection plane, bolts and nuts on the adjustment plates (Figure 4.19) of all four wall connections are loosen and elevations are adjusted by the set-screws on the angle brackets. As the elevations are changed, connection plane is reoriented around x and y axes. Level of the connection plane is checked via the spirit level for both axes with each elevation change and parallelism of the plane to the ground is adjusted iteratively. After the angular error of the connection plane around x and y axes remain in ±4 arcsec on each location on it, bolts and nuts on the adjustment plates are tightened.

4.6.3.2 Aligning the Camera Positioning System

Before leveling the camera positioning system, alignment of camera positioning x-axis and laser positioning x-axis must be satisfied. For this purpose, a laser system is assembled. In this system there is only a single laser source of which the projection line is aligned along the x axis (i.e. perpendicular to the standard one). Beam exit angle and projection line angle of this system is adjusted on a visual calibration platform with a sub-millimeter accuracy on the projection plane with 1.5 m projection distance. The laser system with the reoriented laser source is attached to the laser beam positioning system connection plane of the upper structure by taking the edge of the connection plate (CNC laser cut) as the reference. The projected laser line represents the laser beam positioning system x-axis alignment. This laser beam taken as the reference of calibration system x-axis alignment and camera positioning system is adjusted accordingly. For this purpose, laser position is measured at the two ends of the x-axis and the orientation of the bed is adjusted until the same position value is obtained. The configuration of the laser system is represented in Figure 4.27.

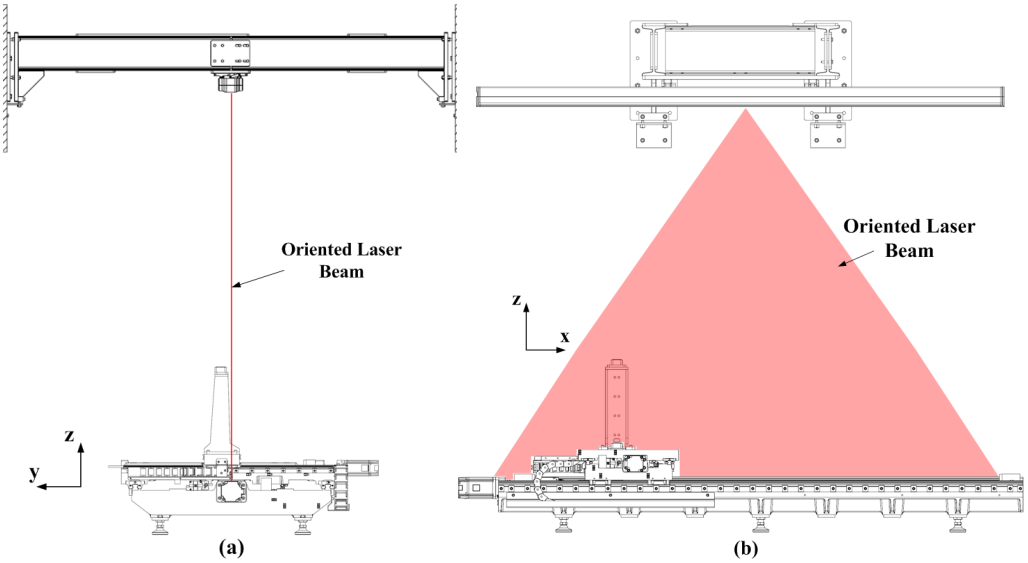

Figure 4.27: Laser line method for camera positioning system alignment (a) front view, (b) side view

The basic problem with the setting of the alignment of camera positioning system is to move the bed smoothly (on x-y plane) in small ranges. To be able to set the alignment of the camera positioning system, a special adjustment method is developed. In this method, the bed is lowered and placed on special supports at the two ends. These supports are manufactured by precision grounding one face of 50 × 100 × 500 ST-37 steel blocks (two blocks for each support). Steel balls of 4 mm diameter are placed between the blocks together with lubricant (special ball bearing grease). Consequently, the camera positioning system can be easily manipulated with smooth translations. A photo and a schematic of the mentioned support system are presented in Figure 4.28.

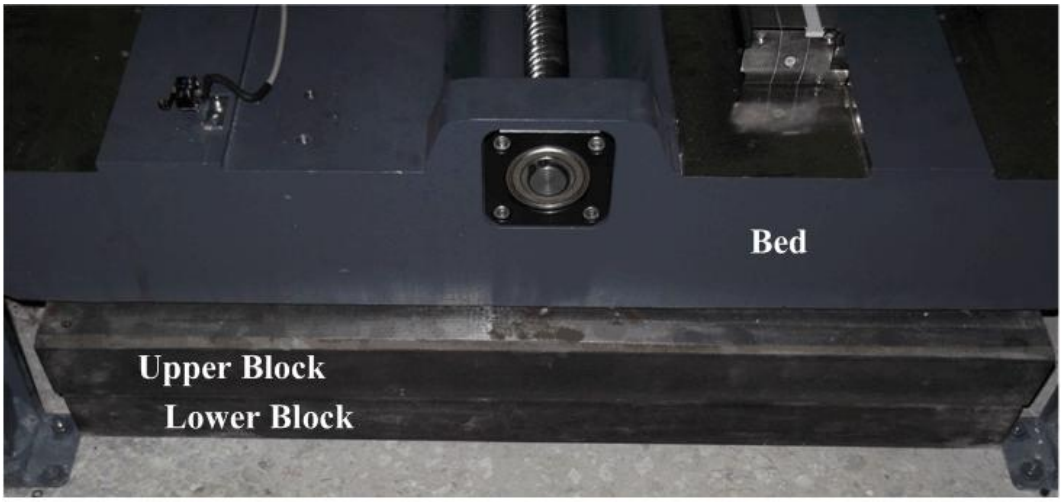

(a)

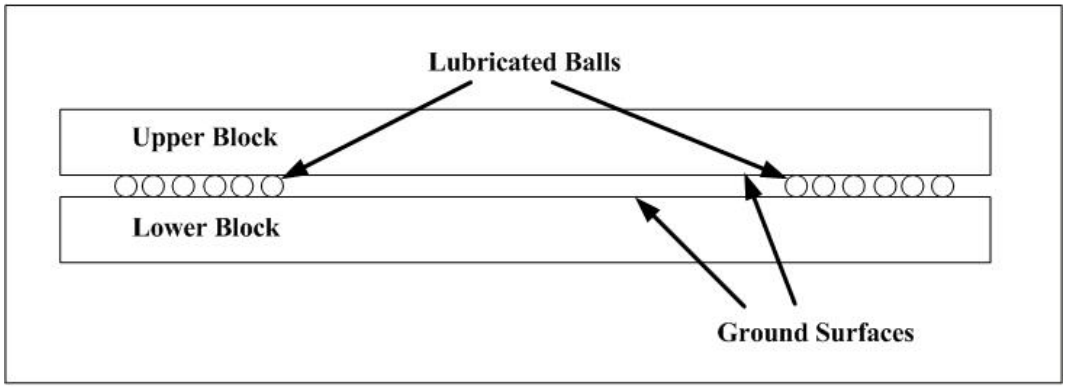

(b)

Figure 4.28: A photo (a) and schematic (b) of the supports

In order to adjust the orientation of the bed properly, an adjustment mechanism consisting of fixed supports and ball ended setscrews (M10) is constituted. The ball ended setscrews enable to apply a point force along the axial direction of the screw. A photo of these setscrews is given in Figure 4.29. The supports used in this mechanism are fixed to the ground at the four corners of the bed via anchor screws as illustrated in Figure 4.30. After the desired orientation on x-y plane is obtained, setscrews (M5) perpendicular to the ball ended setscrews are tightened and the rotations of the ball ended setscrews are restricted. At the end of this procedure, camera positioning system is fixed on x-y plane.

Figure 4.29: Ball ended setscrews

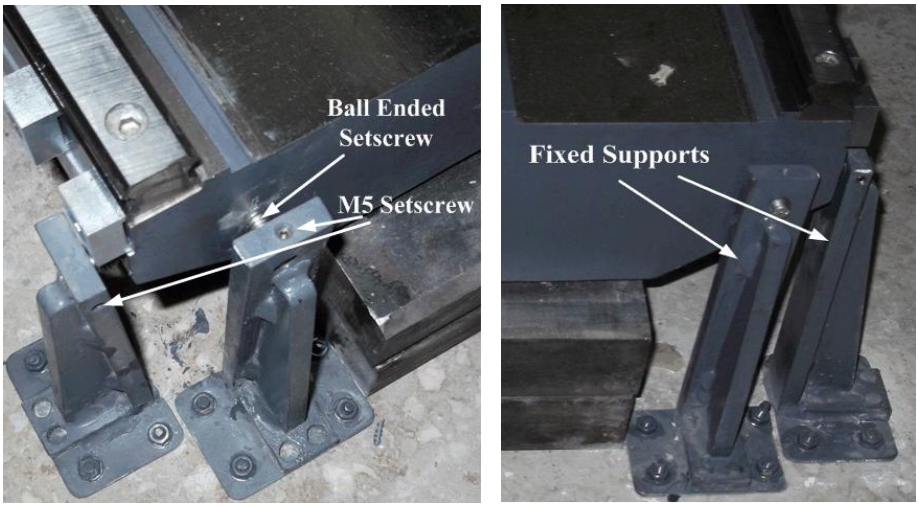

Figure 4.30: Adjustment mechanisms at the corners of the bed

4.6.3.3 Leveling the Camera Positioning System

After the alignment of the camera positioning system along x-axis is set, the last condition to be satisfied is the parallelism of the camera positioning system to the connection plane of the laser beam positioning system. Parallelism of the connection plane to the ground is satisfied by using the precision spirit level (Figure 4.26) as elaborated in Section *4.6.3.1 Leveling the Laser Beam Positioning System Connection Plane*. In order to level the camera positioning system, the same spirit level is utilized while the height of the bed is adjusted via six machine feet (Figure 4.12)

from the bottom of the bed. During this adjustment process the spirit level is placed on the table on which the camera housing is attached. The system is supported by four feet at the corners first. The saddle is translated along x-axis while the change in the bubble position on the vial of the spirit level is monitored. In four-foot condition, angular change during translation is dominantly caused by sagging of the bed. This condition is illustrated in Figure 4.31. At each step of the saddle along x-axis, table is translated on the saddle by aligning the spirit level along y-axis. During this translation, bubble position is monitored again. This time, sagging is less effective. The feet are adjusted to obtain a symmetrical behavior w.r.t. the geometric center of the bed. Following this procedure, angular deviations along the axes are adjusted iteratively.

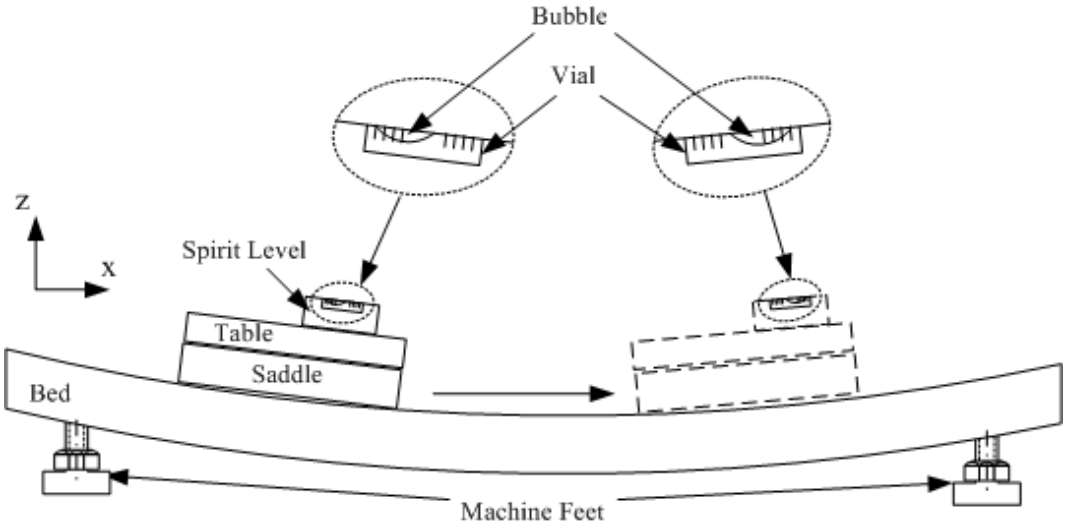

Figure 4.31: Illustration of the camera positioning system leveling

After the adjustments on four feet, two more feet are attached to the bed to minimize the effect of the sagging. Saddle is translated along x-axis to both sides of the additional feet repeatedly and the two feet are adjusted iteratively. At the end of leveling procedure, parallelism of the camera positioning system to the ground is satisfied in several arc seconds range. A detailed tests about this parameter is performed in Section *7.4.1 Spirit Level Tests*.

.

4.7 Closure

In this chapter, development of the calibration setup is explained in details. For the first step, problem definition and the design specifications are introduced. In this part, laser line viewing concept is determined before the overall conceptual design. Concept design is established on the base of laser line detection method in which the laser lines are directed towards the camera sensor plane and the laser positions are determined by positioning the camera precisely on the projection area. Conceptual design is carried out with concept development of the system parts and methods.

In this section, different alternatives for the sub-functions are evaluated. At the end of concept design part, four different concepts are generated for the overall calibration system and a best concept is selected on the basis of Pugh's concept selection method. In detailed design, properties of the system parts and working principles are explained. Engineering calculations of some elements are also included in this section. After the design of the system, manufacturing of the system parts is presented. In this section, all methods and technologies which are used during the manufacturing of the system elements are explained. Finally, assembling procedure of the manufactured system is elaborated.

Some photos of the overall system are given in the following figures. Upper side of the calibration system on which the laser beam positioning system is connected is presented in Figure 4.32. Overall camera positioning system is seen in Figure 4.33. Figure 4.34 shows the saddle, table, and camera platform together with the lower and upper cameras.

Figure 4.32: Upper side of the calibration system together with the laser beam positioning system

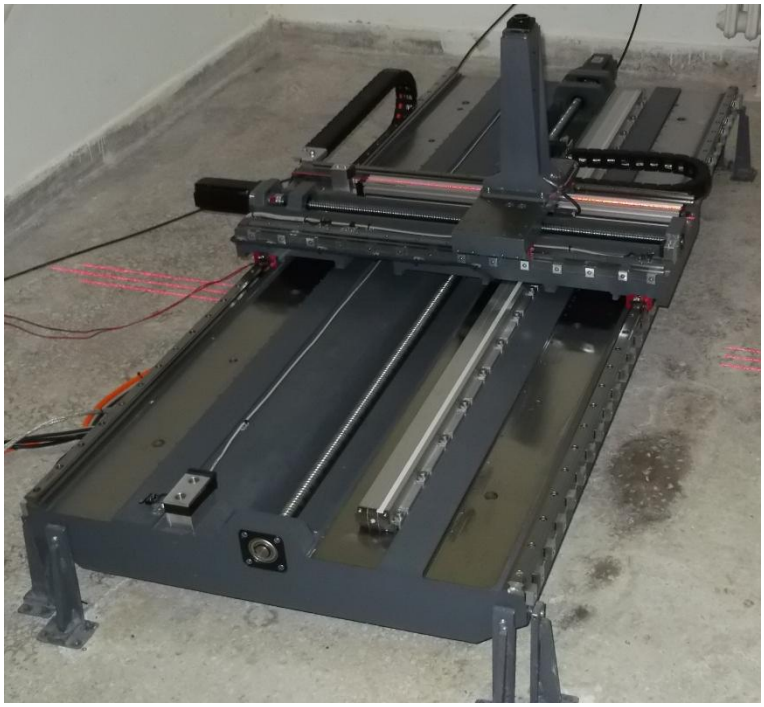

Figure 4.33: Camera positioning system

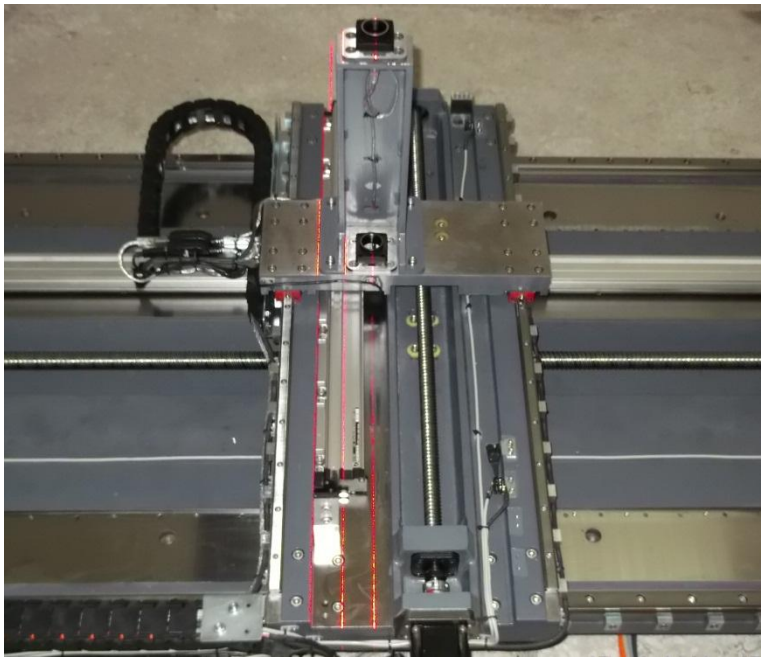

Figure 4.34: Saddle, table and camera platform

CHAPTER 5

CALIBRATION SYSTEM MODELING

5.1 Introduction

In this chapter of the thesis, a kinematic model for the laser beam calibration system is developed. For this purpose, each element of the calibration system with its relative position is determined and a coordinate frame is appropriately placed on it. Homogeneous transformation matrices (HTMs) between the coordinate frames are obtained. Moreover, exit aperture of the laser source is modeled according to some assumptions such that the laser line on the projection surface behaves like the real one. Finally, using the transformation matrices and the model of the laser exit apertures of stationary and movable laser sources, position/orientation of the laser lines are obtained with respect to the relevant frames. The model simulated according to the real calibration procedure. Consequently, the real translational and angular errors of the laser beam positioning system are compared with the measured ones under the static and dynamic errors of the laser positioning system and calibration mechanisms. This kinematic model provides considerable information about the calibration system precision and the parameters which require special care.

5.2 Elements of the Calibration System

Elements of the calibration system related to the kinematic model are bed (base table), saddle, table, camera mounting stage, lower/upper cameras, laser beam positioning system, and stationary/movable laser sources. The descriptions about these elements follow.

- Bed (Base Table)

Upper plane of this table is also the x-y plane of the global reference frame. This table is mounted on the ground and the saddle moves on this table by means of linear guideways. Any form and assembly errors on this table upper plane will manifest themselves as the errors of saddle frame with respect to reference frame.

- Saddle

This part moves along the x-axis of the global reference frame. The coordinate frame on this table is named as “Saddle Frame”. Translational position of this frame along x-axis of the global reference frame changes between 0 and 1600 mm.

- Table (Camera Platform)

This part moves on the saddle by means of linear guideways. This motion is along the y-axis of the saddle frame ranging from -300 to +300 mm.

- Camera Mounting Stage

This element of the system is attached onto the table. It is used for the housing of the cameras. It also gives an offset to the cameras along z-axis of the current frame. To prevent the shadowing of the upper camera to the lower one, an offset along y-axis for upper camera mounting is also given on this part.

- Upper/Lower Cameras

In order to get snapshots the laser lines and determine their position, two CCD cameras are employed in the calibration system. One of them is attached onto the lower connection of the camera mounting stage, and the other one is mounted on the upper one.

- Laser Beam Positioning System

The laser beam positioning system is the system which is to be calibrated and controlled by the calibration system. Laser sources are located along the x-axis of the laser system. This system is attached to a fixed place w.r.t. global reference frame.

- Stationary/Movable Laser Source

Laser source includes a light source and accompanying optics. In the kinematic model, each light source is named as "Laser Focal Point". The laser lens, which is the exit of the laser rays, is modeled as an elliptical aperture. The laser beams pass through this elliptical-shape-exit and then reach to the camera surface. Position of the stationary laser is fixed according to global reference. Movable laser source translates along the guideways.

5.3 Coordinate Frames

A 3D coordinate frame is attached to the elements of the calibration system. There are six different coordinate frames together with the global reference frame. These frames are:

- R: global reference frame,
- S: saddle frame with respect to global reference frame,
- C_1: lower camera frame with respect to saddle frame,
- C_2: upper camera frame with respect to lower camera frame,
- F_1: stationary laser frame with respect to global reference frame,
- F_2: movable laser frame with respect to stationary laser frame.

A schematic representation of the coordinate frames of the camera positioning system is seen in Figure 5.1.

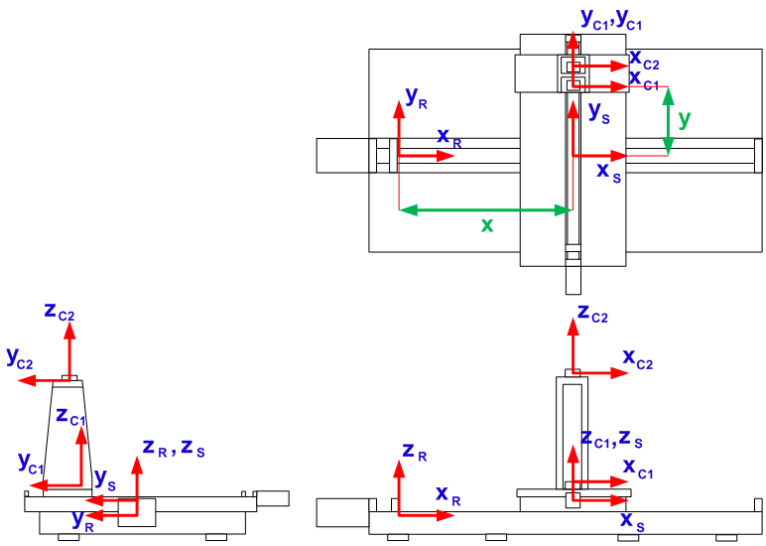

Figure 5.1: Schematic representation of the camera positioning system coordinate frames

As can be seen from Figure 5.1, the saddle frame is translated along the x-axis of global reference frame and lower camera frame is translated along the y-axis of the saddle frame. Note that, Upper camera frame is fixed to the lower camera frame. Stationary laser frame and movable laser frame are illustrated in Figure 5.2.

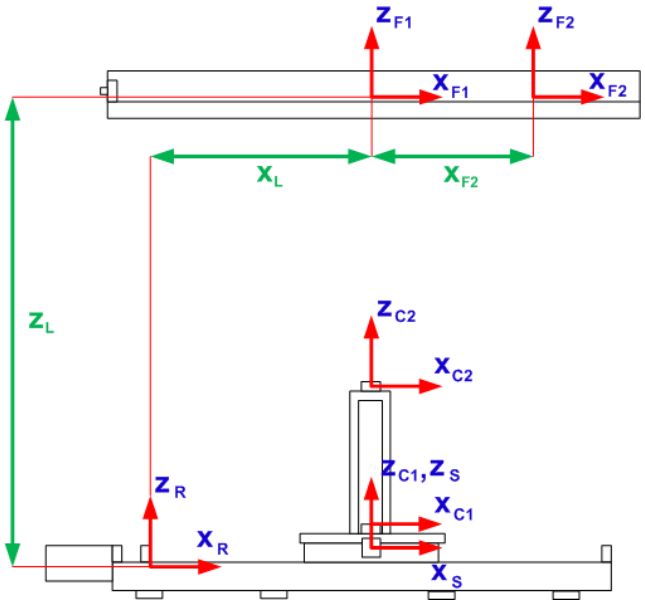

Figure 5.2: Schematic representation of the laser system frame and laser focal point frame together with the global reference frame

Figure 5.2 implies that stationary laser frame is fixed at a position (x_L, z_L) on x-z plane of the global reference frame. Position and orientation errors of this frame caused by the improper mounting of the laser system are static errors of the stationary laser fame. Movable laser frame is translated along the x-axis of stationary laser frame.

5.4 Homogeneous Transformation Matrices

In the development of the kinematic model, spatial transformation which is a mathematical tool allowing coordinate transformation from one reference frame to another (Bajd, 2010) is used. In this transformation, 3D homogeneous transformation matrices between the related coordinate frames are obtained. Equations (5.1), (5.2) , and (5.3) show the transformation of coordinates of a point P_c from coordinate frame *f* to coordinate frame *R*.

$$ {}^{f}P_c = \begin{bmatrix} x_f \\ y_f \\ z_f \\ 1 \end{bmatrix} \tag{5.1} $$

$$ {}^{R}P_c = {}^{R}_{f}T \cdot {}^{f}P_c \tag{5.2} $$

$$ {}^{R}_{f}T = \begin{bmatrix} c\varepsilon_y c\varepsilon_z & -c\varepsilon_y s\varepsilon_z & s\varepsilon_y & x+\delta_x \\ s\varepsilon_x s\varepsilon_y c\varepsilon_z + c\varepsilon_x s\varepsilon_z & -s\varepsilon_x s\varepsilon_y s\varepsilon_z + c\varepsilon_x c\varepsilon_z & -s\varepsilon_x c\varepsilon_y & y+\delta_y \\ -c\varepsilon_x s\varepsilon_y c\varepsilon_z + s\varepsilon_x s\varepsilon_z & c\varepsilon_x s\varepsilon_y s\varepsilon_z + s\varepsilon_x c\varepsilon_z & c\varepsilon_x c\varepsilon_y & z+\delta_z \\ 0 & 0 & 0 & 1 \end{bmatrix} \tag{5.3} $$

where *c* and *s* represent trigonometric cosine and sine functions, respectively. ε's and δ's are angular and translational errors of relevant axis, respectively. *x*, *y*, and *z* are the coordinates of the origin of the relevant frame w.r.t. reference frame.

Since there is no angular positioning in the calibration setup, only the components related to translational positions, translational errors, and angular errors are included in (5.3).

Equation (5.1) shows the coordinates of the point P_c with respect to coordinate frame *f*. Matrix operation given in (5.2) gives the same point with the coordinates w.r.t. coordinate frame *R*. The main issue in this operation is to obtain the homogeneous transformation matrix between the two coordinate frames given in (5.3).

The procedure shown in equations (5.2), (5.3), and (5.1) is implemented in MATLAB software and a function **`cordtrans`** is developed for this purpose. This function is one of the main parts

of the kinematic model of the calibration system. The relevant M-file of **`cordtrans`** is given in appendix. The function accepts an input of a vector with nine elements. The output of the function is a 4-by-4 matrix (homogeneous transformation matrix). Elements of the input vector are:

- Translational x position of the frame *f* w.r.t frame *R*,
- Translational y position of the frame *f* w.r.t frame *R*,
- Translational z position of the frame *f* w.r.t frame *R*,
- Translational error of frame *f* along x-axis of frame *R*,
- Translational error of frame *f* along y-axis of frame *R*,
- Translational error of frame f along y-axis of frame *R*,
- Angular error of frame *f* around x-axis of frame *R*,
- Angular error of frame *f* around y-axis of frame *R*,
- Angular error of frame *f* around z-axis of frame *R*.

In the kinematic model, camera plane and laser focal points are determined according to global reference plane.

In order to determine the camera plane w.r.t. global reference plane, coordinates of the points on the camera planes are transformed two times. At the first time, they transformed to saddle frame. Then, the points obtained with respect to saddle frame are transformed to the global reference frame. The equivalent HTM is calculated by means of the matrix multiplication operation between the homogeneous transformation matrices at the two steps. This operation can be given as:

$$ {}^{R}_{C}T = {}^{R}_{S}T \cdot {}^{S}_{C}T \tag{5.4} $$

where ${}^{S}_{C}T$ is the transformation matrix between the camera and saddle coordinate frames. Similarly, ${}^{R}_{S}T$ is the transformation matrix between the saddle and global reference coordinate frames. The resultant matrix ${}^{R}_{C}T$ is the transformation matrix between the camera and global reference frames.

An important parameter about matrices ${}^{S}_{C}T$ and ${}^{R}_{S}T$ is that the angular and translational error parameters inside the matrices are the functions of translational positions. As can be seen from Figure 5.1, lower camera frame is translated along y-axis of saddle frame and saddle frame is translated along the x-axis of the global reference frame. Then, the translational and angular error components in ${}^{S}_{C}T$ are functions of y, and the error components in ${}^{R}_{S}T$ are functions of x. In other words, for each x and y positions of the lower camera and saddle, different error values are executed.

Although, the stationary laser focal point is defined w.r.t. global reference frame, inputs of movable laser focal point are given w.r.t. stationary laser frame. Hence, in order to obtain the

movable laser focal point coordinates w.r.t. global reference frame, following matrix multiplication should be performed.

$$ {}^{R}_{F2}T = {}^{R}_{F1}T \cdot {}^{F1}_{F2}T \tag{5.5} $$

where ${}^{R}_{F2}T$ is the transformation matrix between movable laser frame and global reference frame. Similarly, ${}^{R}_{F1}T$ is the transformation matrix between the stationary laser frame and global reference frame. Translational and angular error parameters inside the matrix ${}^{R}_{F1}T$ are static errors which have no dependency to the translational position input. The error components of this matrix are caused by the mounting inaccuracies of the laser positioning system. However, translational and angular error components of transformation matrix between the movable laser frame and the stationary laser frame, ${}^{F1}_{F2}T$, are functions of x (i.e. the translational position of the movable laser focal point along the x-axis of stationary laser frame).

5.5 Obtaining the Laser Projection on the Camera x-y Plane

A straightforward method for determination of the laser projection on the camera plane is developed for the kinematic model of the calibration system.

In this method, laser exit is modeled according to the projected laser line behavior. Laser exit has a diameter of 5 mm. Laser source has a fan angle of 45º and straightness tolerance of 0.1 mm for 1 m projection distance. Depending upon this specification, a laser lens exit model is developed.

It is assumed that laser beam segments pass through an elliptical aperture located on a plane at -6 mm on z-axis of each laser frame. A schematic view of the exit aperture model is given in Figure 5.3.

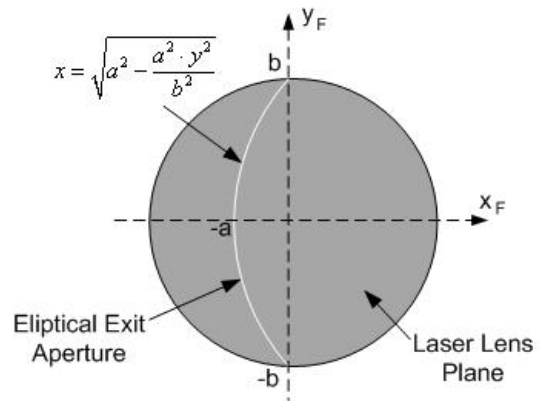

Figure 5.3: Schematic view of laser exit aperture model

Parameters of the elliptical exit are determined such that y-intercept is determined by laser exit diameter and x-intercept is obtained from the straightness specification of the laser source.

In the developed model, finite number of laser beams emitted from laser focal point. Each one of these beams passes through a point on the elliptical exit aperture. Eventually, each beam intersects the camera sensor plane. The set of the points intersecting the camera sensor plane forms the projected elliptical laser curve with the pre-determined straightness error. This model is illustrated in Figure 5.4.

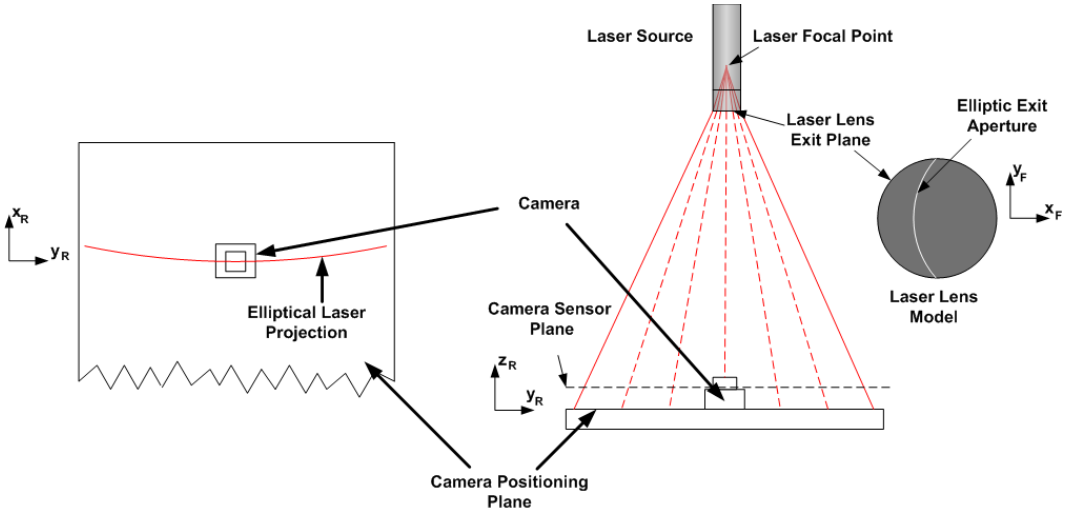

Figure 5.4: Schematic illustration of laser lens modeling and determination of laser projection curve on the camera sensor plane

In the model, camera planes, focal point of each laser source, and the points on the elliptical exits of each laser are determined with respect to global reference plane under the effect of introduced errors. Hence, intersection of the camera plane and the line passing through the laser focal point and a specified point on elliptical laser exit is calculated. This action is repeated for finite number of points on elliptical laser exit.

In order to generate the points on the elliptical laser exit, function **`ellipse`** is developed. Inputs of this function are straightness error of the laser projection for 1 m projection distance and number of the points on the elliptical curve with constant increments.

In determination of the intersection of a plane and a line passing through two certain points in 3D space, a function **`intersect_plane`** is developed. Inputs of this function are two points through which the line passes and any three points on the plane. Input vectors are in the form given in Equation (5.6). Elements of each vector are the coordinates of the related point.

$$ {}^{L}P_1 = \begin{bmatrix} {}^{L}x_1 \\ {}^{L}y_1 \\ {}^{L}z_1 \end{bmatrix} \; {}^{L}P_2 = \begin{bmatrix} {}^{L}x_2 \\ {}^{L}y_2 \\ {}^{L}z_2 \end{bmatrix} \; {}^{P}P_1 = \begin{bmatrix} {}^{P}x_1 \\ {}^{P}y_1 \\ {}^{P}z_1 \end{bmatrix} \; {}^{P}P_2 = \begin{bmatrix} {}^{P}x_2 \\ {}^{P}y_2 \\ {}^{P}z_2 \end{bmatrix} \; {}^{P}P_3 = \begin{bmatrix} {}^{P}x_3 \\ {}^{P}y_3 \\ {}^{P}z_3 \end{bmatrix} \tag{5.6} $$

The plane formed by the points ${}^{P}P_1$, ${}^{P}P_2$, and ${}^{P}P_3$ given in (5.6) has a plane equation given in (5.7).

$$ Ax + By + Cz + D = 0 \tag{5.7} $$

One of the main problems is to determine the coefficients of the plane equation in (5.7) by using the coordinate information of the points on it. These coefficients are determined by calculating the following determinants.

$$ A = \begin{vmatrix} 1 & {}^{P}y_1 & {}^{P}z_1 \\ 1 & {}^{P}y_2 & {}^{P}z_2 \\ 1 & {}^{P}y_3 & {}^{P}z_3 \end{vmatrix} \tag{5.8} $$

$$ B = \begin{vmatrix} {}^{P}x_1 & 1 & {}^{P}z_1 \\ {}^{P}x_2 & 1 & {}^{P}z_2 \\ {}^{P}x_3 & 1 & {}^{P}z_3 \end{vmatrix} \tag{5.9} $$

$$ C = \begin{vmatrix} {}^{P}x_1 & {}^{P}y_1 & 1 \\ {}^{P}x_2 & {}^{P}y_2 & 1 \\ {}^{P}x_3 & {}^{P}y_3 & 1 \end{vmatrix} \tag{5.10} $$

$$ D = -\begin{vmatrix} {}^{P}x_1 & {}^{P}y_1 & {}^{P}z_1 \\ {}^{P}x_2 & {}^{P}y_2 & {}^{P}z_2 \\ {}^{P}x_3 & {}^{P}y_3 & {}^{P}z_3 \end{vmatrix} \tag{5.11} $$

After determining the plane equation coefficients, lie equation parameter is determined as in (5.12) for the point intersecting the plane.

$$ t = \frac{A \cdot {}^{L}x_1 + B \cdot {}^{L}y_1 + C \cdot {}^{L}z_1 + D}{A \cdot \left({}^{L}x_1 - {}^{L}x_2 \right) + B \cdot \left({}^{L}y_1 - {}^{L}y_2 \right) + C \cdot \left({}^{L}z_1 - {}^{L}z_2 \right)} \tag{5.12} $$

Finally, the coordinates of the intersection point is found by substituting this parameter in (5.12) into the line equation:

$$ P = {}^{L}P_1 + t \cdot ({}^{L}P_2 - {}^{L}P_1) \tag{5.13} $$

The calculated point P in (5.13) is the intersection point of the line and the plane. After determining the intersection points with respect to global reference frame, locations of the same

points with respect to camera frame are determined by multiplying each point by the inverse of the homogeneous transformation matrix between the camera frame and the global reference frame.

5.6 Input Matrices

In the kinematic model, system matrices including the relative positions and static/dynamic errors of the system elements are taken as a ".mat" file. The system matrices are as follows:

- F1 (1×9): stationary laser input matrix w.r.t. global reference frame,
- F2 (n×9): movable laser input matrix w.r.t. stationary laser frame,
- S (n×9): Saddle input matrix w.r.t. global reference frame,
- C1 (m×9): Lower camera input matrix w.r.t. saddle frame,
- C2 (1×9): Upper camera input matrix w.r.t. lower camera frame.

where m and n are the number of measurement points (i.e. measurement resolution) along y-axis of the saddle frame and x-axis of the global reference frame, respectively.

5.7 Error Vectors

The aim of the kinematic model is to determine the difference between the real errors and the measured ones. For this purpose six different error vectors are assigned in the model. Each element of the vectors represents the relevant error (real or measured) at the relevant x-position of the movable laser. The error vectors are the followings:

- **`E_pos_mov_real`**: Real positioning errors of the movable laser w.r.t. the stationary laser,
- **`E_line_angle_real`**: Real projection line angle errors of the movable laser w.r.t. the stationary laser,
- **`E_exit_angle_real`**: Real beam exit angle errors of the movable laser w.r.t. the stationary laser,
- **`E_pos_mov_measured`**: Measured positioning errors of the movable laser w.r.t. the stationary laser,
- **`E_line_angle_measured`**: Measured projection line angle errors of the movable laser w.r.t. the stationary laser,
- **`E_exit_angle_measured`**: Measured beam exit angle errors of the movable laser w.r.t. the stationary laser.

5.8 Measurement of Position, Projection Line Angle, and Beam Exit Angle

During the measurements, relevant raw (depending on the nominal x and y positions) of the input matrices of saddle and lower camera are used for current x and y positions.

Lower camera takes measurements along the laser projection between the y-axis limits (-300 mm, 300 mm) for the nominal fixed x-position of the laser projection line.

At each position (x, y), laser projection on the lower camera plane is calculated w.r.t. lower camera frame. Location of the laser projection line is calculated with function **`cam_measure`** which is given in appendix. Line angle of the laser projection is calculated via the function **`line_angle`**.

For the calculation of the position and the beam exit angle **`cam_measure`** is executed with the laser projection curve when the lower camera frame is at y = 0 w.r.t. the saddle frame. After that, upper camera y-axis offset is compensated (i.e. Lower camera is located at y = -40 mm.) and **`cam_measure`** is executed for the projection curve on the upper camera plane w.r.t. upper camera frame. Hence, the same portion of the laser beam is measured at two different elevations. Dividing the difference between the two measurements (measurements of the lower camera and upper camera) to the z-axis offset of the upper camera w.r.t. the lower camera gives the beam exit angle of the laser. Position errors on the lower camera plane caused by the laser source positioning and laser beam exit angle are decoupled by using the calculated laser beam exit angle. Hence, laser source positioning error is calculated by subtracting the position change caused by the laser beam exit angle from the measured position error on the lower camera.

5.9 Simulation Steps

A single run of the kinematic model simulates a real calibration procedure in which the laser source positioning error, laser projection line angle error, and laser beam exit angle error are measured. In the model, some static and dynamic errors are given to the laser beam positioning system. These errors are determined by considering the assembly of the laser system to the calibration setup, attachment of the laser sources to the laser system, and the precision of linear positioning elements of the laser system. Consequently, movable laser source positioning errors, projection line errors, and beam exit angle errors w.r.t stationary laser are calculated along its travel. These parameters (i.e. position error, projection line angle error, and beam exit angle error) are also calculated by the camera measurements under the effects of the static and dynamic errors of the camera positioning system. Difference between the real errors and the measured ones presents the calibration system measurement capability under the given conditions.

The mentioned calibration simulation consists of several steps. These steps are elaborated in this section.

Step 1: Assignment of the input matrices,

Step 2: Calculation of the positions of the points on the elliptical exits on the laser sources in 3D w.r.t. the coordinate frame of the relevant laser frame,

Step 3: Assignment of the error vectors (empty at the beginning),

Step 4: Determination of the real error components (laser source position, projection line angle, and beam exit angle) for each nominal x position and putting these values to the elements of the real error vectors,

Step 5: Determination of the stationary laser focal point and the points on its elliptical exit w.r.t. global reference frame,

Step 6: Determination of the camera planes w.r.t. global reference frame for nominal x position of the stationary laser,

Step 7: Measurement of laser source position, projection line angle, and beam exit angle of the stationary laser

Step 8: Determination of the stationary laser focal point and the points on its elliptical exit w.r.t. global reference frame for the initial nominal x position of the movable laser,

Step 9: Determination of the camera planes w.r.t. global reference frame for initial nominal x position of the movable laser,

Step 10: Measurement of laser source position, projection line angle, and beam exit angle of the movable laser for its initial nominal position,

Step 11: Calculation of the movable laser errors for the laser source position, projection line angle, and beam exit angle by subtracting the measured parameters of the movable laser from those of stationary laser and assigning these values (i.e. calculated errors) as the first elements of the measured error vectors,

Step 12: Repeating steps 8 to 11 for each nominal x position (depending on the selected x-axis position resolution) of the movable laser successively,

Step 13: Calculating the measurement errors by taking the difference of relevant measured and real error vectors,

Step 14: Plotting the data.

For a sample calculation, following static errors are executed with the model.

- Rotational error of the laser system (stationary laser source) around z-axis: 0.005 rad
- Translational error of the upper camera along x-axis: 3 mm
- Translational error of the upper camera along y-axis: 3 mm
- Translational error of the upper camera: 1 mm
- Laser line straightness for 1 m projection distance: 0.1 mm

The output graphs are presented in Figure 5.5, Figure 5.6, and Figure 5.7. Figure 5.5 is for movable laser source positioning error w.r.t. the stationary laser. As can be seen from the upper sub-plot, real positioning error is zero for each position since the dynamic error components of the movable laser source are all zero. Calibration system measurements deviates from the real error due to the given system errors. The lower sub-plot presents the measurement error. In Figure 5.6, projection line angle error is given. Under this condition, maximum measurement error is about 8

μm. Similar to the laser source position error; real projection line angle error of the movable laser w.r.t. stationary laser is zero for all positions. The measured values of this parameter increases with the positioning distance due to the given errors. It reaches to about 0.4 arcsec at 1600 mm positioning distance. Real and measured beam exit angle errors of the movable laser w.r.t. stationary laser are both zero along the positioning axis. This means that the given errors affect the beam exit angle of both stationary and movable laser in the same amount with the same direction.

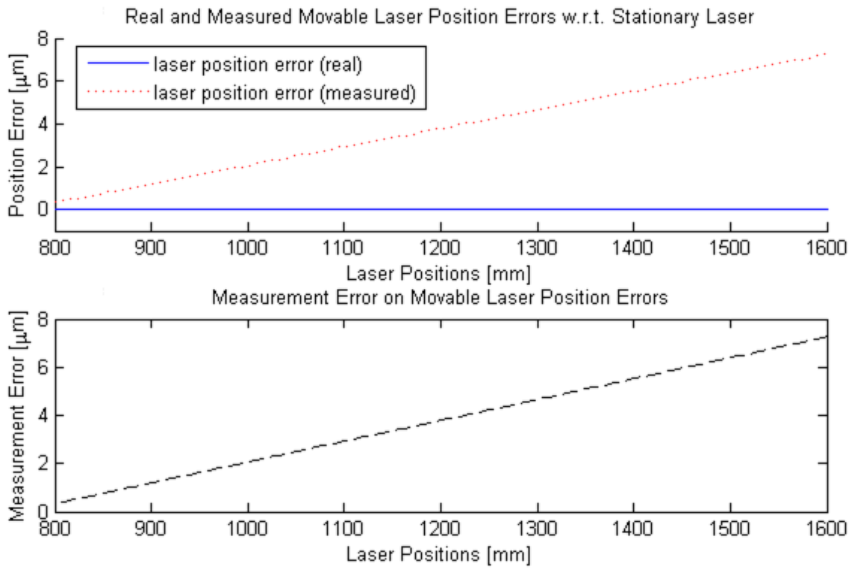

Figure 5.5: Output of the kinematic model for the laser source position with the given errors

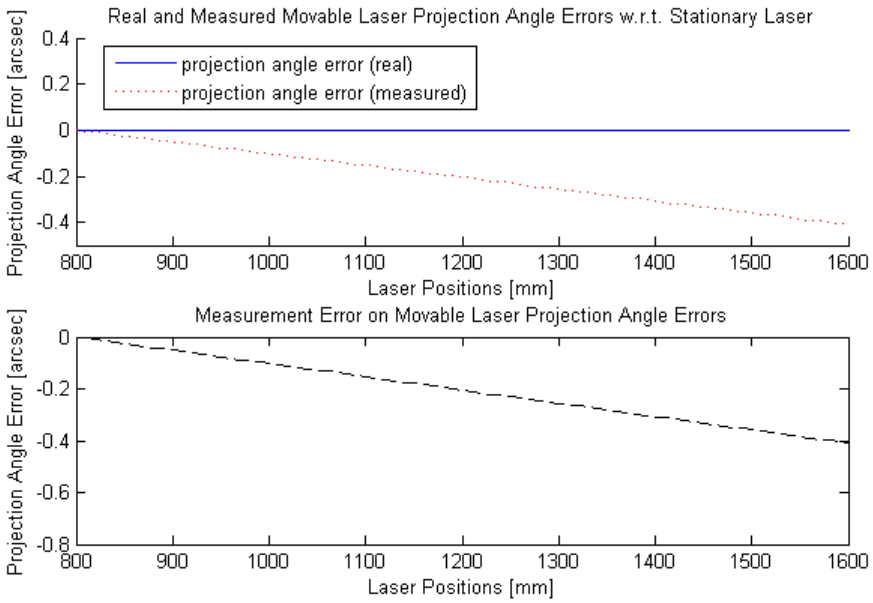

Figure 5.6: Output of the kinematic model for the projection line angle with the given errors

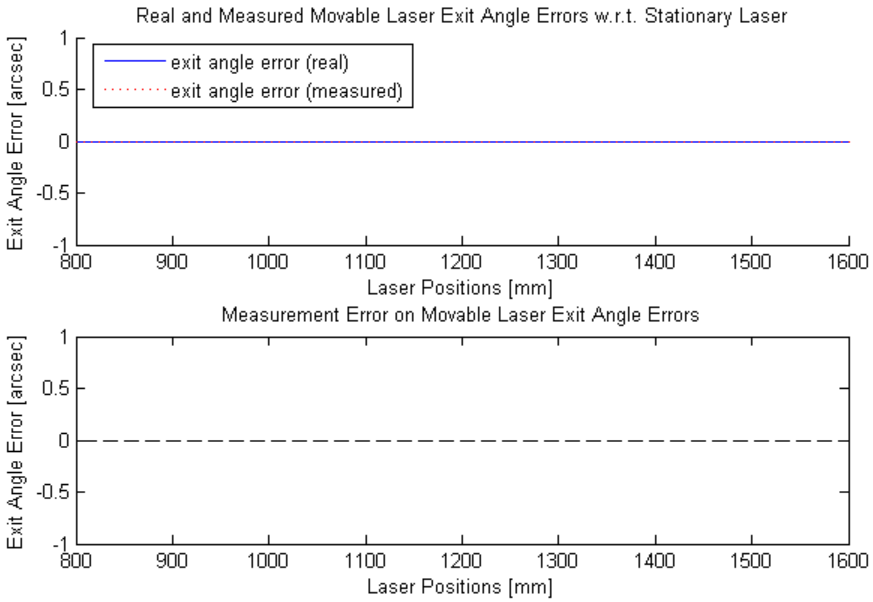

Figure 5.7: Output of the kinematic model for the beam exit angle with the given errors

5.10 Determination of the Static and Dynamic Errors

According to the design specifications presented in Section *4.2 Problem Definition and Design Specifications*, developed system must have measurement accuracy of: i) ±20 μm for laser source position, ii) ±8 arcsec for projection laser line angle, iii) ±3 arcsec for laser beam exit angle.

There are static (constant with camera and movable laser position) and dynamic (change with camera or movable laser position) error components affecting resultant measuring accuracy. In order to determine the effects of the error components on the overall measuring accuracy, these components are divided into two groups as static and dynamic errors. A series of calculations are performed and the results are presented in this section.

5.10.1 Static Errors

Some errors in the calibration system are independent from the camera and movable laser positions. In the kinematic model, these are named as static errors. These types of errors are originated from improper attachment of elements and misalignments of the axes.

There are sixteen different static error components in the calibration system kinematic model. Magnitude of each component is determined intuitively according to the relevant assembling capability. Note that the magnitudes are all given as positive in this step. These errors are listed in the following table.

Table 5.1 Static error estimations

Coordinate Frame	**Error Component**	**Magnitude**	**Unit**
F1	δ_y	5.000	mm
F1	ε_x	0.005	rad
F1	ε_y	0.003	rad
F1	ε_z	0.003	rad
F2	δ_y	2.000	mm
F2	δ_z	3.000	mm
F2	ε_x	0.010	rad
C1	ε_x	0.005	rad
C1	ε_y	0.005	rad
C1	ε_z	0.005	rad
C2	δ_x	3.000	mm
C2	δ_y	3.000	mm
C2	δ_z	3.000	mm
C2	ε_x	0.005	rad
C2	ε_y	0.005	rad
C2	ε_z	0.005	rad

The estimated error values listed in Table 5.1 are used in the kinematic model. Note that although the error components of movable laser and lower camera changes with position, some of the error components are seen on the estimated static error table. Static errors are major parts of these components and entered to each position as the same value. Dynamic parts are relatively smaller and to be added up to these static parts in the following section. The obtained results are presented in Figure 5.8, Figure 5.9, and Figure 5.10.

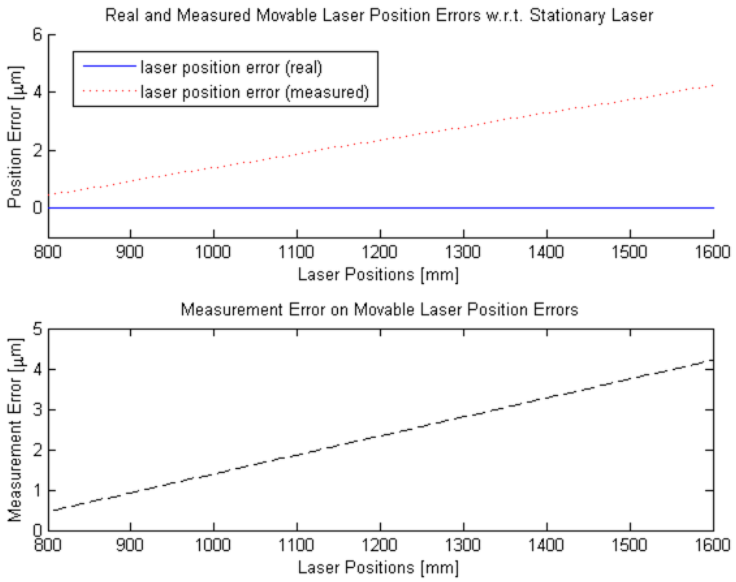

Figure 5.8: Laser source position error output for the estimated static inputs

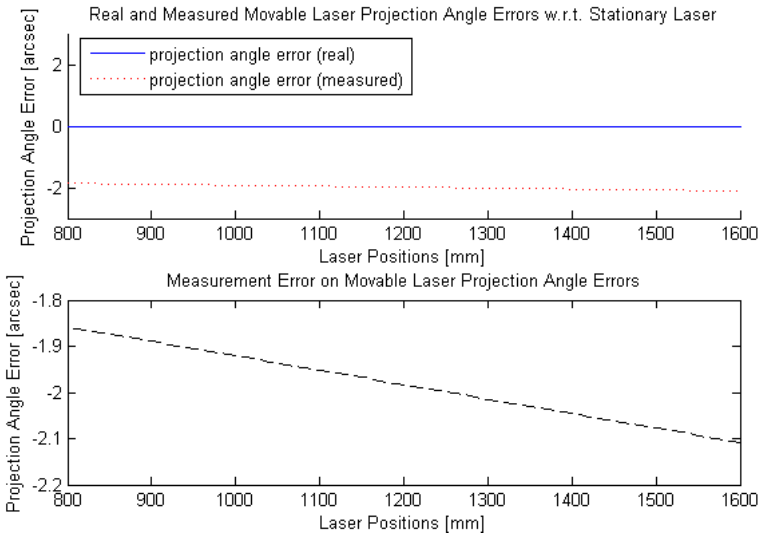

Figure 5.9: Projection laser line angle error output for the estimated static inputs

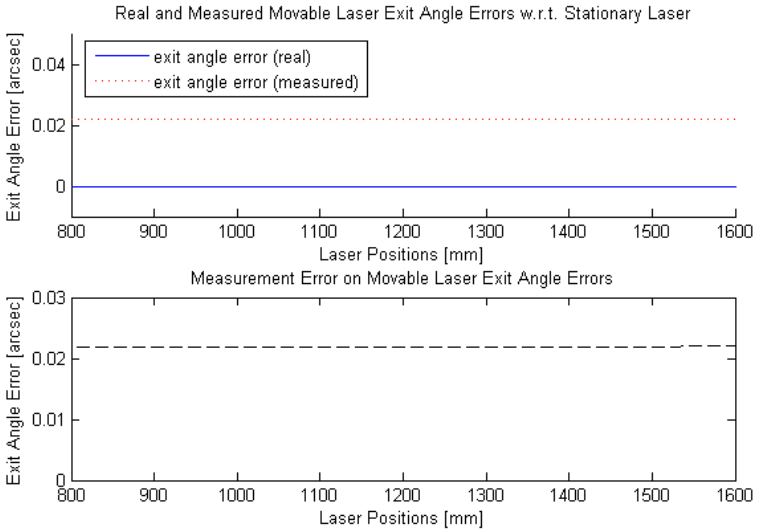

Figure 5.10: Beam exit angle error output for the estimated static inputs

Under the effect of the estimated static error inputs maximum errors of laser position, projection line angle, and beam exit angle measurements are computed as 4 μm, -2.1 arcsec, and 0.022 arcsec respectively.

In order to determine the sign (i.e. positive or negative) of each static error component raising the measurement error, each component is tested one by one. At each step, one item from Table 5.1 is excluded and the three errors (i.e. measurement errors of laser position, projection line angle, and beam exit angle) are recalculated. If the calculated maximum measurement error is less than the initial one, this means that the sign of the relevant error component is to be taken as positive for the relevant measurement error calculation. Otherwise, it should be negative. This procedure is presented in Table 5.2. E_{pos}, E_{line}, and E_{exit} represent the maximum measurement errors of laser source position, projection line angle, and beam exit angle respectively. Note that selected sign of an error component may be different for different measurement errors. Hence, the sign combinations of the static error components are handled independently for each one of the three measurement error calculations.

According to the sign selection of each static error component individually, resultant maximum measurement errors change. Using the same magnitudes presented in Table 5.1 and the signs specified in Table 5.1, maximum measurement errors due to the static error components are computed as 6 μm, -2.103 arcsec, and 0.251 arcsec for laser source position, projection line angle, and beam exit angle respectively. System requirements are ±20 μm, ±8 arcsec, and ±3 arcsec.

Table 5.2: Sign determination of estimated static errors

Trial #	E_{pos} [mm]	E_{line} [arcsec]	E_{exit} [arcsec]	Excluded Item	Effect of Inclusion		
1	0.004	-2.103	0.022	-	E_{pos}	E_{line}	E_{exit}
2	0.005	-2.101	0.032	F1 δ_y	-1	1	-1
3	0.004	-2.099	0.018	F1 ε_x	1	1	1
4	0.003	-2.099	0.022	F1 ε_y	1	1	1
5	0.001	-2.085	0.017	F1 ε_z	1	1	1
6	0.005	-2.098	0.022	F2 δ_y	-1	1	1
7	0.003	-2.104	0.022	F2 δ_z	1	-1	1
8	0.004	-1.040	0.022	F2 ε_x	1	1	1
9	0.005	-2.103	0.041	C1 ε_x	-1	1	-1
10	0.003	-2.103	0.022	C1 ε_y	1	1	1
11	0.003	-2.103	0.218	C1 ε_z	1	1	-1
12	0.003	-2.103	0.022	C2 δ_x	1	1	1
13	0.003	-2.103	0.011	C2 δ_y	1	1	1
14	0.003	-2.103	0.022	C2 δ_z	1	1	1
15	0.003	-2.103	0.022	C2 ε_x	1	1	1
16	0.003	-2.103	0.022	C2 ε_y	1	1	1
17	0.003	-2.103	0.025	C2 ε_z	1	1	-1
			Maximum Error:		0.006 [mm]	-2.103 [arcsec]	0.251 [arcsec]

5.10.2 Dynamic Errors

Elements of the calibration system which are subjected to translational motion cause different errors for different positions along the translation axes due to several reasons such as:

- Geometric and dimensional inaccuracies of linear guideways, ball screws, and timing belt of the laser beam positioning system,
- Geometric and dimensional inaccuracies of planes which are precision ground for linear guideways and linear encoders,
- Static and dynamic deflections of the bed and the saddle under the influence of weight,
- Positioning errors of the motors.

These types of errors are named as dynamic errors in the kinematic model. Different from the static errors, effects of dynamic errors on the measurements are tested by running the model

repetitively while the errors are defined as a random number in a pre-determined band. After the results are obtained, maximum measurement errors calculated are taken in the consideration. If the obtained errors are exceeds the limits presented presented in Section *4.2 Problem Definition and Design Specifications*, the error bands are updated.

Dynamic errors are included in the calculations together with the static error inputs determined in the previous section. Since the laser source position measurement error seems to be more critical than the other two measurement errors, sign combination given for this error is used.

Translational and rotational errors of movable laser frame (F2) and saddle frame (S) change with x position while those of the lower camera change with y position. At each step, model is executed 200 times. After several updates, error bands presented in Table 5.3 are determined to satisfy the requirements of the measurement errors. Under the effects of the dynamic errors presented in Table 5.3 and static errors presented in Section *5.10.1 Static Errors* maximum measurement errors of laser source position, projection line angle, and beam exit angle are computed as 19 μm, 5 arcsec, and 2 arcsec respectively.

Table 5.3: Dynamic error tolerances

Coordinate Frame	**Error Component**	**Magnitude**	**Unit**
F2	δ_x	±0.100	mm
F2	δ_y	±0.002	mm
F2	δ_z	±0.002	mm
F2	ε_x	±0.0005	rad
F2	ε_y	±0.0005	rad
F2	ε_z	±0.0005	rad
S	δ_x	±0.005	mm
S	δ_y	±0.002	mm
S	δ_z	±0.003	mm
S	ε_x	±0.00003	rad
S	ε_y	±0.00005	rad
S	ε_z	±0.000025	rad
C1	δ_x	±3.000	mm
C1	δ_y	±0.005	mm
C1	δ_z	±0.005	mm
C1	ε_x	±0.005	rad
C1	ε_y	±0.005	rad
C1	ε_z	±0.005	rad

5.11 Closure

In this chapter a kinematic model representing the calibration system together with the laser beam positioning system is developed. System elements are elaborated initially and coordinate frames of relevant elements are presented. Utilization of homogeneous transformation matrices and

assumption made to create the kinematic model are clarified. Inputs and outputs of the model together with the execution procedure and the employed MATLAB functions presented. In the final section, tolerance bands for static and dynamic errors of the calibration system are determined via the kinematic model developed.

CHAPTER 6

SYSTEM INTEGRATION

6.1 Introduction

This chapter is dedicated to the integration of calibration system elements. In this part of the thesis, the main elements (hardware and software), communication structure, and working principles of the calibration system are clarified. Calibration procedure is also elaborated.

6.2 Calibration System Hardware

The basic components of the calibration system are as follows: i) servo drives of the translational axes, ii) linear encoders, iii) limiting and homing switches, iv) lower and upper cameras, and v) laser beam positioning system.

Actuation and position control of the translational axes (x-axis and y-axis) are carried out by Delta ASDA-A2 AC servo drivers. 750 W and 400 W models are used for x and y axes respectively. These devices facilitating the motion control of rotational or translational systems are quite useful and user friendly system elements facilitating the motion control of rotational or translational systems. These drivers work with set parameters. Each parameter is associated with a register. By writing to these registers, mechanical and electronic parameters can be adjusted. Note that these parameters can be set by means of a PC or the keypad onboard. Heidenhain LS type optical linear encoders are used in the calibration system as the precise position feedback devices. These encoders have 250 nm measurement resolution with ±3 µm accuracy. The encoders are connected to motor drivers. Omron SS-5GL2 type limit switches and Omron EE-SX674 slot type photo-micro-sensor homing switches are used on the axes. These switches are connected to digital input pins of the drivers and defined as the limit and homing signals setting the related parameters. Type of the homing action is also defined with these parameters. Lower and upper cameras are mounted to camera stage and connected to PC by means of USB port. Since the standard cables of the cameras are shorter than the required length (about 5 m), USB to USB active extension cables are used. Laser beam positioning system elaborated in Chapter 3 is connected to the system via RS-232.

Schematic of the calibration system is presented in Figure 6.1. This figure represents the block diagram of the setup. PC is the host controller of the system. Motor drivers and laser positioning system are controlled by the software run by the PC. Data collected from the cameras is also executed by this software.

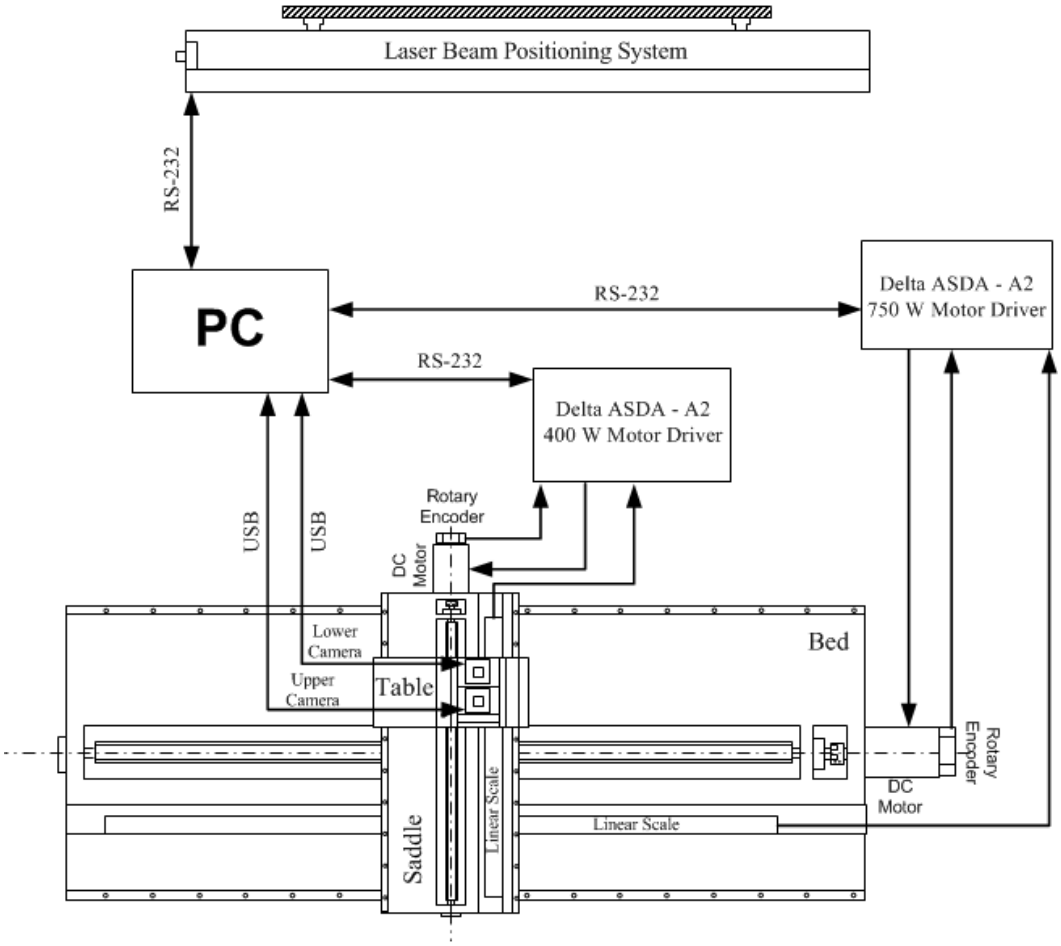

Figure 6.1: Schematic of the calibration system hardware

6.3 Communication Structure of the System Elements

As can be seen from Figure 6.1, system PC is in communication with servo drivers, laser system, and cameras. *Modbus* protocol is implemented for the communication between the PC and the derivers. A special protocol is developed for the control of the laser beam positioning system. Camera communication is carried out via the C# libraries supplied by the camera manufacturer Point Grey Research Inc. company.

- Servo Drivers

All operations about the servo drivers like control, state monitoring, and programming are implemented via serial communication. Desired communication mode is selected by setting the communication parameters of the drivers. In the calibration system communication mode parameter of each driver is set to 0 in order to select RS-232 serial communication interface. Other communication parameters, which should be set for proper communication, are communication address setting, transmission speed, and communication protocol.

- Communication Address Setting

When using serial communication interfaces each servo drive has a pre-assigned communication address. The computer of the system controls each servo drive according to its communication address. For this reason, communication slave address of each driver in the network should be set to a pre-determined number in hexadecimal format.

- Transmission Speed Selection

This parameter is used to set the data transmission speed of the communications. In the calibration system the data transmission speed is selected as 500K bits/sec.

- Communication Protocol Selection

This parameter is to set the communication protocol. There are several communication mode alternatives (such as modbus ASCII and modbus RTU) according to number of data bits, parity (even, odd, or non-parity) bit, and number of stop bits of the data in communication.

In modbus American Standard Code for Information Interchange (ASCII) mode, each 8-bit data in message is sent as two ASCII characters between the master and the slave (PC and servo drive). Similarly, in modbus RTU (Remote Terminal Unit) mode, each 8-bit data is the combination of two 4-bit hexadecimal characters. Comparing to ASCII mode, transmission speed of RTU mode is better.

Format of each data package in ASCII mode is given in Table 6.1.

Table 6.1: Data package in ASCII mode

Start	Start character ':'
Slave Address	Communication address: 1-byte consists of 2 ASCII characters
Function	Function code: 1-byte consists of 2 ASCII characters
Data (n-1)	Contents of data: n word = n × 2-byte consists of n × 4 ASCII characters n≤10
…	
Data (0)	
LRC	Error checking: 1-byte consists of 2 ASCII characters
End 1	End code 1: (CR)
End 0	End code 0: (LF)

According to data package format given in Table 6.1, the communication protocol in ASCII mode starts with a start character ':'. Slave address is expressed with 2 ASCII characters. Function represents the application performed with the data such as writing single word, writing n words, or reading n words. Each function has a specific hexadecimal code. LRC (longitudinal redundancy check) is an error check which is calculated by summing all the bytes in package up and taking 8-bit two's complement of the sum. CR (carriage return) and LF (line feed) is a special sequence of characters specifying the end. Format of each data package in RTU mode is given in Table 6.2.

Table 6.2: Data package of RTU mode

Start	A silent interval of more than 10 ms
Slave Address	Communication address: 1-byte
Function	Function code: 1-byte
Data (n-1)	Contents of data: n word = n × 2-byte n≤12
…	
Data (0)	
CRC	Error checking: 1-byte
End 1	A silent interval of more than 10 ms

According to data package format given in Table 6.2, the communication protocol in RTU mode starts with a silent interval and ends with a silent interval as well. There are communication address, function code, contents of the data, and CRC (cyclical redundancy check) between start and end.

Although communication transmission speed of RTU mode is higher than that of ASCII mode, it must be guaranteed that there is no delay in the communication for RTU mode since it takes silent interval of more than 10 ms as start or end signal.

In the calibration system, communication with servo drives is implemented via modbus ASCII mode with even parity, 8 data bits, and 1 stop bit.

- Cameras

Communication interface between the system computer and cameras is USB. Libraries provided by the manufacturer are used in the data collection from the cameras.

- Laser Positioning System

As mentioned before, communication with laser positioning system is performed via RS-232 interface. Laser positioning system has its own protocol. A character is assigned for each command in the system control. These commands are listed in Table 6.3. Any of the characters listed in Table 6.3 is sent to the laser positioning system and the system performs the related task.

Table 6.3: Command list of the laser positioning system

Command	Character	Task
Serial number	's'	gets for the serial number consisting of alphanumeric characters and saves it.
Set move range	'r'	gets a 4-digit number in unit of mm and set the taken value as the movement range
Set homing distance	'h'	gets a 16-bit count specifying the encoder count corresponding to the homing distance of the laser system
Set end distance	'e'	gets a 16-bit count specifying the encoder count corresponding to the end distance of the laser system
Set conversion constant	'v'	makes a full cycle motion and calculates the conversion of encoder count to mm and saves it
Set backlash	'b'	gets a 2-digit number (in encoder count) and sets it as the backlash of the drive system
Get system data	'i'	sends package including the system information
Get encoder count	'w'	sends the current encoder count
Move to position	'x'	gets a 4-digit number (position in mm) and actuates the motor to send the laser sources to the relevant position
Test run	'o'	gets a 4-digit number (in msec) and performs a full cycle motion with 10 mm increments with the given time
Clear memory	'f'	clears the memory
Command list	'c'	sends a list including all commands and corresponding command characters

6.4 Calibration System Software

Software of calibration system is developed in Visual C# environment. All system elements are integrated by using this software.

The main form (i.e. the interface) of the software is given in Figure 6.2. *Status Window* on the form is used to inform the user about the process. *Data Window* is utilized to present informative data about the relevant action. *Clear* buttons at the bottom of each window are used to clear the screens in the windows.

Connect button sets the connections of servo drives, laser system, and cameras. The information about the connections is reported on the status window. *Laser Go* button sends the laser sources to the entered position (in mm). *Enable X-Axis* and *Enable Y-Axis* buttons force the drivers to servo-on state. *X-Axis Go* and *Y-axis Go* buttons sends the camera to the entered x and y positions respectively.

Camera group box consists of camera setting buttons, *Auto Threshold* button, and *Camera Info* button for the two cameras (i.e. top camera or bottom camera). *Set Shutter* and *Set Gain* buttons are utilized to adjust the shutter time and the gain of the relevant camera in milliseconds and in dB respectively. *Set Threshold* button is employed in the setting of the intensity threshold value in 16-bit count. *Auto Threshold* button is used to compute the intensity level on the camera sensor and

set a threshold value automatically. *Camera Info* button prints the information (serial number, image mode, frame rate etc.) of the relevant camera on the status window.

Measurements group box buttons activates the measurements requiring double camera. *Start Camera Test* button initializes the double camera static test explained in 7.6Section *7.6 Time Dependent Camera Tests*. Laser location data collected in this test is stored in a text file. *Exit Angle* button triggers the sequence for the beam exit angle measurement of a single laser beam.

Group box with the name of *Camera Specific* includes the methods carried out via single camera. These are line angle, laser location, and straightness measurements. Depending on the camera selection relevant action is activated by the relevant buttons.

Start Calibration button is used to start the calibration procedure according to the selected laser system unit type. This procedure is elaborated in the following section.

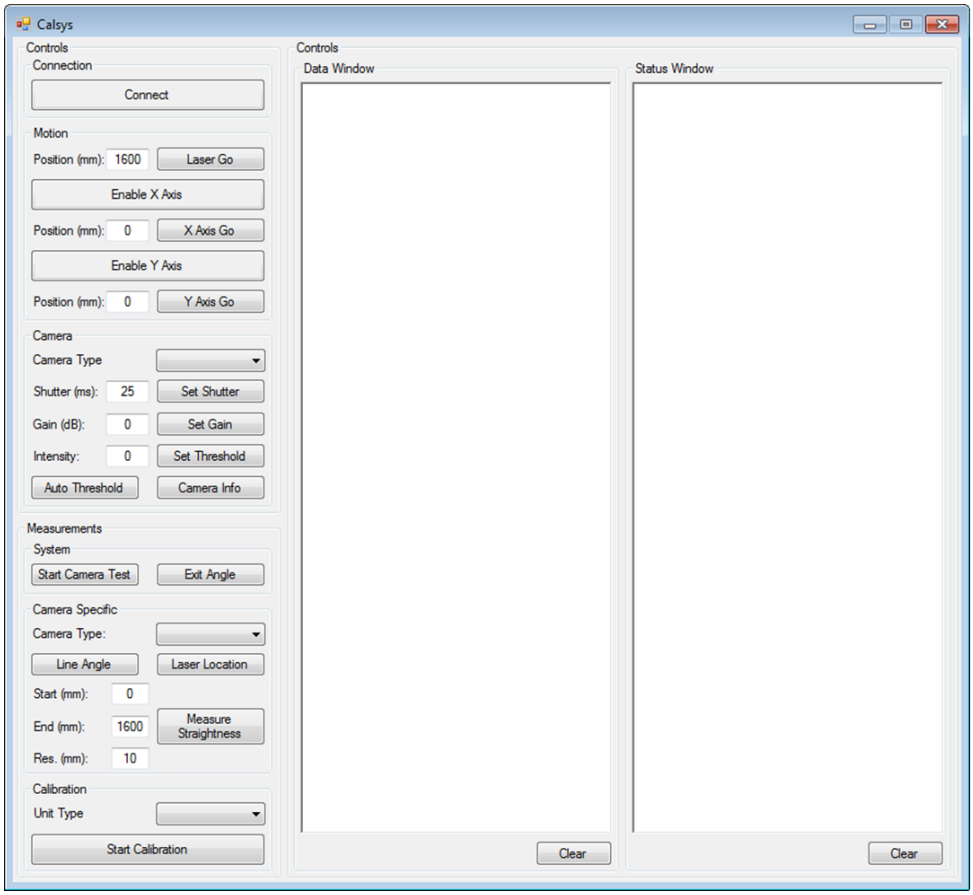

Figure 6.2: Main form of the developed software

6.5 Calibration Procedure

In this section, laser calibration procedure is elaborated step by step. Throughout the procedure, system elements are controlled by the calibration system software via the communication interfaces presented in Section *6.2 Calibration System Hardware*.

When the calibration is initialized, the lower camera is translated to the pre-determined calibration start position (x:740 mm, y: 300 mm) and search laser method is started. In this method, lower camera is translated along x-axis. Meanwhile, intensity level on the camera sensor is tested. When the amount of the pixels having the specified intensity (20,000 out of 65535 counts) reaches to the pre-determined number *n* (n=1000), the current position is assigned as the initial position of the laser source. This method is illustrated in Figure 6.3. For each laser found, the software generates a laser object. The detected position is added to this object. After finding a laser, camera is translated further. The remaining two laser lines are detected similarly. At the end of the laser search method, three laser objects are generated with their initial positions and their tags as *encoder side laser*, *motor side laser*, and *center laser*. These names are given according to the laser beam positioning system stepper motor and rotary encoder.

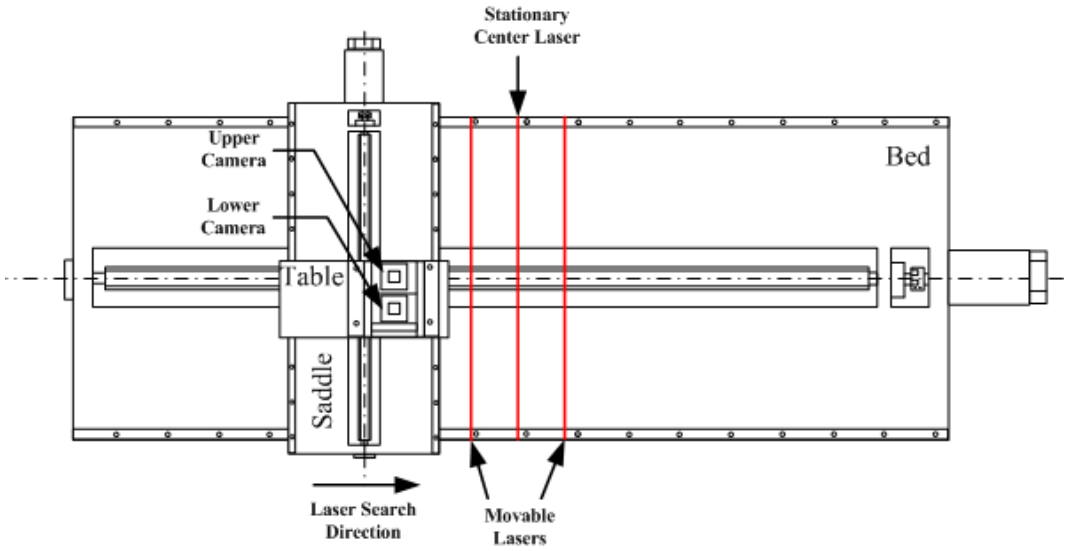

Figure 6.3: Illustration of laser searching in the calibration

After the positions of the three laser lines are determined, cameras are sent to laser line measurement start position along y-axis while they are positioned to stationary center laser position along x-axis. Without changing the x-axis position, stationary center laser line is scanned along the y-axis by translating the cameras with 15 mm resolution for each measurement. Laser line measurement is illustrated in Figure 6.4. At each position along the laser line, upper and lower cameras measure the x position of the incident portion of the laser on the sensor. For this purpose, centroid calculation method elaborated in Section *7.5.1.1 Centroid Calculation Method (CCM)* and line fit method presented in Section *7.2.2 Algorithm Development* are utilized. Mid-point of the line fit is assigned as the laser position for current y position on lower and upper camera planes

separately. When the data collection of the center laser is completed, cameras are positioned to laser line measurement start positions of encoder side and motor side movable laser lines respectively. Same procedure is followed for the movable laser lines.

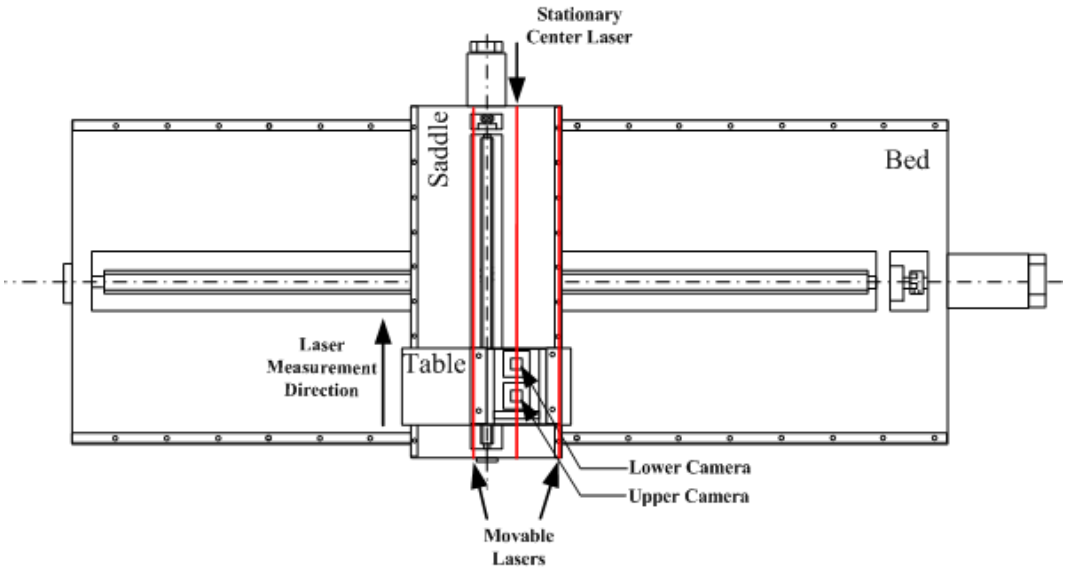

Figure 6.4: Illustration of laser line measurements

At the end of laser line measurements for initial position of movable lasers, a discrete data about the three laser lines is available. A graph presenting this data is shown in the following figure.

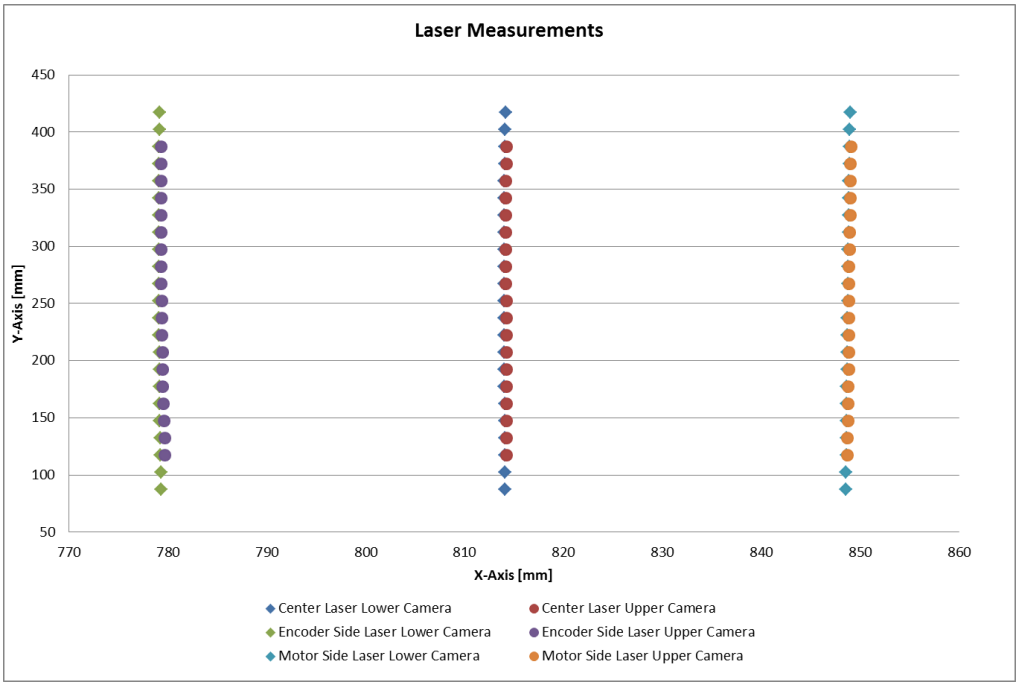

Figure 6.5: Measurement data of the three lasers for initial position

By using this data, two line fits are calculated for center laser (one for lower camera, one for upper camera). More detailed view of the center laser data presented in Figure 6.5 is shown in Figure 6.6 together with the computed line fits for both lower and upper cameras. As can be seen from the graph, laser projection is not a straight line. Line fit method is used to minimize the laser form errors and obtain a comparable data. The offset along the x-axis between the data obtained from lower and upper cameras is used to calculate the beam exit angle of the laser. For this purpose, difference between the mid-points of the line fits is divided by the z-offset of the upper camera. By using this angle and the distance between the laser beam positioning system and the lower camera, laser position error on the projection surface caused by the laser source positioning and laser beam exit angle are decoupled. Angle (i.e. slope) of the line fit computed with lower camera data is assigned as projection line angle. These three parameters (laser source position, projection line angle, beam exit angle) are set to the center laser object in the software.

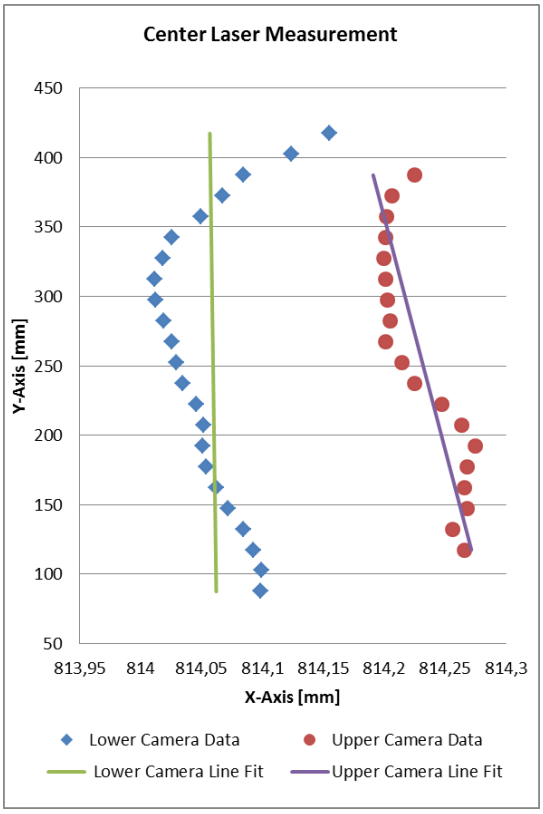

Figure 6.6: Center laser measurement data and computed line fits

Similar to the center laser, a line fit for each camera data collection of each laser is computed. A detailed view of the same data of movable laser sources presented in Figure 6.5 and obtained line fits are shown in Figure 6.7.

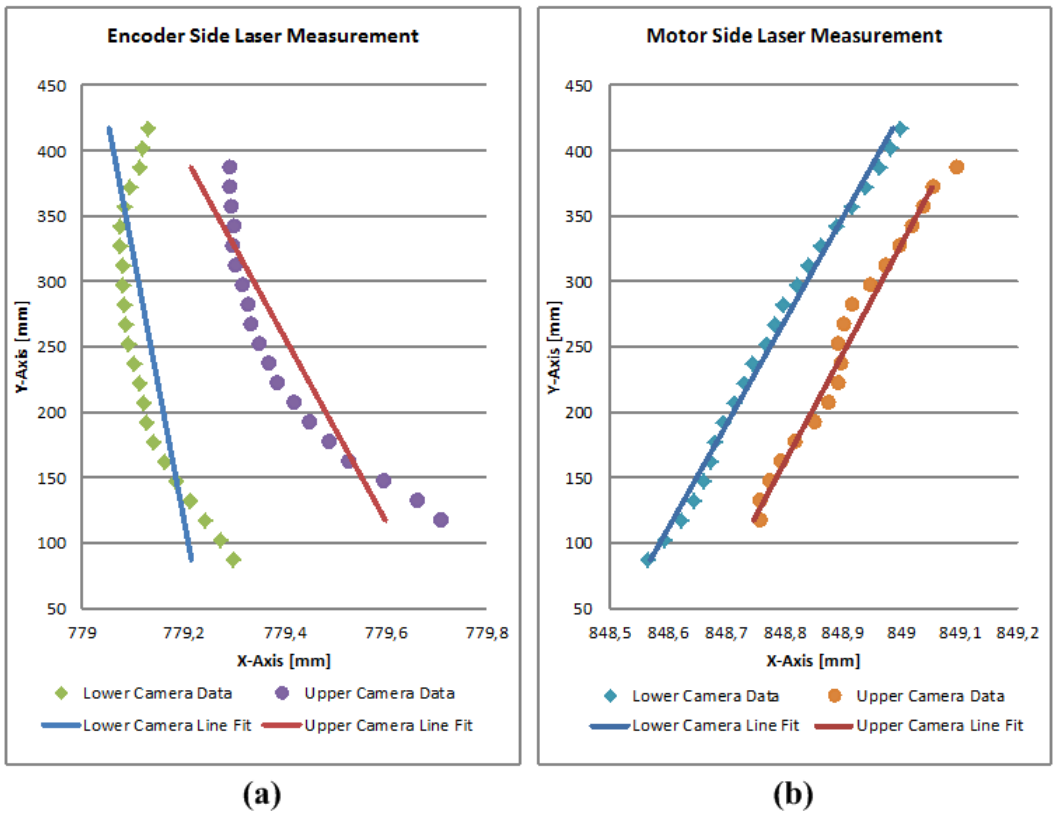

Figure 6.7: Measurement data of the movable laser sources together with the relevant line fits, (a) encoder side laser, (b) motor side laser

Laser source position, projection line angle, and beam exit angle are calculated with the same method explained for center laser. Difference between these calculated values and the value corresponding center laser parameter indicate the relevant error of the laser.

Movable laser sources are translated 40 mm apart from each other and the three parameters (laser source position, projection line angle, and beam exit angle) of the movable laser sources are recalculated for the current x-position. These values are also subtracted from those of stationary center laser. Hence, new error values are obtained for the new position. The same procedure is followed for each nominal x-position of the laser sources with resolution of 20 mm. Finally, a file including the error data of both movable laser sources w.r.t. nominal x-position is generated. In Section *7.7 Calibration of a Laser Beam Positioning System*, data collected in a calibration procedure is presented.

6.6 Closure

In this chapter, how the system elements work together (as a whole) is elaborated. System elements are divided into two groups as hardware and software. Properties of the hardware are presented. Communication structure with the relevant interfaces is also clarified. In the system software section, the interface of the calibration system is elaborated. Finally, a calibration procedure is explained step by step.

CHAPTER 7

TESTS AND MEASUREMENTS

7.1 Introduction

Throughout this thesis study, several tests and measurements are conducted to understand the properties of the system elements and verify the performance of the calibration setup. These tests and measurements consist of the studies about the camera measurements, vibration tests, mechanical system verifications, and the calibration of a laser beam positioning system. All these tests and measurements with their evaluations are presented in this chapter.

The initial tests are carried out for the camera as preliminary camera tests. Before the detailed design of the calibration setup, these tests are performed to understand the camera properties and requirements for precise laser position measurements. After these camera tests, vibration measurements are performed in the calibration room to see the convenience of the room for the calibration setup.

After the manufacturing and assembling of the calibration setup, verification tests are performed on the camera positioning system via two auxiliary linear encoders and a precision spirit level. These tests are followed by the camera tests on the calibration system. These tests are performed to select the most suitable parameters for camera measurement.

Another test for system measurements is performed to see the effect of the time of the day to the performance of the measurements. For this purpose, position of a stationary laser is measured by the two cameras simultaneously for 24 hours. Effects of the time on the measurements of both cameras are monitored and the results are compared.

Finally, calibration and quality control of a laser beam positioning system is conducted and the errors of this commercial product are documented.

7.2 Preliminary Camera Tests

Before the detailed design of the calibration system, a CCD camera meeting the system requirements is determined from the market and a series of preliminary tests are conducted to see the capabilities of the camera, imaging methods, and the environment.

In this part of the thesis, properties of the camera, setups where the tests are conducted, used algorithms, conducted laser position detection test, and evaluation of these test results are presented.

7.2.1 Properties of the Camera

For the laser detection device a CCD camera search is carried out in the market. Research parameters were pixel size of the sensor, software development capability, technical support, global shutter availability, and possible shutter times.

At the end of the research, Chameleon 1.3 Mp monochrome CCD camera of Point Grey Inc. imaging company is selected. This camera has a Sony progressive scan interline transfer ICX445 1/3" CCD image sensor. Resolution of the sensor is 1296(H) × 964(V) with pixel size of 3.75µm × 3.75µm. The camera give 16 bit monochrome data output. It presents a 7.5 fps frame rate with full image at 16 bit. This value may be increased up to 30 fps with suitable windowing operations on the sensor. There is a programmable global shutter on the camera with adjustable shutter time of 0.01 to 10 milliseconds. The camera is purchased with a software development kit (SDK) including very useful libraries for various imaging applications. Communication with the camera is carried out with USB 2.0 interface.

7.2.2 Algorithm Development

The camera sensor consists of a pixel array and its output is a 2D (1280 × 960) array whose elements are intensity (light strength) values for all pixels. A gray scale image of camera snapshot is given in Figure 7.1.

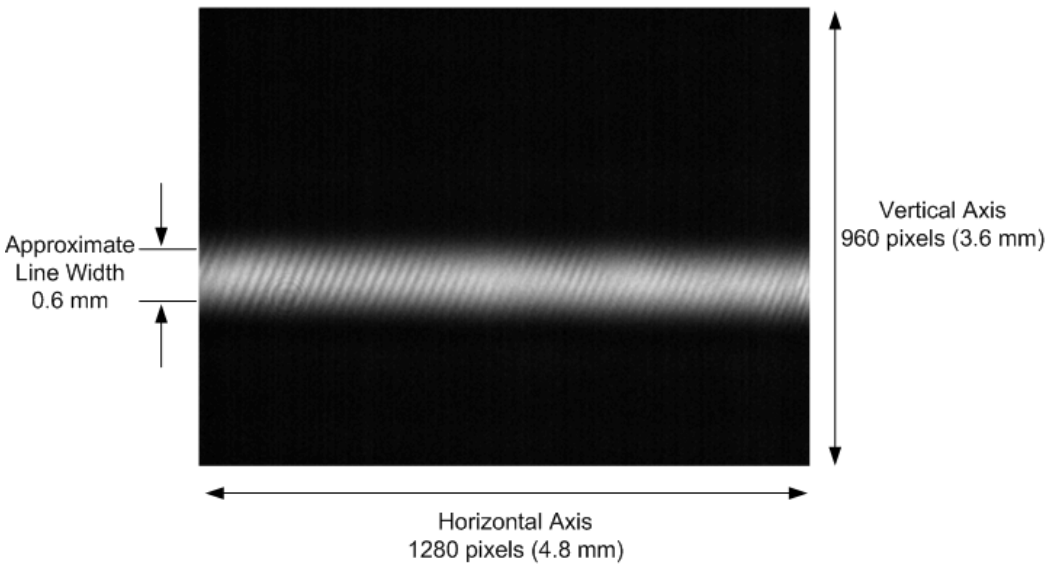

Figure 7.1: A snapshot of laser line on the camera sensor

There are three basic problems about the determination of the laser line position on the camera sensor with micrometer range repeatability. The first one is the sensor based intensity fluctuations of the pixels. The second one is the irregularities of the image caused by sensor mirror and

possible dust particles. The third one is the position change due to vibration coming from the environment.

The first problem is caused by small instantaneous fluctuations of the pixel intensity values. This effect can be filtered by taking several successive images, calculating the average intensity value of each pixel for these successive snapshots, and using the average value of each pixel as the intensity value. Note that ten successive snapshots are used during tests.

The second problem is due to the interference of the protection glass in front of the CCD sensor. The effect can be seen on Figure 7.1, as inclined linear patterns along the laser line. Sakuo Matsui and Chao Zhang (Matsui, 2002) are faced with a similar problem in their study while developing an alignment method for 50 m distance with a laser and CCD camera. They eliminate the problem by removing the cover glass. The images before and after removal are given in Figure 7.2.

Figure 7.2: CCD images, (a) with cover glass (b) without cover glass) (Matsui, 2002)

The linear patterns seen on Figure 7.2 (a) disappear after the removal of the cover glass. Removal of the protection glass in front of the CCD sensor is considered in this study. However, the damage risk to the sensor outweighs the benefits gained from the removal of this glass cover.

The third problem, which is the dominant factor of the camera tests, is environmental factor. In order to see the effect of this factor several tests in different environments are conducted. These environments and the tests are explained in the following parts.

Considering the form of the incident light and other parameters mentioned above, an algorithm is developed for laser position detection using pixel based intensity values. Basic idea of the algorithm is to find a centroid along the laser line width (i.e. vertical axis according to Figure 7.1), for each vertical pixel lying along the laser line and then to fit a line to these centroid points.

There are several centroid calculation methods in literature. These are explained in Chapter 2. Determination of the most suitable centroid calculation method for this application is a procedure which is conducted in Section *7.5 Calibration System Camera Tests*. For this preliminary camera tests which are aimed to determine the effects of environmental factors like vibration, an intuitive method is selected and the tests are carried out accordingly.

The method used for centroid determination is squared center of gravity method. In this method, sum of the multiplications of pixel index and square of intensity value of the pixel is divided by sum of the squares of the intensity values of the current series. The formulation as follows:

$$y = \frac{\sum_{i=1}^{960} i \cdot I_i^2}{\sum_{i=1}^{960} I_i^2} \tag{7.1}$$

The laser line on the camera sensor shown in Figure 7.1 has a Gaussian intensity distribution along the vertical axis of the image. The intensity distribution along a single pixel series is shown in Figure 7.3.

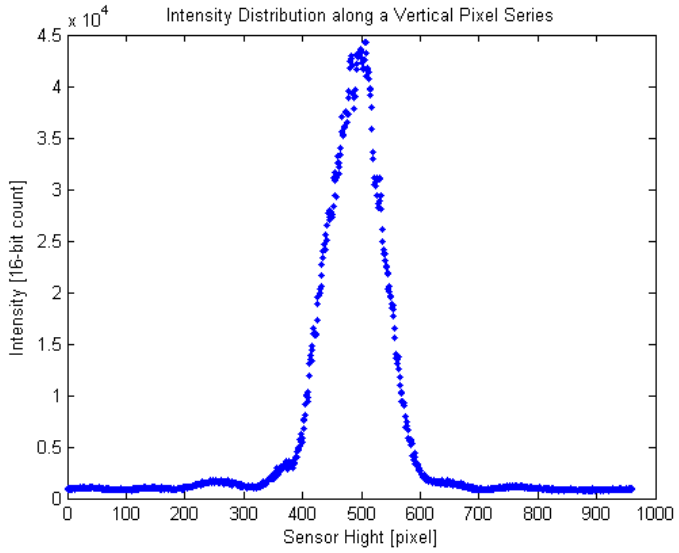

Figure 7.3: Intensity distribution of the laser line on the camera sensor along a vertical pixel series

Aim of the method given in (7.1) is to determine centroid of the intensity distribution shown in Figure 7.3 for each pixel series.

Second step which is to fit a line to determined centroid points is carried out by using least square method. Intensity distribution on which a line is fitted on the camera sensor is given in Figure 7.4.

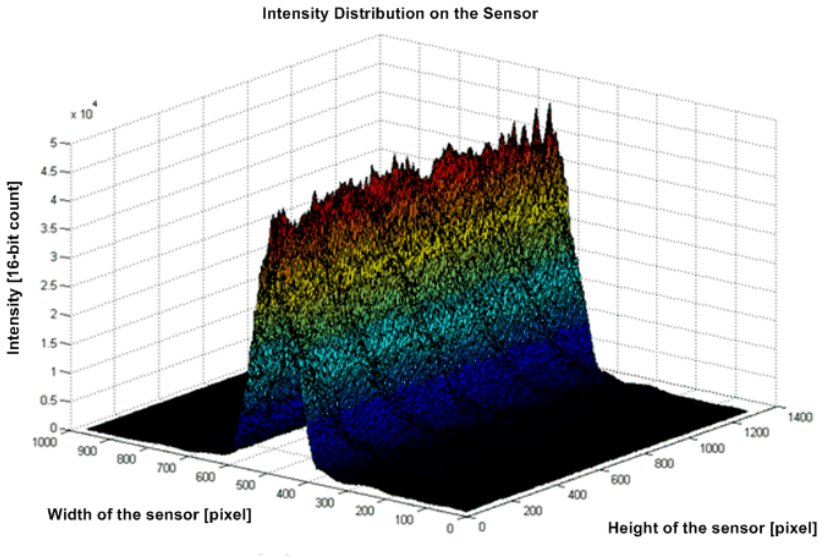

Figure 7.4: Laser line intensity distribution on the camera sensor

The laser line intensity distribution seen on Figure 7.4 has a Gaussian distribution along the sensor width just like the one represented in Figure 7.3 and it has a uniform distribution along the sensor height. Centroid points and the line fit are presented in Figure 7.5. Dots represent the centroid points of each vertical pixel series and the red line is the line fit calculated with least square method.

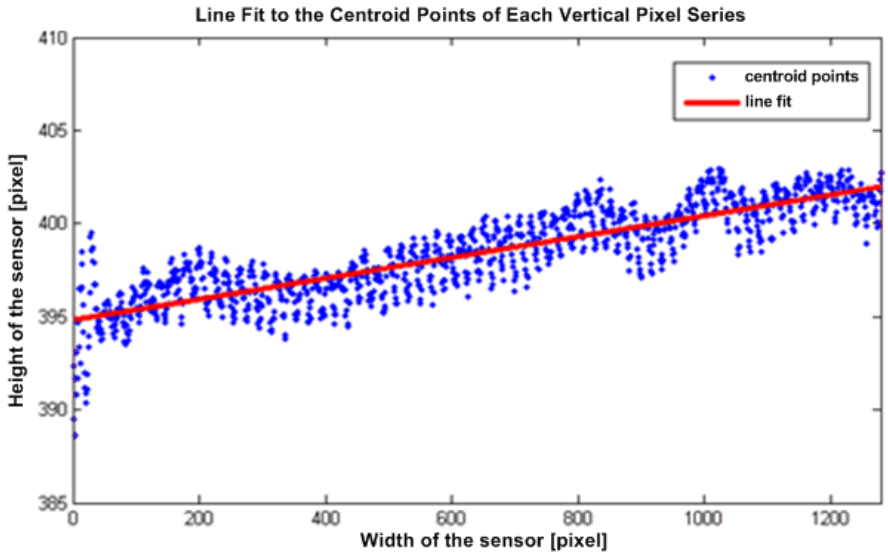

Figure 7.5: Line fitting to the centroid data

To summarize, to determine the position of the line segment on the camera sensor, ten successive snapshots are taken each time, average of these 10 snapshots for each pixel is calculated, an average matrix is obtained for each position measurement, centroid of each vertical pixel series of this matrix is determined by using square centroid method, and a line fit is calculated for the centroid points aligning along the laser line by using least square method.

7.2.3 Test Setups

For preliminary camera tests, four different setups in four different environments are established. These are test setups in an office, on the table of a CNC machining center, on the granite table of a coordinate measuring machine (CMM), and on concrete block of a vibration test laboratory.

During the test special mountings laser source is driven by a standard control card of the laser positioning system. For attenuation of the laser strength a ND3 filter is used. This filter decreases the light intensity to the 1/1000 of the original one. Calculation for determination of the filter grade is given in Section *4.4.2 Engineering Calculations.*

The first set-up is established in an office of a steel construction building by means of aluminum sigma profiles. Distance between the laser source and the camera is approximately 1 m. The problem with this setup is the disturbances emanating from the environment. The office is located on the second floor of a three-story building in which there are R&D offices of several companies. The construction of the building is prone to vibratory movements. Especially in the working hours of the day, vibration sources like walking people, closing doors, operating equipment etc. affects the laser position stability.

The second set-up is assembled on a CNC table. Camera and laser source connections are fixed to the table by means of clamps. Laser source – camera distance is again set to 1 m. Reason for selection such a place for laser position measurement is the establishment method of the related CNC machine. Before the placement of this CNC machine, a hole of several meters deep is dug on the ground and it is filled with a special mixture with concrete in order to prevent the machine table from the vibrations coming from the industrial environment. During the tests, some machine tools around the test setup are running. In spite of the establishment of the machine center, disturbances coming from other machines are affected the stability. This test is also gives idea about the machining accuracies of the related machine tool.

The third setup is put on the granite plate of a CMM in an industrial environment. Camera and the laser source are placed in a 1 m distance apart from each other. Two different tests are conducted on this table. In the first one camera and laser source casings are not fixed to the table but freely put on the table surface. In the second test, camera and laser casings are fixed to the granite plates by using claps. Although the room in which the CMM is placed is apart from the machine shop, the machine tools working in the machine shop next to the CMM room are possibly affected the measurements.

The fourth setup is placed on a concrete block of a vibration laboratory. Distance between the camera and the laser source is again approximately 1 m. For this case, camera and laser source cannot be clamped; they are freely placed on the block instead. The advantage of this laboratory is that it is on the basement of a single-floor-building and there are few disturbance sources around. Moreover, the concrete block is embedded in a several meters deep.

7.2.4 Laser Position Detection Tests

In the test procedure, fifty successive measurements are taken for a stationary laser source. In each measurement, the method explained in Section *7.2.2 Algorithm Development* is carried out. Average of all the fifty measurements is taken. Then, difference of each measurement from the average line is plotted. Showing all the plots on the same graph expresses fluctuations of the laser line positions caused by several parameters like camera stability, algorithm performance, laser instability, and vibrations disturbances.

Figure 7.6 shows the behavior of the laser line under the effects of the disturbances. This figure presents one of the tests taken in the office. Lines with the same color represent the successive ten measurements. Totally fifty measurements are taken for each test.

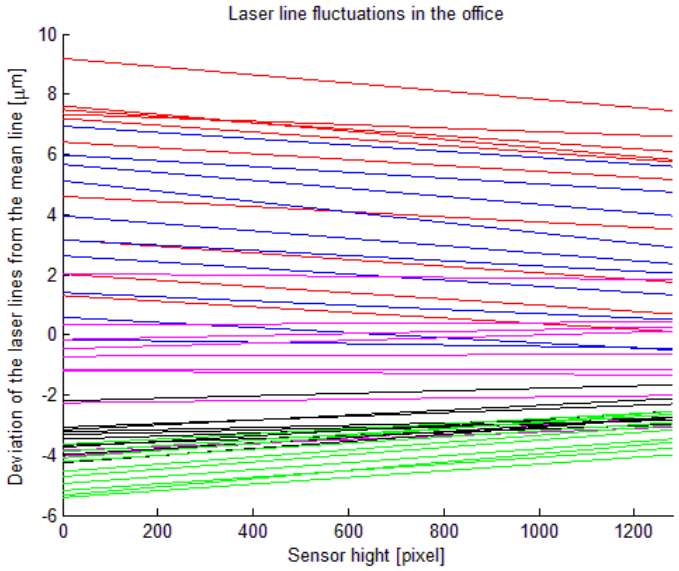

Figure 7.6: Fluctuations of successive fifty laser line position measurements in the office

Hundreds of tests are conducted in the office. Similar results shown in Figure 7.6 are obtained each time. Generated line fits from the camera data are deviates from their mean value. As can be seen in Figure 7.6, laser lines deviates between -6 µm and +9 µm. Whenever an extra disturbance like shutting a door is interfered, this deviation value reaches up to ±15 µm.

Using exactly the same method used in office tests and the same laser source - camera distance, some tests are conducted on a CNC machining center table. Camera and the laser source are fixed to the table by means of clamps. Deviations of the laser line on the sensor observed during this test are shown on the graph given in Figure 7.7. As can be seen from the graph given in Figure 7.7, laser line position deviates about ±6 µm.

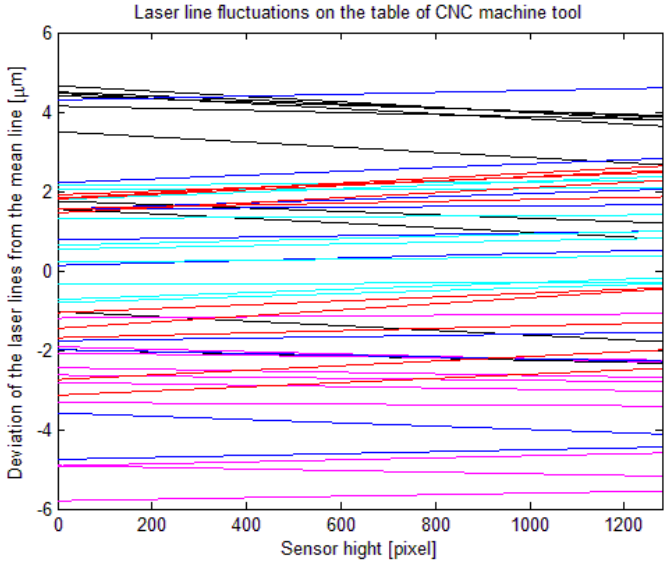

Figure 7.7: Fluctuations of successive fifty laser line position measurements on the CNC Machine

The third test setup is established on the granite table of a CMM. Two different tests are conducted for this case. In the first test, camera and laser casings are put on the granite table freely without any fixing. The same laser source - camera distance with the previous test setups is used. The obtained laser behavior is shown in Figure 7.8.

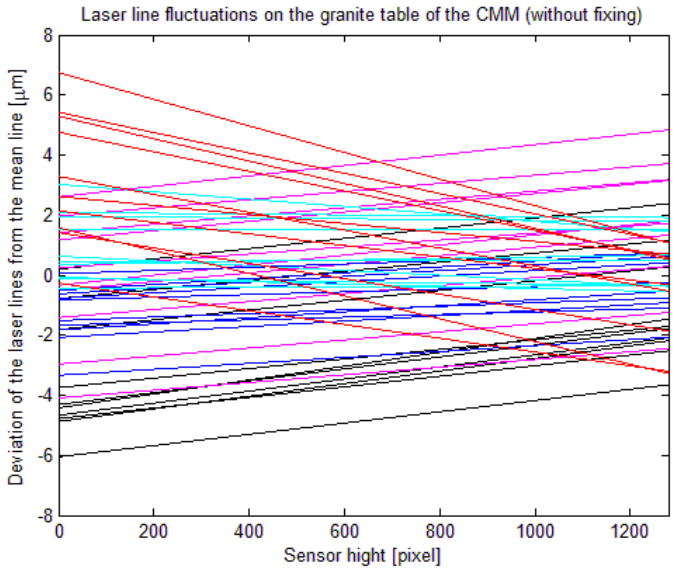

Figure 7.8: Fluctuations of successive fifty laser line position measurements on the granite table of the CMM (without fixing)

In this case laser line measurements deviate about ±7 µm. In order to determine the vibration effect, camera and laser source casings are fixed to the granite table by clamps and the same test is conducted. The result is given in Figure 7.9.

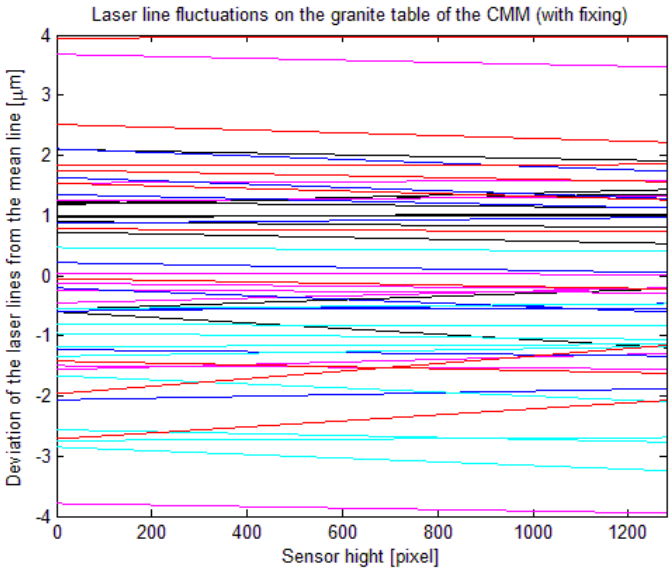

Figure 7.9: Fluctuations of successive fifty laser line position measurements on the granite table of the CMM (with fixing)

According to the result given in Figure 7.9, laser line fluctuation is decreased to ±4 µm by fixing the camera and laser source to the granite table.

The last test setup is established in a vibration test laboratory. Camera and laser source are freely placed on the concrete block in the laboratory. Obtained results are given in Figure 7.10.

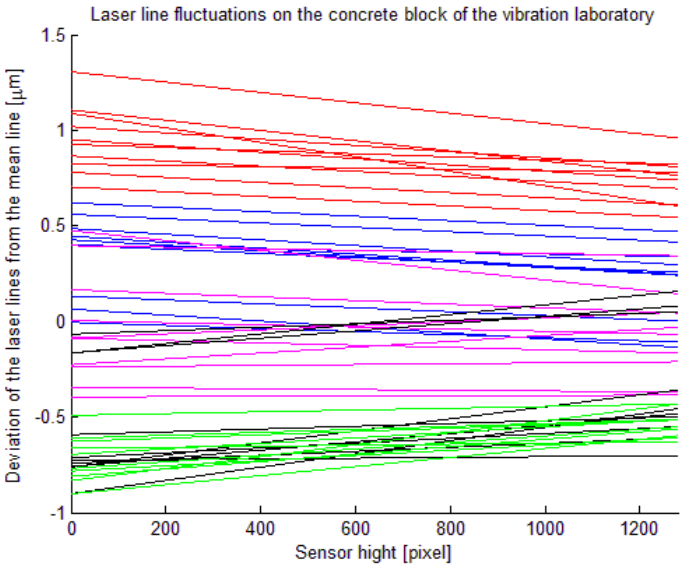

Figure 7.10: Fluctuations of successive fifty laser line position measurements on the concrete block of the vibration laboratory

Figure 7.10 shows that the laser line fluctuations are limited to ±1.5 µm under the condition of the vibration test laboratory.

Results of the preliminary camera tests prove that one of the main parameters about the laser line position detection is vibration disturbance. Thus, vibration removal is one of the most important considerations during the calibration setup development.

7.3 Calibration Room Vibration Tests

Preliminary camera tests show that one of the most important factors about the laser position determination is vibration. For this reason, a suitable place for the calibration system is searched. A room on the same floor (ME-D 01) with the vibration test laboratory where one of the test setups for the preliminary camera tests is established is determined as the most suitable place for the calibration system. In order to verify this, a series of vibration tests are conducted on the ceiling, floor, and the walls of the room.

During the vibration tests Dytran 3035B piezoelectric accelerometers are used for vibration sensors. Resolution of the accelerometer is 100 mV/g where g=9.81 m/s^2. For acquisition of the data, HP 3560A portable dynamic signal analyzer is utilized. Signal conditioning is carried out by ICP (Integrated Circuit Piezoelectric) amplifier embedded inside HP 3560A. The collected data is transferred to the PC by means of RS232 communication interface and HP Standard Data Format (SDF) Utilities DOS executable programs. Then, the data are processed by MATLAB.

For each test, four different analyses are conducted. These are time history with and without integration, and linear spectrum with and without integration.

As an example, averaged linear spectrum with integration of the measurement taken from front wall is given in Figure 7.11. After these measurements, rms value of each signal is calculated. Calculated rms value of the signal shown in Figure 7.11 is 7.81×10^{-7}.

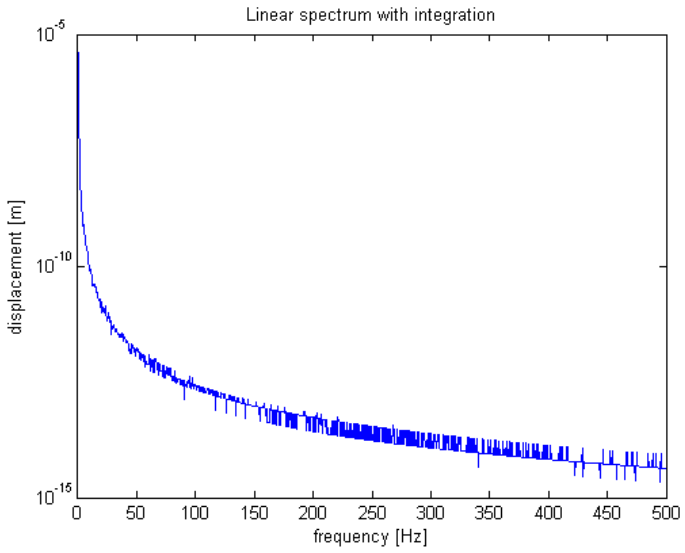

Figure 7.11: Linear spectrum of the vibration measurement taken from front wall

Calculated rms values for signals obtained from time history without integration, time history with integration, averaged linear spectrum without integration, and averaged linear spectrum with integration are given in Table 7.1 for floor, ceiling, right wall, left wall, and front wall. Time history is collected as acceleration with unit of g (gravitational acceleration - 9.81 m/s^2). Linear spectrum is expressed as meters.

Table 7.1: Calculated RMS values of the signals

	Floor	**Ceiling**	**Left Wall**	**Right Wall**	**Front Wall**
Time Hist. w/o Integration [g]	1.46×10^{-6}	1.96×10^{-6}	1.20×10^{-6}	1.68×10^{-6}	1.54×10^{-6}
Time Hist. w/ Integration [g]	1.54×10^{-6}	1.48×10^{-6}	1.04×10^{-6}	1.40×10^{-6}	1.68×10^{-6}
Linear Spec. w/o Integration [m]	5.47×10^{-7}	7.38×10^{-7}	5.93×10^{-7}	5.43×10^{-7}	5.60×10^{-7}
Linear Spec. w/ Integration [m]	7.31×10^{-7}	7.95×10^{-7}	9.62×10^{-7}	8.73×10^{-7}	7.81×10^{-7}

The obtained results given in Table 7.1 shows that vibration disturbance coming from the walls, ceiling, and the floor is less than 1.7010^{-6} g in acceleration and 9.7×10-7 m (below 1μm) in displacement. These are promising results for the calibration system and justify the reason for the selection of the room to establish the calibration system.

7.4 Camera Positioning System Verification Tests

In order to satisfy the system requirements about the laser position and angle measurements of the calibration setup, the precision of the camera positioning system has a great importance. Design, manufacturing, and assembling of the system are carried out on the basis of the precision requirements presented in Section *4.2 Problem Definition and Design Specifications*.

Camera positioning system has two translational axes on which the saddle and the table are positioned. Rotational changes of the saddle and the table during the positioning along these translational axes inversely affect the measurement accuracy of the calibration setup. Axes of the rotational errors of the saddle and the table are illustrated in Figure 7.12 and Figure 7.13 respectively. The saddle illustrated in Figure 7.12, translates along x-axis of the camera positioning system. Hence, the pitch error is around y-axis, roll error is around x-axis, and yaw error is around z-axis.

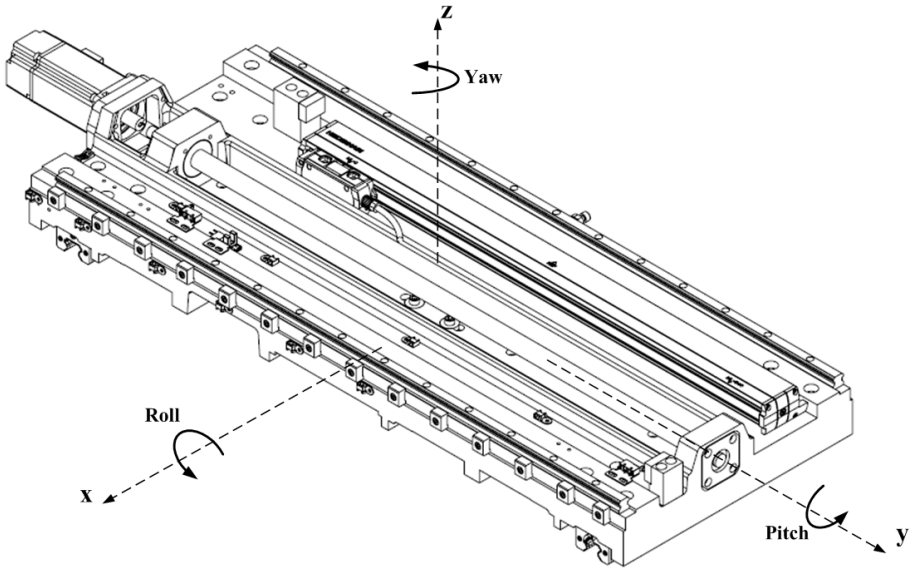

Figure 7.12 Illustration of roll, pitch, and yaw axes of the saddle

The table presented in Figure 7.13 translates along y-axis of the camera positioning system. Consequently, the pitch error is around x-axis, roll error is around y-axis, and yaw error is around z-axis.

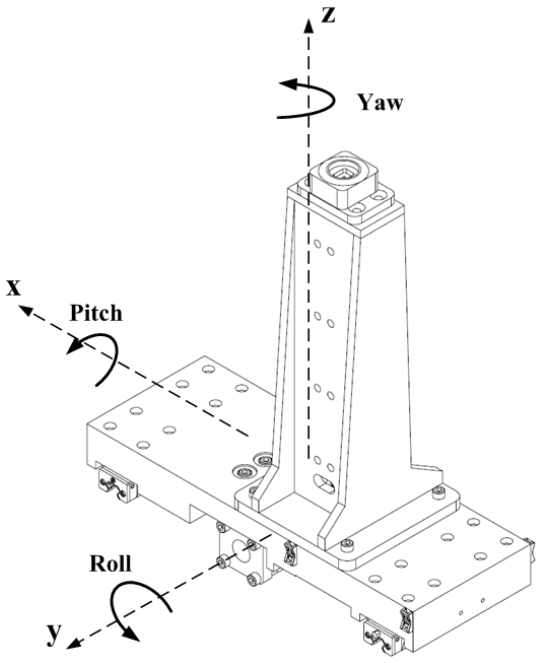

Figure 7.13 Illustration of roll, pitch, and yaw axes of the table

In the system verification tests, pitch and roll errors of the saddle and the table are measured via precision spirit level given in Figure 4.26. Yaw error of the saddle is measured by performing a double encoder test. Depending on this test, translation error of the saddle is also estimated.

7.4.1 Spirit Level Tests

Pitch and roll errors of both the saddle and the table are measured via the precision spirit level presented in Figure 4.26 and elaborated in Section *4.6.3.1 Leveling the Laser Beam Positioning System Connection Plane*.

In order to measure the pitch angle change of the saddle during the translation along x-axis, the spirit level is placed on the table when the table is in the middle of the saddle (i.e. in the middle of y-axis). Saddle is translated along x-axis with 10 mm increments. During these measurements, spirit level is aligned along x-axis. After each movement, it is necessary to wait about 15 seconds for the stabilization of the spirit level. The collected data for the pitch angle change of the saddle during the translation of 1600 mm is presented in Figure 7.14. Maximum and minimum values of the pitch angle shown in this figure are 9 arcsec and -11 arcsec respectively. This corresponds to a dynamic pitch angle error of ±10 arcsec. This value is slightly less than the dynamic pitch error of the saddle determined according to system requirements in Section *5.10.2 Dynamic Errors*. Pitch error tolerance of the saddle (εy) presented in Table 5.3 is 0.0005 rad which corresponds to 10.3 arcsec.

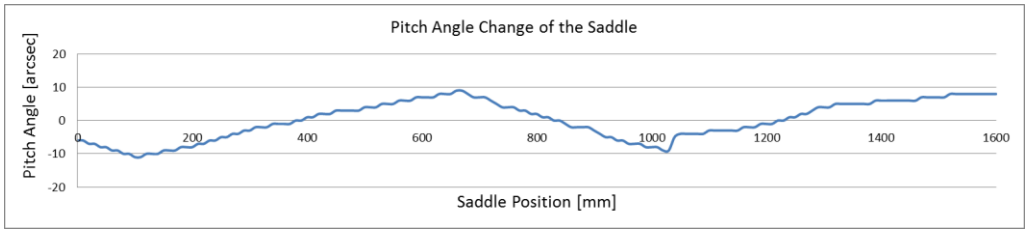

Figure 7.14: Pitch angle change of the saddle with the position

The same test is performed for roll angle change of the saddle during the translation along x-axis. However, no significant change is observed on the spirit level. Similarly, pitch angle and roll angle changes of the table during the translation along y-axis are not significant. This implies that the change of the mentioned angles during the translation is less than 4 arcsec. This condition satisfies the requirements for these three errors (εx of the saddle, εx of the table, and εy of the table) presented in Table 5.3.

7.4.2 Double Linear Encoder Tests

One of the important parameters of the camera positioning system is the yaw error of the saddle (i.e. rotational error of the saddle around the z-axis). In order to measure this parameter, two additional linear encoders (Heidenhain LS 176C) are attached to two sides of the saddle. In position control, feedback is provided by a Heidenhain LS 177 type linear encoder which is connected to x-axis motor driver. Data generated by the auxiliary linear encoders are collected via the main control cards used in the laser beam positioning system (presented in Section *3.2.5 Electronic Control System*) and stored in PC. The schematic of the double encoder test is shown in Figure 7.15.

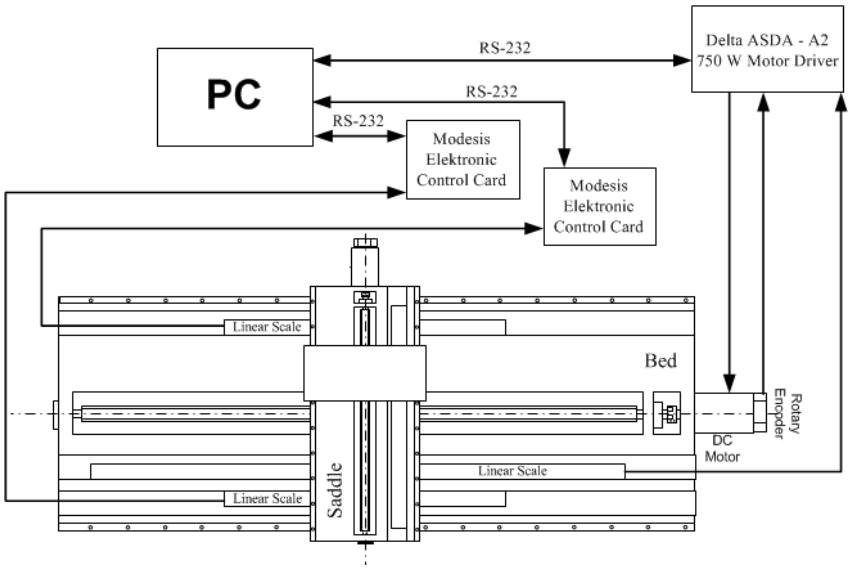

Figure 7.15: Schematic of the double linear encoder test

Utilizing the data obtained from the auxiliary encoders, yaw error of the saddle is calculated. Depending on the same data positioning error is also estimated. In order to elaborate the method followed during these calculations, the orientation of the saddle under the effects of positioning and yaw error is illustrated in Figure 7.16. The abbreviations presented in the figure are as follows:

- P_n: nominal position,
- P_p: position of the primary encoder
- P_{A1}: position of auxiliary encoder 1
- P_{A2}: position of auxiliary encoder 2

Calculation of yaw error is expressed as:

$$\alpha = \tan^{-1}\left(\frac{(P_{A2})-(P_{A1})}{d}\right) \tag{7.2}$$

where α is the yaw angle and *d* is the distance between the auxiliary encoders (given as 600 mm). Positioning error of the saddle is estimated by the equation given by:

$$e = \frac{(P_{A2})-(P_{A1})}{3} + (P_{A1}) - P_n \tag{7.3}$$

where *e* is the positioning error of the saddle. Equation (7.3) is generated on the basis of linear relationship between the encoder heads as presented in Figure 7.16.

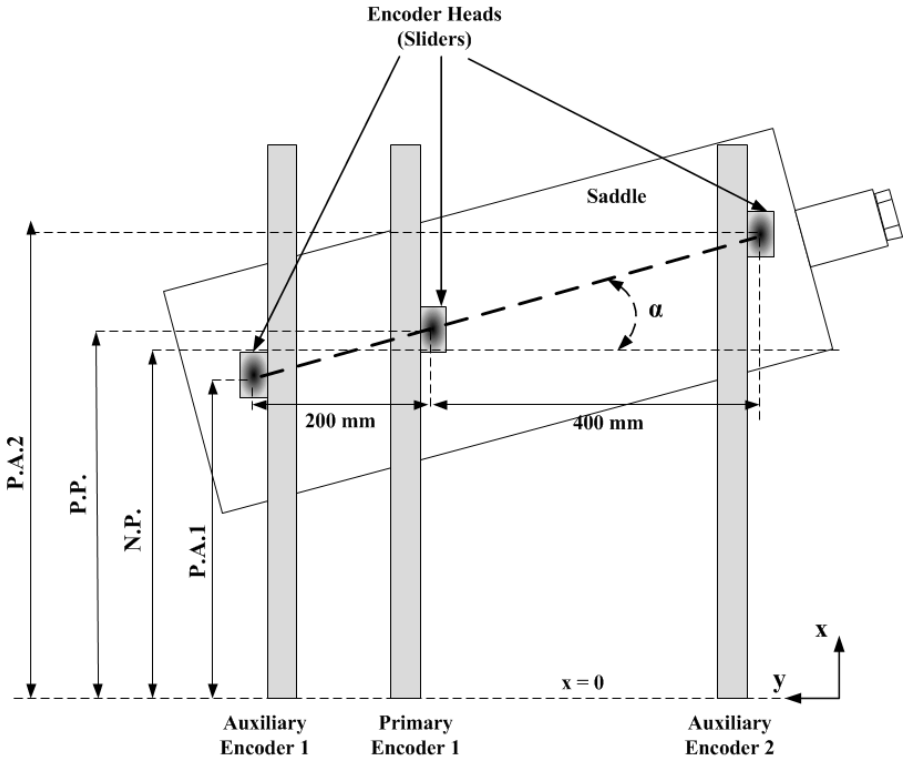

Figure 7.16: Illustration of the saddle orientation under the effects of both translation and yaw errors

Measuring distance of the auxiliary encoders are 540 mm. During the tests, 500 mm of the translational x-axis is monitored by taking position measurements of 1 mm resolution. Yaw data collected in the first test which is performed in the forward direction of the saddle is presented in the following figure.

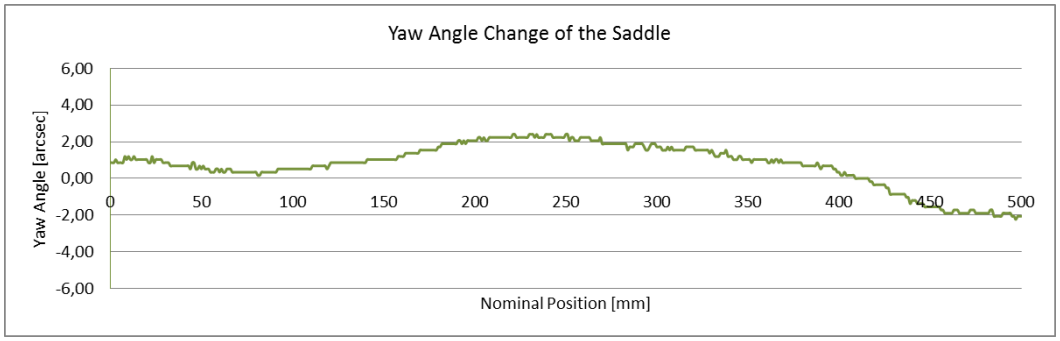

Figure 7.17: Yaw angle change of the saddle with the x-axis position

Yaw angle of the saddle changes between -2.23 arcsec and 2.41 arcsec in 500 mm translation. This corresponds to a yaw error of ±2.32 arcsec. Depending on the same test, positioning error of the saddle is also calculated according to the Equation (7.3) and presented in the following figure.

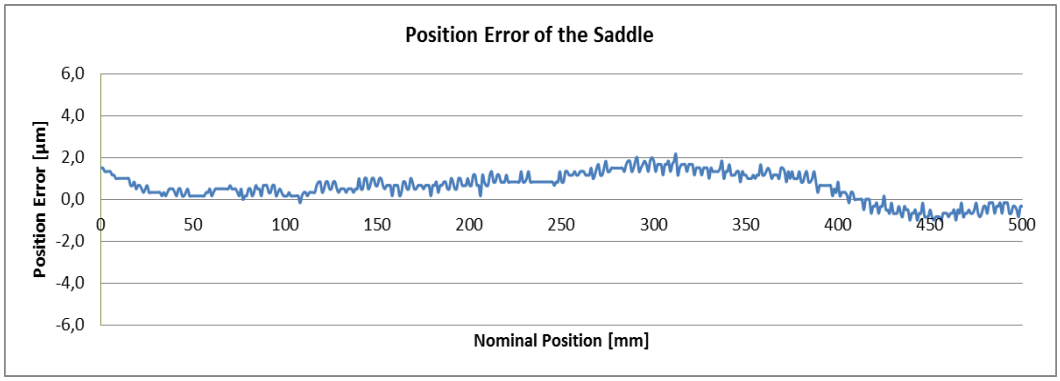

Figure 7.18: Position error of the saddle along x-axis

Position error of the saddle presented in Figure 7.18, changes between 0.002 mm and -0.001 mm. Depending on this test, positioning error of the saddle is estimated as ±1.5µm for the measurement range of 500 mm.

The same test is performed 10 times in forward and reverse direction of the saddle. Maximum yaw error and maximum position error are measured as ± 2.41 arcsec and ±2.2 µm in the measurement range of 500 mm. Depending on these results, yaw end position error of the saddle are assumed to be below the limits presented in Table 5.3 as ±0.000025 rad (±5.2 arcsec) and ±5 µm respectively, for the full movement range.

7.5 Calibration System Camera Tests

In order to select the most suitable parameters for camera measurements, a series of tests are carried out. In this section, relevant parameters are elaborated and the performed tests are presented with their results.

7.5.1 Test Parameters

There are several parameters related to camera measurements. Some of these parameters are related to algorithms used in position determination and some are related to geometrical, mechanical, and environmental conditions. During the tests, effects of each parameter is tried to be determined. Test parameters and their explanations are included in this section.

7.5.1.1 Centroid Calculation Method (CCM)

Basic idea about determination of the laser line position is to find centroid of intensity distribution along each pixel series which are perpendicular to laser line. There are several methods to find the centroid of an intensity distribution. Convenience of the method changes according to application, device, working condition, and data distribution. Along the pixel series on which a centroid is searched, intensity is distributed in a Gaussian manner. The sensing device is a monochrome CCD camera with 3.75 μm × 3.75 μm pixel size and 1280 × 960 pixel resolution.

To determine the most convenient method, some tests should be conducted and the methods should be compared using the same data at each time. Centroid calculation methods compared in camera tests are Gaussian fit method, centroid method, squared centroid method, and binary centroid method. Methods are basically explained in literature review part. Some of the methods are not exactly the same as the ones explained in literature review. Some modifications are conducted.

- Gaussian Fit Method

Since the intensity distribution of the laser line is close to a Gaussian form, one of the ideas considered to determine the laser centroid is to fit a Gaussian curve to each pixel series along the lateral direction of the laser line. Gaussian function can be expressed as:

$$f\left(x,K,\sigma,\mu\right)=K\cdot\exp\left(-\frac{\left(x-\mu\right)^2}{2\sigma^2}\right) \tag{7.4}$$

where x is the current pixel position in the pixel series, K and μ are peak height and peak position respectively, σ is the width parameter. Parameters K, μ, and σ are calculated with an iterative method. An intensity distribution of a pixel series with Gaussian fit curve is presented in Figure 7.19.

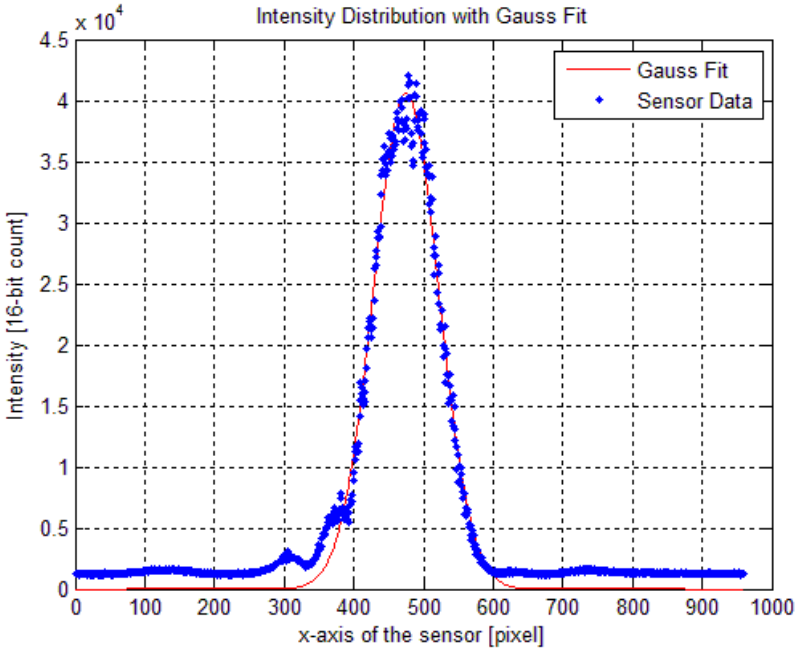

Figure 7.19: Intensity distribution of a pixel series with fitted Gaussian Curve

According to Gaussian fit represented on Figure 7.19, peak position or the centroid of the distribution is at 474.86 in pixels. It corresponds to 1.7807 mm from the edge of the sensor.

- Centroid Method

Centroid (or center of gravity) method is applied by multiplying the intensity value of each pixel by its pixel location and dividing by the sum of the intensity values. The equation is given by (2.3).

$$\overline{x} = \frac{\sum_{i=1}^{n} x_i \cdot I_i}{\sum_{i=1}^{n} I_i} \tag{7.5}$$

- Squared Centroid Method

This method is very similar to the centroid method but this time intensity values are replaced by their squares:

$$\overline{x} = \frac{\sum_{i=1}^{n} x_i \cdot I_i^2}{\sum_{i=1}^{n} I_i^2} \tag{7.6}$$

- Binary Centroid Method

In this method centroid is calculated by Equation (2.3) but intensity values in the equation are one or zero depending on the intensity value of the related pixel and the pre-determined threshold value. Pixels having intensity values greater than the threshold taken as intensity of one while the others are taken as zero.

7.5.1.2 Threshold

In order to filter the background noise, a constant threshold value is applied to intensity data generated by the camera. Hence, intensity values less than this specified level are assumed to be zero.

Binary centroid method is always used with a threshold level. The other methods are applied with both threshold and grey scale (without threshold) approaches. For an unsaturated image, maximum intensity values are generally about 50,000 ~ 60,000 in 16-bit counts. Used threshold values during the tests are 10,000, 20,000, and 30,000. It is estimated that this method can minimize the effect of background noise on the measurements.

7.5.1.3 Number of Snapshots for Pixel Intensity Value Averaging

During the centroid determination of each pixel series several snapshots are taken and the average value of each pixel for these successive images is determined before the centroid calculation. It is estimated that this method can minimize the instantaneous intensity fluctuations of the pixels.

7.5.1.4 Shutter Time of the Camera

The camera of the system has a global shutter. By adjusting this parameter intensity levels on the camera sensor can be controlled. Shutter time of the camera can be adjusted from 0.01 ms to 10 s. Excessive shutter time results in saturated sensor. Several shutter time alternatives are used during the camera tests.

7.5.1.5 Part of the Sensor on which the Laser Line Is Located

Dimension of the sensor on the lateral direction of the laser line is 3.6 mm. Laser line has a width about 0.6 mm. The effect of the location of the laser line along the width of the sensor is also tested during the tests. For a uniform sensor, it is expected that the laser line location on the sensor

does not affect the accuracy of the measurements. Different tests are conducted when the laser line is at the right side, left side and middle of the sensor.

7.5.1.6 Motor State

When the servo motors are off, the ball screws are free to rotate. When they are on, the ball screws are locked at the current position. However, this time there is the risk of motor vibrations. Whether the servo motors are in action or not during the measurements is an important parameter to be decided. For this purpose, measurement tests are compared when the servo motors are in power on and power off states.

7.5.1.7 Windowing on the Sensor

The camera used in the study is capable of defining an active region on the sensor. In other words, only the cells in the region specified by a rectangle are active in imaging. In this method, only the cells which are close to the laser line are in action. Hence, the speed of the imaging is increased. There are 960 CCD cells along the vertical axis of the camera sensor. In the tests, 300 of them are employed and the measurement results are inspected. Two snapshots of the camera with and without windowing are given in Figure 7.20.

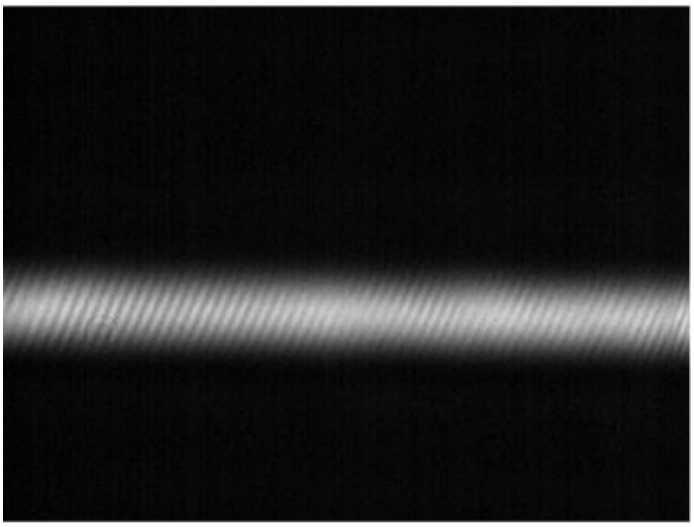

(a)

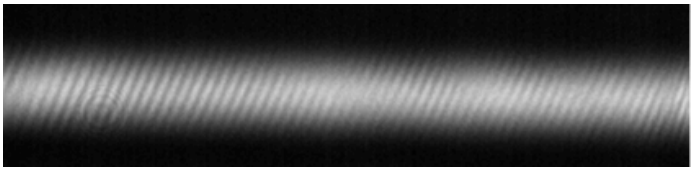

(b)

Figure 7.20: Camera snapshot, (a) full image 1280x960 (b) windowed image 1280x300

7.5.2 Test Procedure

In the previous section, parameters affecting the measurement performance are elaborated. To be able to compare the results systematically, some reference conditions are determined and under these almost constant conditions, effects of changes on the related test parameters are inspected. Actually, to provide an exactly constant reference condition in which all the parameters remain constant is not possible since each test takes some time and during this time interval, parameters like sensor temperature and time span in which the laser source is open change inevitably. To minimize the effects of such parameters, tests in which these parameters are accepted to be constant are handled after about 30 minutes later than all the components are energized.

For the first step of the test procedure, all centroid calculation methods (CCMs) are tested under a specific reference condition. For this purpose, 15 different sets of data each of which includes 50 successive images are collected under the reference condition. Each CCM is applied to all images. Note that every CCM is applied to the same data to be able to obtain comparable results. For each set of data including 50 successive images centroid of each pixel series is calculated by using a specific method and a line fit is performed for each image. Hence, standard deviation of the tip points of 50 line fits is calculated where smaller standard deviation is always favorable.

At the end, 15 standard deviation values for each CCM are obtained. Average of these standard deviations is calculated for each method and the method giving the smallest one is selected as the CCM.

After determining the best CCM, all other parameters are tested by using this CCM. At each test, a best condition (having the smallest standard deviation) is selected for each parameter.

7.5.3 Test Results

Camera tests are conducted according to the procedure explained in the previous section. All parameters elaborated in Section *7.5.1 Test Parameters* are tested. These tests and their results are presented in this part.

7.5.1.8 Tests for Centroid Calculation Method

At the first step, CCMs are tested. For this purpose, a reference condition is determined and all CCMs are tested accordingly. The determined reference condition includes the followings:

- Camera is positioned to the middle of each axis which represents the reference coordinates (x=800, y=0 mm).
- Both laser line angle on the sensor and laser beam exit angle are adjusted such that they are almost zero.

- Laser line is directed to the middle of the sensor along horizontal direction (321st - 640th pixels).
- Shutter time is adjusted to 13 msec.
- Both axis of the positioning system servo motors are set to servo-on state.
- System is kept at this condition about 30 minutes before tests.
- Camera is set to full image condition (no windowing).

After providing this reference condition, following steps are carried out:

- 10 snapshots are taken for averaging of each image data to be saved.
- At each test, 50 successive images are taken and 15 data sets are collected.
- A threshold of 20,000 is applied to data.
- Centroid of each pixel series of each image is calculated and a line fit is formed for each image.
- Standard deviation of the start points (y=0 in pixels) of the line fits is calculated.
- Standard deviation of the end points (y=1280 in pixels) of the line fits is calculated.
- The bigger one of the two standard deviation values is taken.
- This procedure is repeated 15 times and the average of the 15 deviations is calculated.

The value obtained from this procedure is the measure of comparison for the related CCM. Obtained test results are given in Table 7.2.

Table 7.2: Test results for CCM

Centroid Calculation Method	Standard Deviation [μm]
Gaussian	0.236
Centroid	0.211
Squared Centroid	0.241
Binary Centroid	0.248

Table 7.2 shows the standard deviation of the tip point positions of line fits formed by using the centroid points obtained by four different CCMs. According to the results centroid (center of gravity) method is selected as the CCM.

7.5.1.9 Threshold Test

Using the same data sets in Section *7.5.1.8 Tests for Centroid Calculation* Method, threshold values of 0, 10,000, 20,000, and 30,000 are applied. The obtained results are given in Table 7.3.

Table 7.3: Test results for threshold determination

Centroid Calculation Method	**S.D. with Threshold at 0 [μm]**	**S.D. with Threshold at 10,000 [μm]**	**S.D. with Threshold at 20,000 [μm]**	**S.D. with Threshold at 30,000 [μm]**
Gaussian	0.201	0.217	0.236	0.241
Centroid	0.195	0.199	0.211	0.217
S. Centroid	0.212	0.225	0.241	0.256
B. Centroid	0.222	0.230	0.248	0.261

Test results given in Table 7.3 shows that the threshold has an adverse effect on the standard deviation of the line position estimations. These results show that the back ground noise has no effect on the measurements. Attenuation of the ND filter may eliminate this type of disturbances. No threshold condition is selected after these results.

7.5.1.10 Tests for Number of Snapshots in Pixel Intensity Value Averaging

A new set of tests is conducted to determine the number of snapshots to be taken for intensity averaging of each image. During the tests, Centroid method with no threshold is used. 15 data sets are collected for each condition. Each set includes 50 images. Tests are repeated for 1 snapshot, 5 snapshots, 10 snapshots, and 20 snapshots conditions. The results are given in Table 7.4.

Table 7.4: Test results for number of snapshots

Number of Snapshots	Standard Deviation [μm]
1	0.413
5	0.325
10	0.302
20	0.359

According to test results given in Table 7.4, best results are obtained by using 10 snapshots for each image.

7.5.1.11 Shutter Time Tests

For four different shutter times, four sets of data are collected. All data sets are tested according to centroid method with no threshold with 10 snapshot numbers for each image. Results are given in Table 7.5.

Table 7.5: Test results for shutter time

Shutter Time [msec]	Standard Deviation [μm]
8	0.422
15	0.377
20	0.221
25	0.421

In the tests of which the results are given in Table 7.5, sensor is saturated for 25 msec shutter time. Tests results show that the best results are obtained for the shutter time just before the saturation limit.

7.5.1.12 Part of the Sensor Tests

Parameters up to this point are tested when the laser line is at the middle section of the sensor. Tests at this step are to observe the effect of the line location on the sensor. For this purpose, three sets of data are collected when the laser line is at left side, right side, and middle of the sensor. Results are presented in Table 7.6.

Table 7.6: Test results for part of the sensor

Part of the Sensor [pixels]	Standard Deviation [μm]
1^{st} - 320^{th}	0.301
320^{th} - 640^{th}	0.285
640^{th} - 960^{th}	0.292

According to test results given in Table 7.6, the location of the line along the sensor width has no significant effect on the measurements as long as the whole line width is inside the sensor area.

7.5.1.13 Motor State Tests

Four sets of tests are conducted for motor state parameter when the servo motors are at power off and power off states. During the tests centroid method with no threshold is used with 10 snapshot numbers for each image. Shutter time is set as 20 msec. Results are presented in Table 7.7.

Table 7.7: Test results for motor state

Motor State	Standard Deviation [μm]
x-axis off	0.861
y-axis off	0.351
Both axes off	1.311
Both axes on	0.302

Test results given in Table 7.7 indicate that free axes have a negative effect on the measurements. According to these results, motors should remain energized during the measurements.

7.5.1.14 Windowing Tests

Two sets of data are conducted for this parameter. In the first set, a full image of the sensor is executed. In the second set, a window of 300 pixels is formed around the laser line as shown in Figure 7.20 (b). Best conditions determined up to this point are used in the tests. These are centroid method with no threshold, 10 snapshots for intensity averaging of each image, shutter time of 20 ms, laser line at the middle of the sensor, and servo motor on. Results are shown in Table 7.8.

Table 7.8: Test results for windowing

Window Condition	Standard Deviation [μm]
Windowing to Pixel Range of 300^{th} - 600^{th}	0.455
Full Image	0.321

Test results given in Table 7.8 shows that full sensor images are superior to windowed images. However, this method increases the speed of the camera up to three times. If the speed of the camera becomes a bottleneck for the system, windowing may still be a preferable alternative.

7.5.4 Evaluation of Test Results

Results of the tests show that the most suitable CCM is centroid method in which the intensity value of each pixel is multiplied by the pixel location and divided to sum of the intensity values.

Threshold shows a negative effect on the standard deviation of the laser line positions. This shows that the background noise has not a significant negative effect on the measurements. This may be due to the ND filter in front of the sensor. This filter attenuates the light power to 1/1000 of the original one. Under this condition a negligible amount of light other than the laser line passes from the filter.

The image averaging method of taking several snapshots to obtain a single image by taking the mean value of each pixel presents a positive effect on the measurements. By this way, instantaneous pixel intensity fluctuations can be minimized.

Shutter time of the sensor has a significant effect on the measurements. Test results show that high shutter time is preferable in general. However, when the sensor is saturated, high intensity pixels reach to the same level and their contributions become equal. This affects the line deviations adversely. In other words, high shutter time is favourable provided that the sensor is not saturated.

Laser line location on the sensor has not a significant effect on the measurements. This is the result of the uniformity of the sensor.

Tests which are conducted with different motor states show that when the servo motors are at power on state, system takes more repeatable measurements.

Finally, windowing presents an adverse effect on the system. Full sensor images show better performance. However, despite its higher standard deviation, it presents a superior camera speed. Under some conditions, windowing may be a considerable alternative.

7.6 Time Dependent Camera Tests

In order to see the effect of the time of the day on the camera measurements a long period time test is carried out with the cameras. In this test, the methods determined in Section *7.5 Calibration System Camera Tests* are applied during measurements.

Starting from 08:30 pm on Monday, both cameras measure the position of a stationary laser for 36 hour (until 8:30 am on Wednesday). Temperature difference is about 4 °C between the night and daytime. Measuring and saving a single position data takes about 3 seconds for both cameras. In other words, about 43,000 position measurements are performed by each camera simultaneously. The obtained data is presented in Figure 7.21.

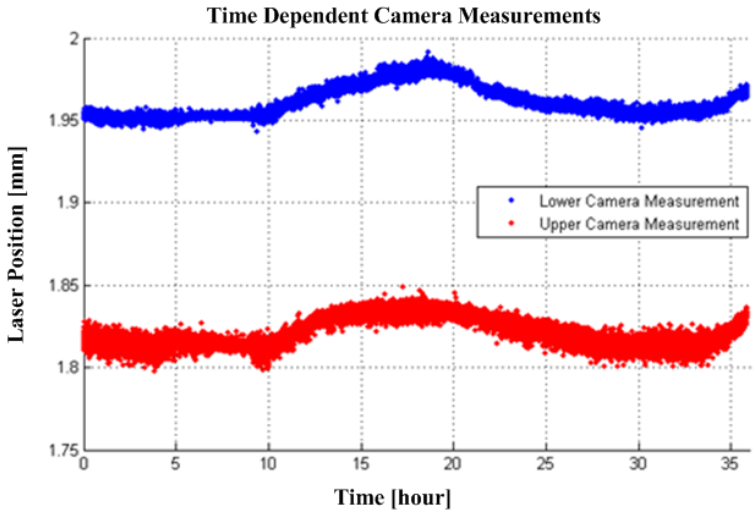

Figure 7.21: Time dependent camera measurements

In the lower camera data presented in Figure 7.21, laser position changes between 1.943 mm and 1.991 mm. This corresponds to a deviation about 48 µm in long period. This deviation is quite close to the deviation of the position data measured by the upper camera. The minimum and the maximum values of the upper camera measurements are 1.798 mm and 1.850 mm respectively. This corresponds to a deviation of 52 µm. Standard deviation (1 σ) of the lower camera measurements are 9.5 µm while that of the upper camera measurements is 9.1 µm.

Considering the required time for a calibration procedure, behaviour of the measurements in 4.5-hour periods is inspected by taking the most dispersed section of each camera test. For this purpose, lower and upper camera data between the hours 0 and 4.5 are monitored. Corresponding measurements of lower and upper cameras are presented in Figure 7.22 and Figure 7.23 respectively. Standard deviation of the lower camera measurements presented in Figure 7.22 is 1.6 µm and that of the upper camera measurements shown in Figure 7.23 is 3.9 µm.

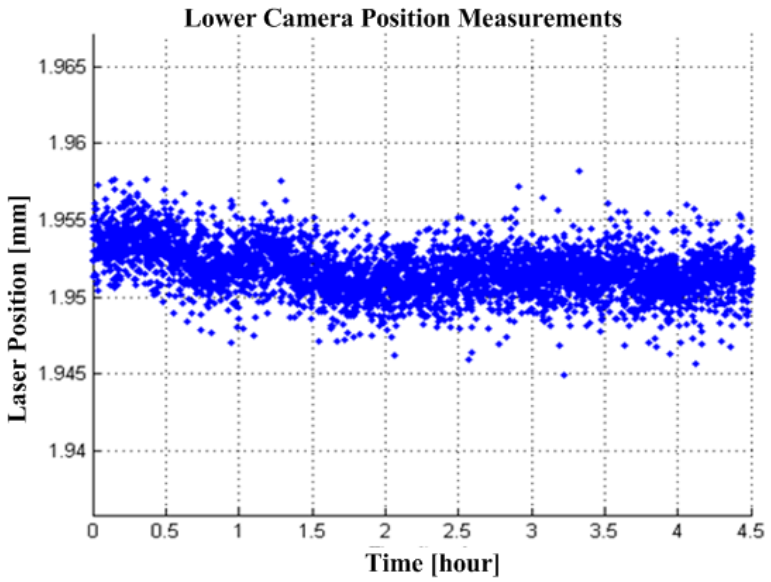

Figure 7.22: Lower camera position measurements between the hours 0 and 4.5

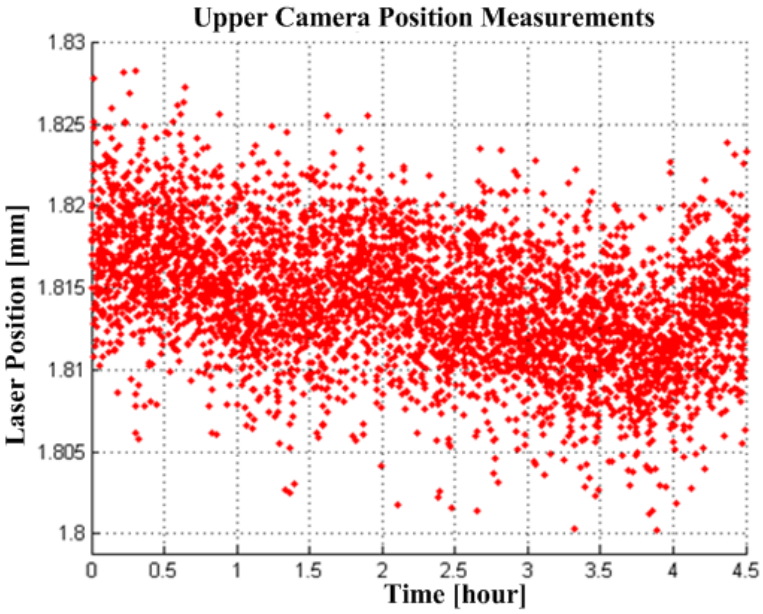

Figure 7.23: Upper camera position measurements between the hours 0 and 4.5

After determining the broadest region of the measurements, the narrowest band for both measurements presented in Figure 7.21 is obtained in time interval corresponding to the period between the hours 5 and 9.5. The relevant graphs are presented in Figure 7.24 and Figure 7.25.

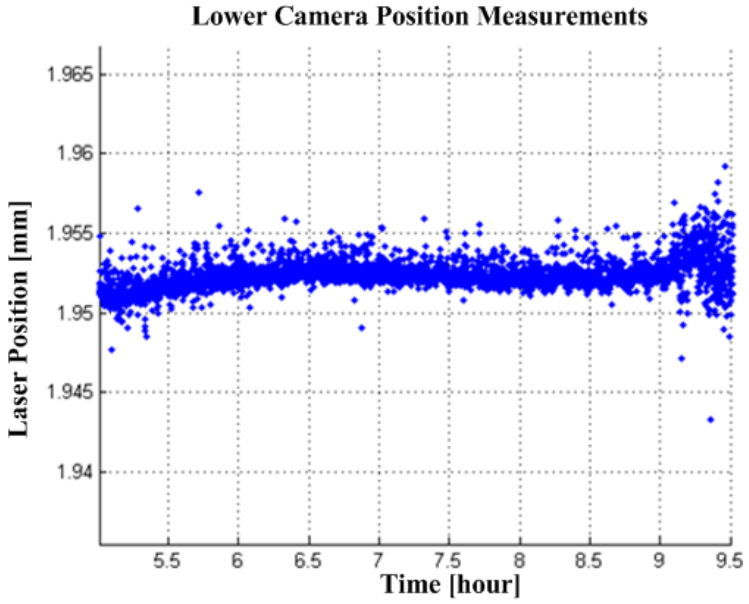

Figure 7.24: Lower camera position measurements between the hours 5 and 9.5

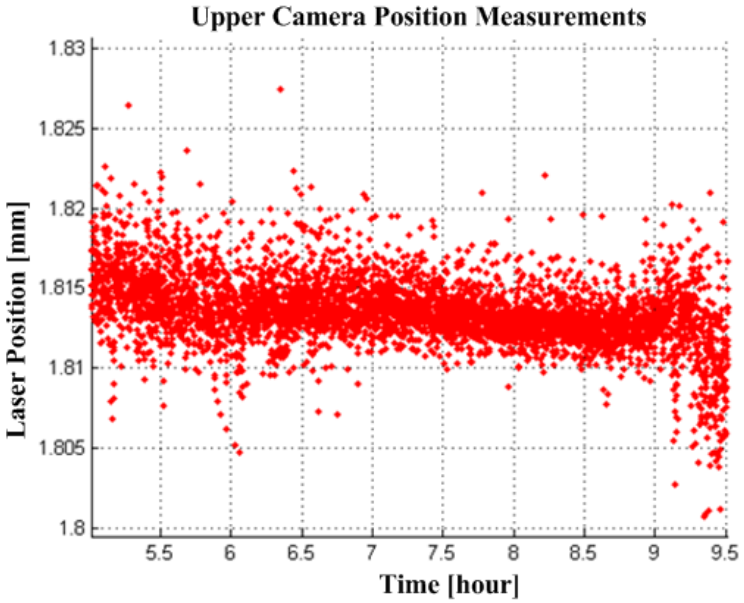

Figure 7.25: Upper camera position measurements between the hours 5 and 9.5

Standard deviation of the measurements of the lower camera presented in Figure 7.24 is 0.8 µm, and it is 1.9 µm for the lower camera measurements presented in Figure 7.25.

Due to the thermal changes and the vibrational effects originated from the environment, measurement performance of the cameras changes w.r.t. time of the day. Note that the changes are similar for both cameras whereas the standard deviation of the measurements performed by the upper camera always relatively grater. The most significant reason is the fact that the upper camera is about 300 mm farther away from the focus distance of the laser although the lower camera is at the focus distance.

7.7 Calibration of a Laser Beam Positioning System

At the end of the study, the calibration system is capable of performing the calibration of the laser beam positioning system. One of the commercial products of Modesis Machine Technologies with the product number of SL0FH01110281 is calibrated on the developed system.

The calibration procedure elaborated in Section *6.5 Calibration Procedure* is carried out. Consequently, required three parameters of the movable laser sources which are laser source position error, projection line angle error, and beam exit angle error w.r.t. the stationary center laser are measured for each position of the movable laser sources with 20 mm resolution along x-axis. Laser source positioning error graph is presented in Figure 7.26.

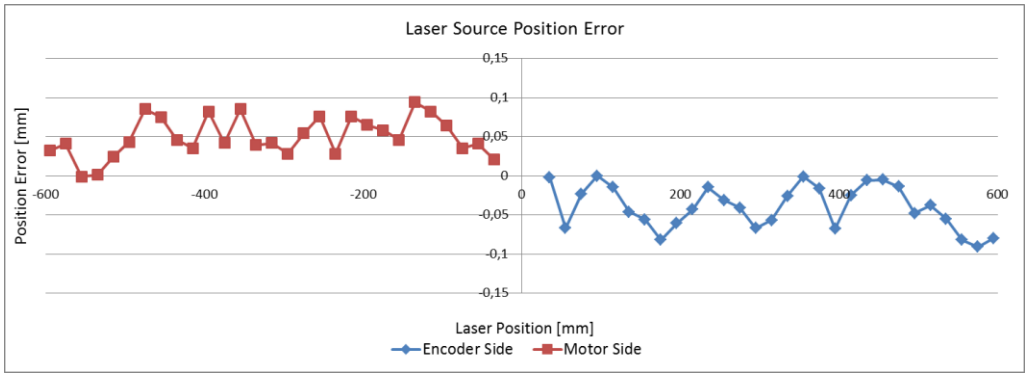

Figure 7.26: Laser source positioning error graphs of movable laser sources

Positioning error of both movable laser sources on the encoder side and on the motor side are presented in Figure 7.26. Positioning error of the encoder side laser source is between 0.0 mm and -0.09 mm. That of the motor side laser source is between 0.00 mm and 0.09 mm. Dominant factor of these errors is the power transmission system of the laser beam positioning system (timing belt and pulley). Projection line angle error graph generated from the output of the calibration system is presented in Figure 7.27.

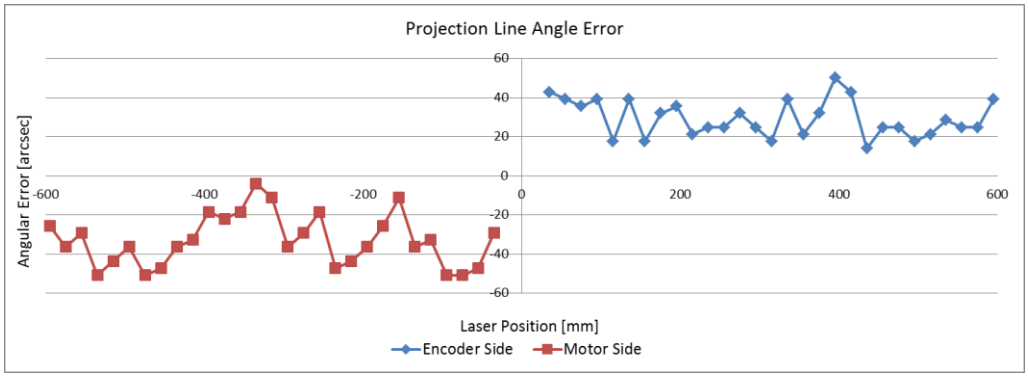

Figure 7.27: Projection line angle error graphs of movable laser sources

Projection line angle error of the encoder side laser which is presented in Figure 7.27 changes between 14 arcsec and 50 arcsec. This error is between 4 arcsec and 51 arcsec for the laser source on the motor side. The significant part of these errors is originated from the linear positioning elements (i.e. linear guideway and carriage] of the laser beam positioning system. Beam exit angle error of the movable laser sources is presented in Figure 7.28.

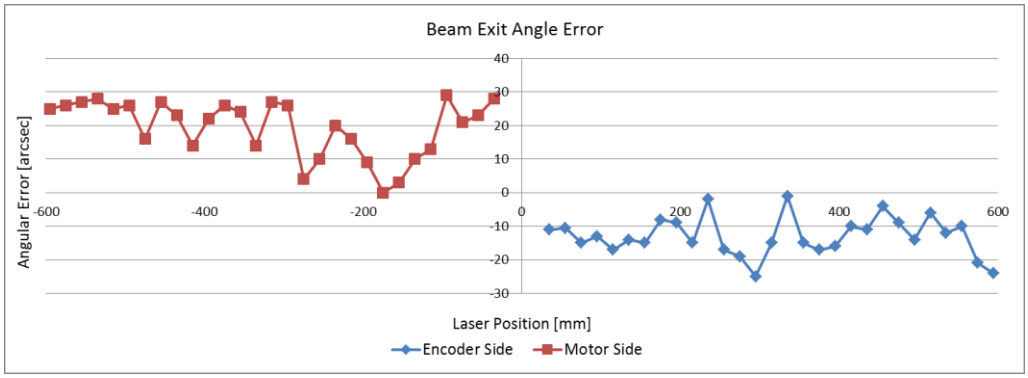

Figure 7.28: Beam exit angle error graphs of movable laser sources

According to the graph given in Figure 7.28, beam exit angle error of the encoder side laser is between -1 arcsec and -25 arcsec whereas that of the motor side laser is between 0 and 29. Similar to the projection line angle error, dominant factor of this error is linear positioning elements and attachment of these elements to the laser system.

7.8 Closure

In this chapter, test and measurements performed in the study are presented. The first test depends on the camera measurements performed on different environments. Results of these measurements indicate that the vibration disturbance is an important parameter for the calibration system. Consequently, a suitable place for the calibration system is searched and some vibration tests are performed for this purpose. These tests are also included in this chapter as *Calibration Room Vibration Tests*. Depending on the system requirements, camera positioning system verification tests are carried out. In these tests, angular errors of both translational axes are monitored. Positioning error of x-axis is also estimated on the basis of a double linear encoder test. Since there are several parameters affecting the laser position measurements of the camera, a series of tests are performed to specify the relevant parameters for precise measurements. After determining the camera measurement parameters a long period time test is performed with the cameras and a stationary laser to see the effect of the day time on the measurements. Finally, calibration results of a laser beam positioning system are presented.

CHAPTER 8

CONCLUSIONS AND FUTURE WORK

8.1 Conclusions

In this study, a calibration system for laser beam positioning systems used in industrial applications is designed and manufactured. The calibration system developed in this study is capable of measuring the laser positions of any kind of laser projection system for a projection area inside the dimensions of 1600 x 600 mm.

Designed system consists of two parts. The first part is the 2D camera positioning system and the second part is the upper side of the calibration system on which the laser projection system is mounted. Camera positioning system parts are designed and manufactured for high stability, high damping for vibration disturbances, and precise dimensional and geometrical properties. Camera position is measured by high-accuracy linear encoders along both axes. Translation system consists of precision elements such as linear guideways with circulating ball baring carriages and ball screws. Both axes are driven by servo motors. For the connection to the mating surfaces of thermally critical parts such as ball screw nut bodies and screw heads of ball screw nut body connections are covered by thermal insulation elements which are made of fiberglass epoxy plates.

Upper side of the calibration system is built as a heavy steel construction against vibration disturbances. IPN 200 I-beams and 10-mm thickness steel plates are used in the construction. The geometrical precision of this structure is also provided via the precision grinding of the mating surfaces. Wall connections of this structure is specially designed and manufactured to enable the angular adjustment of the laser projection system connection plate.

CCD cameras having 3.75 × 3.75 μm pixel size are utilized as the laser position sensor. Special algorithms are developed to measure the laser position precisely. With the developed algorithms, sub-pixel accuracy is obtained for the laser line position measurements on the camera. By conducting a series of tests measurement parameters of the cameras are determined.

In order to specify the accuracy bands of the static and dynamic elements of the calibration system, a kinematic model is developed. The calibration procedure is simulated via the developed model. A tolerance band for each error component is determined in order to satisfy the system requirements.

All system elements are integrated with a host controller PC via serial communication and USB interfaces. Control software is developed in Visual C# platform. Motor drivers, laser beam positioning system, and cameras are controlled via this software.

After the integration of the setup, system verification tests are performed on the camera positioning system. During these tests, critical angular error components of the translating elements are observed. The obtained results are compared with the tolerance bands specified with the kinematic model simulations. All measured parameters remain inside the limits.

Finally, calibration of a laser beam positioning system is accomplished. The measurements of the required parameters (laser positioning error, projection line angle error, and beam exit angle error) are documented.

8.2 Future Work

In addition to the work done in this study, some further studies can be conducted to obtain a more precise, more affective, and fully automatic calibration setup. For the first step, in order to minimize the environmental effects on the measurements, an air conditioning system should be constituted. Long period camera tests show that the thermal changes adversely affects the laser position measurements. Measurement problems caused by thermal effects can be minimized via a suitable air conditioning system.

One of the problems with the calibration system is the measurement speed. In the developed system a single laser position measurement takes about 1.5 seconds. Together with the waiting time after each positioning (for the stabilization of the camera positioning system) this period takes about 5 seconds. A calibration performed with 20 mm resolution along x-axis and 15 mm resolution along y-axis takes about 4.5 hours. Increasing the measurement speed enables to increase the measurement resolution.

In the developed calibration system, angle adjustments are performed by hand. It is possible to make these adjustments via stepper motors which are controlled by the system software. Such an improvement makes the calibration system fully automatic.

REFERENCES

Aalderink B. J. et al., "Experimental Observations of the Laser Keyhole Welding Process of AA5182", International Conference on Applications of Lasers and Electro-optics, November 2005.

ABB, Linear Motors, http://www.baldormotion.com/products/linearproducts/lmcf.asp, Last accessed December 20, 2012.

Aerotech, Inc., Linear Motors Application Guide, http://www.aerotech.com/media/117516/linear-motors-application-en.pdf, Last accessed December 20, 2012.

Bajd T., Mihelj M., "Robotics", Springer, New York, 2010.

Bradley B. D., Chan A. D.C., Hayes M. J. D., "A Simple, Low Cost, 3D Scanning System Using the Laser Light-Sectioning Method", IEEE International Instrumentation and Measurement Technology Conference, May 2008.

Bradley B. D., Chan A. D.C., Hayes M. J. D., "Calibration of a Simple, Low Cost, 3D Laser Light-Sectioning Scanner System for Biomedical Purposes", Carleton University, 2009.

Chida Y., Matsui S., Ohnishi J, "Laser and CCD Camera System for Magnet Alignment on Girder in the Spring-8 Storage Ring", 4th International Workshop on Accelerator Alignment, Japan, November 1995.

Dahotre N. B., Harimkar S. P., "Laser Fabrication and Machining of Materials", Springer, 2008.

Dieter G. E., Schmidt L. C., "Engineering Design", McGraw-Hill, Boston, 2009.

Diode Laser Concepts Inc., Uniform Line Generators Datasheet, http://www.diodelaserconcepts.com/pdf/UniformLineGeneratorInfoSheet.pdf, Last accessed August 10, 2012.

Drake G. W. F., "Springer Handbooks of Atomic, Molecular, and Optical Physics", Springer, 2006.

Edmund Optics Inc., Coherent Lasercam Beam Profiler, http://www.edmundoptics.com/lasers/laser-measurement/laser-beam-analysis/coherent-lasercam-beam-profiler/2780, Last accessed June 7, 2012.

Esersan Makine Ekipmanları, Product Catalogue, http://www.esersan.com/ ESERSAN.pdf, Last accessed July 14, 2012.

Fife K., Gamal A., Wong H. S. P., "A 0.5 μm Pixel Frame-Transfer CCD Image Sensor in 110nm CMOS" IEEE International Electronic Devices Meeting, pp. 1003 - 1006, December 2007.

Hanumolu P. K., "Design of Low Noise, Low Power Linear CMOS Image Sensors", Master Thesis, Worcester Polytechnic Institute, April 2001.

Heidenhain GmbH, Mounting Instructions, p10, Traunreut, 2002.

Hiwin Technologies Corp., Linear Guideway Catalogue, "Linear Guideway Technical Information", p.12, 2012a.

Hiwin Technologies Corp., Ball Screws Catalogue, “Ball Screws Technical Information”, p.29, 2012b

Hou B. et al., “Charge-Coupled Devices Combined with Centroid Algorithm for Laser Beam Deviation Measurements Compared to a Position-Sensitive Device”, Optical Engineering 50 (3), March 2011.

Jukic D., Scitovski R., “Least Squares Fitting Gaussian Type Curve”, Applied Mathematics and Computation 167, pp. 286 - 298, 2005.

Kulcke A., Gurschler C., Gasser C., Niel A., “Image Processing Based Calibration of High Precision Laser Projection Systems”, Photogrammetric Computer Vision, pp. 134 - 137, September 2002.

Lebedev A., “A laser calibration system for the STAR TPC”, Nuclear Instruments and Methods in Physics Research, pp. 163 - 165, 2002.

Lin C. S. et al., “High Speed and High Accuracy Inspection of in-Tray Laser IC Marking Using Line Scan CCD with a New Calibration Model”, Optics and Laser Technology, June 2010.

Matsui S. et al., “Magnet Alignment of the SPring-8 Storage Ring”, 4th International Workshop on Accelerator Alignment, Japan, November 1995.

Matsui S., Zhang C., “Alignment Method for 50m Distance Using Laser and CCD Camera”, Proceedings of the Seventh International Workshop on Accelerator Alignment, Japan, November 2002.

Newport Corporation, Absorptive Neutral Density Filters, http://search.newport.com/i/1/x1/pageType/q1/Products/q2/Optical%20Filters/q3/Neutral%20Density%20Filters/q4/Absorptive%20Neutral%20Density%20Filters/x2/section/x3/chapter/x4/family/nav/1/, Last accessed June 10, 2012.

Point Grey Research Inc., Technical Application Note TAN2008006, “Sensor QE Comparison”, 2011.

Precision Granite Castings, http://www.granitek.co.uk/hVibExorption.html, Last Access Date: 17/07/2012

Ranusawud M., Vacharanukul K., Tonmeanwai A., “Traceability of 633 nm Laser Calibration at Nimt”, IMEKO XIX World Congress, September 2009.

Shortis M. R., Clarke T. A., Short T., “A Comparison of Some Techniques for the Subpixel Location of Discrete Target Images”, Proc. SPIE 2350, Videometrics III, pp. 239 - 250, October 1994.

Song X. H. et al., “Design and Performance Analysis of Laser Displacement Sensor Based on Position Sensitive Detector (PSD)”, Journal of Physics: Conference Series 48, pp. 217 - 222, 2006.

St. John W. D., “Determination of the Beam Centroid of an Obstructed Focused Gaussian Laser Beam”, Optical Society of America, July 2009.

Stache N. C. et al., “Approaches for High-Speed Melt Pool Detection in Laser Welding Applications”, Vision, Modeling, and Visualization (VMV), pp. 217 - 224, November 2006.

Stache N. C. et al., “Automatic Calibration of a Scanner-Based Laser Welding System”, International Congress on the Applications of Lasers and Electro-Optics (ICALEO), pp. 223 - 229, November 2007.

Techno Inc., Techno Linear Catalogue, “Technological information - Stepper or Servo”, p.41, 2011

Tsumaki K. et al. “Magnet Rearrangement for 30 m Long Straight Sections in the SPring-8 Storage Ring”, Proceedings of the Seventh International Workshop on Accelerator Alignment, Japan, November 2002.

Vilaca J. L., Fonseca J. C., Pinho A. M., “Calibration Procedure for 3D Measurement Systems Using Two Cameras and a Laser Line”, Optics and Laser Technology, May 2008.

Vyas A., “Performance of Centroiding Algorithms at Low Light Level Conditions in Adaptive Optics”, International Conference on Advances in Recent Technologies in Communication and Computing, 2009.

Welch S. S., “Effects of Window Size and Shape on Accuracy of Subpixel Centroid Estimation of Target Images”, NASA Technical Paper 3331, 1993.

Wurzbacher T. et al., “Calibration of Laryngeal Endoscopic High-Speed Image Sequences by an Automated Detection of Parallel Laser Line Projections”, Medical Image Analysis 12, pp. 300 - 317, February 2008.

Xinqiao L., “CMOS Image Sensors Dynamic Range and SNR Enhancement via Statistical Signal”, Doctoral Thesis, Department of Electrical Engineering - Stanford University, June 2002.

APPENDIX A

CALCULATION OF X-AXIS BALL SCREW DIMENSIONS

- **Conditions of Use**

Ball Screw Type	:	FSC Super S Series
Quick feed speed	:	300 mm/sec
Movement per pulse	:	250 nm
Motor	:	AC servo motor (100,000 pulse/rev)
Stroke	:	1600 mm
Mounting Method	:	Fixed - Supported
Mounting Distance	:	1900 mm

- **Ball Screw Lead Selection**

Movement per pulse	:	250 nm
Motor resolution	:	100,000 pulse/rev

$$\ell = (0.00025mm) \times (100000\,pulse/rev) = 25mm$$

- **Rotational Speed**

Quick feed speed	:	300 mm/sec
Ball screw lead	:	25 mm

$$\omega = \frac{300mm/\sec}{25mm} \cdot 60\sec/\min = 720rpm$$

- **Minimum Shaft Diameter**

Minimum shaft diameter is calculated from critical speed formula.

Mounting Method	:	Fixed - Supported
Mounting Distance	:	1900 mm

$$d = \frac{(\text{Rotational speed}) \times (\text{Mounting distance})^2}{\text{Coefficient of the mounting method}} = \frac{720 \cdot 1900^2}{15.1 \cdot 10^7} = 17.2mm$$

Root diameter of the ball screw should be greater than 17.2 mm. Root diameter of FSC 20 ball screw is 16.7 mm. That of FSC 25 is 22.32 mm.
Consequently, FSC 25x25 ball screw is selected as the ball screw dimensions of x-axis.

APPENDIX B

CALCULATION OF Y-AXIS BALL SCREW DIMENSIONS

- **Conditions of Use**

Ball Screw Type	:	FSC Super S Series
Quick feed speed	:	1000 mm/sec
Movement per pulse	:	250 nm
Motor	:	AC servo motor (80,000 pulse/rev)
Stroke	:	600 mm
Mounting Method	:	Fixed - Supported
Mounting Distance	:	800 mm

- **Ball Screw Lead Selection**

Movement per pulse	:	250 nm
Motor resolution	:	80,000 pulse/rev

$$\ell = (0.00025mm) \times (80000\,pulse/rev) = 20mm$$

- **Rotational Speed**

Quick feed speed	:	1000 mm/sec
Ball screw lead	:	20 mm

$$\omega = \frac{1000mm/\sec}{20mm} \cdot 60\sec/\min = 3000rpm$$

- **Minimum Shaft Diameter**

Minimum shaft diameter is calculated from critical speed formula.

Mounting Method	:	Fixed - Supported
Mounting Distance	:	800 mm

$$d = \frac{(\text{Rotational speed}) \times (\text{Mounting distance})^2}{\text{Coefficient of the mounting method}} = \frac{3000 \cdot 1900^2}{15.1 \cdot 10^7} = 12.7mm$$

Root diameter of the ball screw should be greater than 12.7 mm. Root diameter of FSC 15 ball screw is 12.37 mm. That of FSC 20 is 16.7 mm.
Consequently, FSC 20x20 ball screw is selected as the ball screw dimensions of x-axis.

APPENDIX C

M - FILES OF FUNCTIONS USED IN THE KINEMATIC MODEL

- **ellipse**

The m-file represents the function **ellipse** which generates a vector of which the elements are points on the elliptical curve of the laser exit.

INPUTS:

str_err: straightness of the laser at 1 m projection distance

n: number of the points taken on the elliptical curve

OUTPUTS:

curve: vector including the coordinates of the elliptical curve in 3D

Table D.1: MATLAB code of the function "**ellipse**"

```
function [curve]=ellipse(lens_dist,str_err, n)

h=-lens_dist;     % distance between the laser focal point and
                  % the laser exit
fanangle=45/180*pi;         % exit fan angle of the laser source
a=(abs(h)*str_err)/1000;    % x-intercept of the ellipse
b=abs(h)*tan(fanangle/2);   % y-intercept of the ellipse

% y-coordinates of the points on the elliptical curve
y=linspace(-b,b,n);

% x-coordinates of the points on the elliptical curve
x=sqrt(a^2-(a^2).*(y.^2)/b^2);

% z-coordinates of the points on the elliptical curve
z=ones(1,length(y))*h;

curve=[x;y;z];

end
```

- **intersect_plane**

The function **intercect_plane** finds the position of the intersection point "P" of a line (passing through two points PL1 and PL2) and a plane (including three points PP1, PP2, and PP3)

INPUTS:

PL1, PL2: points on the line

PP1, PP2, PP3: points on the plane

OUTPUTS:

P: intersection point of the line and the plane

Table D.2: MATLAB code of the function **"intersect_plane"**

```
function [P]=intercect_plane(PL1, PL2, PP1, PP2, PP3)

% A planar equation of Ax+By+Cz+D=0;
A=det([1 PP1(2) PP1(3); 1 PP2(2) PP2(3); 1 PP3(2) PP3(3)]);
B=det([PP1(1) 1 PP1(3); PP2(1) 1 PP2(3); PP3(1) 1 PP3(3)]);
C=det([PP1(1) PP1(2) 1; PP2(1) PP2(2) 1; PP3(1) PP3(2) 1]);
D=-det([PP1(1) PP1(2) PP1(3);PP2(1) PP2(2) PP2(3);PP3(1) ...
    PP3(2) PP3(3)]);

% Points on the line
x1=PL1(1); y1=PL1(2); z1=PL1(3);
x2=PL2(1); y2=PL2(2); z2=PL2(3);

% Parameter of the line in 3D "P=P1+(P2-P1)*t"
t=(A*x1+B*y1+C*z1+D)/(A*(x1-x2)+B*(y1-y2)+C*(z1-z2));

P=PL1+t*(PL2-PL1);

end
```

- **line_angle**

The m-file represents the function **line_angle** which computes the angle of the line connecting the end points of a given 2D curve (2xn)

INPUTS:

curve: vector including the coordinates of a curve

OUTPUTS:

angle: angle of the line connecting the two tip points of the curve (in radians)

Table D.3: MATLAB code of the function **"line_angle"**

```
function angle=line_angle(curve)

n_points=length(curve); % number of pnits
x1=curve(1,1); y1=curve(2,1); % first point
x2=curve(1,n_points); y2=curve(2,n_points); % last point
if x1==x2
    angle=pi/2;
else
    angle=atan2(-(y1-y2),-(x1-x2));
end

end
```

- **cam_measure**

Function **cam_measure** calculates the x position of the projected curve corresponding to y=0.

INPUTS:

curve_res: number of the points on the curve

curve_C_laser: vector including the points on the curve

OUTPUTS:

measurement: x-position of the projected laser curve on the camera center

Table D.4: MATLAB code of the function **"cam_measure"**

```
function measurement=cam_measure(curve_res,curve_C_laser)

for i=1:(curve_res-1)

    if (curve_C_laser(2,i)*curve_C_laser(2,i+1)<=0)
        y1=curve_C_laser(2,i);
        y2=curve_C_laser(2,i+1);
        x1=curve_C_laser(1,i);
        x2=curve_C_laser(1,i+1);
    break;
    end
end

measurement=(y1*x2-y2*x1)/(y1-y2);

end
```

- **cordtrans**

The m-file represents the function **cordtrans** which generates the homogeneous transformation matrix between two coordinate frames.

INPUTS:

Pose: matrix including the translational and rotational components of a frame w.r.t. a reference frame.

OUTPUTS:

T: homogeneous transformation matrix between the frames.

Table D.1: MATLAB code of the function **"cordtrans"**

```
function [T]=cordtrans(Pose)

X=Pose(1); Y=Pose(2); Z=Pose(3);    % translational position
dX=Pose(4); dY=Pose(5); dZ=Pose(6); % translational errors
Ex=Pose(7); Ey=Pose(8); Ez=Pose(9); % rotational errors

T=[cos(Ey)*cos(Ez) -cos(Ey)*sin(Ez) sin(Ey) X+dX;

sin(Ex)*sin(Ey)*cos(Ez)+cos(Ex)*sin(Ez)...
-sin(Ex)*sin(Ey)*sin(Ez)+cos(Ex)*cos(Ez)...
-sin(Ex)*cos(Ey) Y+dY;

-cos(Ex)*sin(Ey)*cos(Ez)+sin(Ex)*sin(Ez)...
cos(Ex)*sin(Ey)*sin(Ez)+sin(Ex)*cos(Ez)...
cos(Ex)*cos(Ey) Z+dZ;

0 0 0 1];

 end
```